AD-A069 074 HARRIS CORP MELBOURNE FL GOVERNMENT SYSTEMS GROUP F/G 22/2
CODING FOR NAVY UHF SATELLITE COMMUNICATIONS (PHASE II).(U)
AUG 78 N00039-77-C-0259
UNCLASSIFIED JA-1126 NL

| OF |
AD
A069074

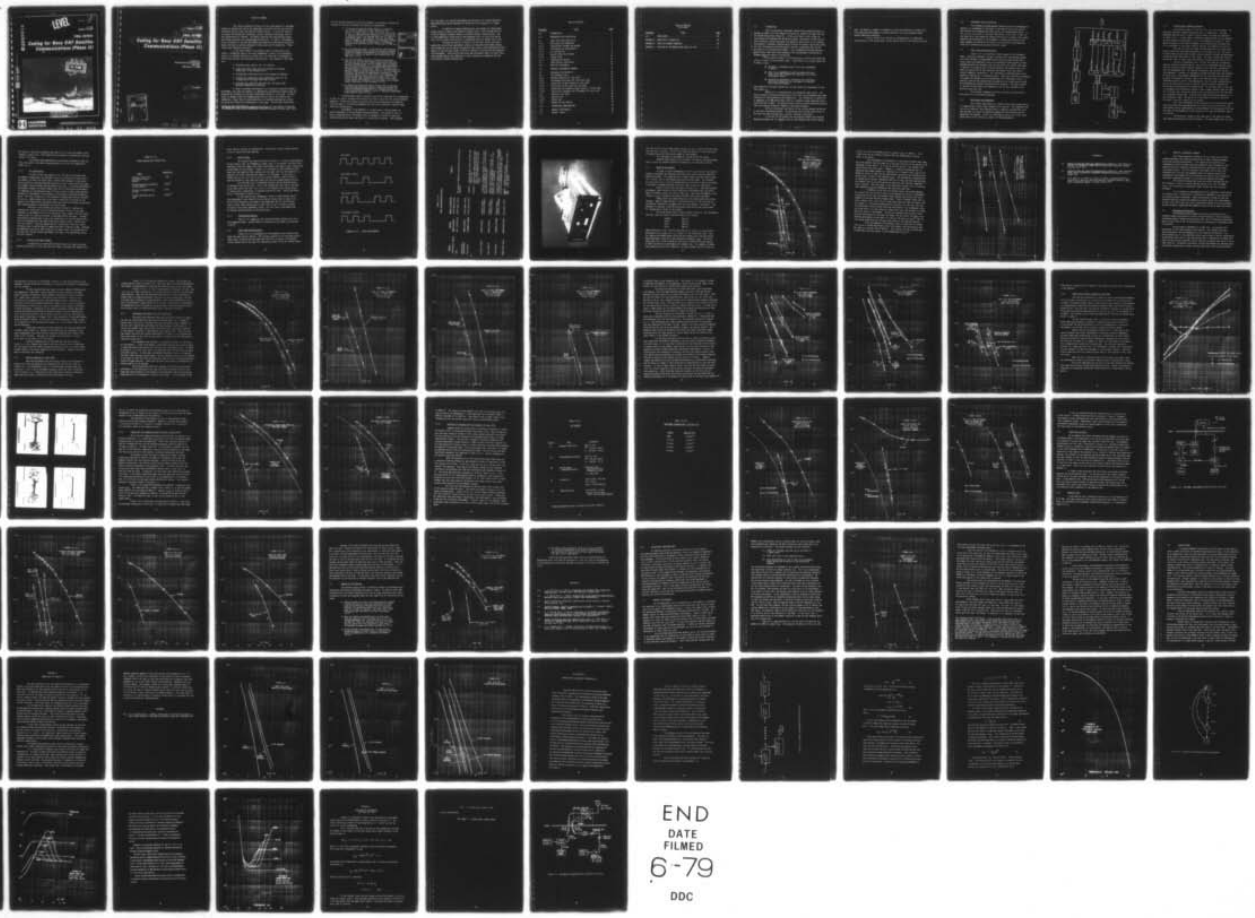

END
DATE
FILMED
6-79
DDC

LEVEL II

JA 1126
N00039-77-C-0259

FINAL REPORT

Coding for Navy UHF Satellite Communications (Phase II)

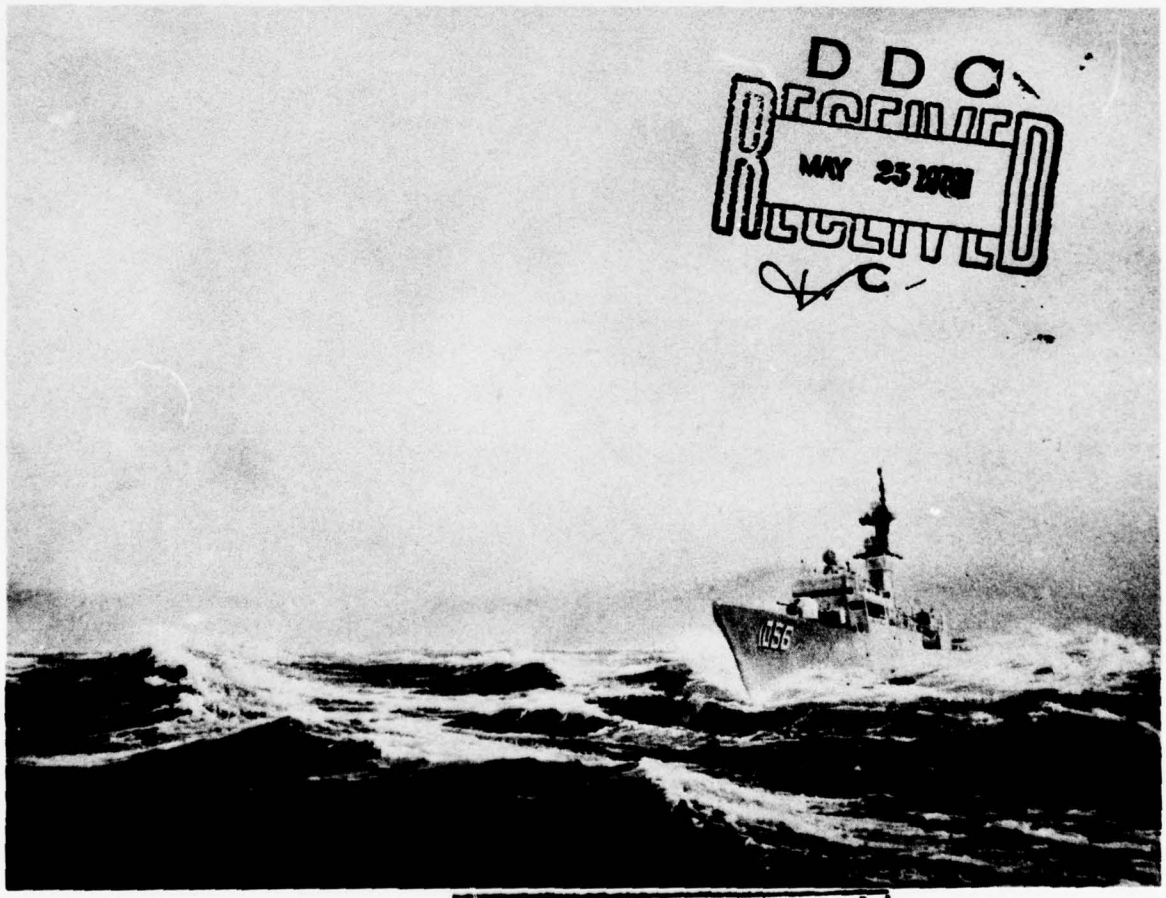

HARRIS
COMMUNICATIONS AND INFORMATION HANDLING

HARRIS CORPORATION Government Systems Group
Communications Systems P.O. Box 37, Melbourne, FL 32901 (305) 727-4000

(14) JA-1126

(15) New N00039-77-C-0259

(9) FINAL REPORT.

(6) Coding for Navy UHF Satellite Communications (Phase II).

Prepared For:
Naval Electronic Systems Command
PME 106-1
Washington, D. C. 20360

(11) 11 Aug 1978

(12) 90 p.

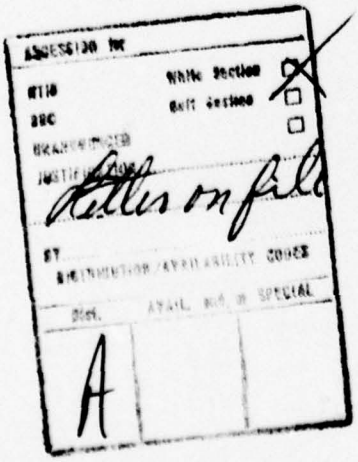

89652

EXECUTIVE SUMMARY

This report presents the results of the second phase of a two-phase program to evaluate and verify the advantages associated with the use of error-correction coding in Navy UHF satellite communications. In the first phase of the study, the problem was formulated, various techniques considered, and the most appropriate are selected. The chosen technique was convolutional coding and Viterbi decoding, with pseudorandom interleaving. In Phase I, performance of this technique in the Navy UHF SATCOM environment was predicted by analytical means, and shown to provide substantial coding gain and RFI protection. These results were reported previously.*

In the second phase of the program, which is addressed by this report, a breadboard codec of the type recommended in Phase I was implemented. Since it is intended primarily as a test unit, the codec has a high degree of flexibility and many user-selectable configurations. Key features of the codec are:

- Selectable code rates of 1/2, 2/3, and 3/4
- Longer-than-usual code constraint lengths for enhanced coding gain in the presence of RFI
- Pseudorandom interleaver which can be enabled or bypassed
- Internal bit synchronizer with performance within 0.4 dB of theoretical for E_s/N_o from 0 dB to 10 dB
- Hard decision, three-bit soft decision, and analog (NRZ baseband) demodulator interfaces

In order to evaluate performance in an accurately simulated shipboard environment, the codec was tested in a comprehensive experimental program using the Shipboard RFI Simulator at the Naval Postgraduate School as a test bed. In these tests, an AN/WSC-3 Satellite Communications Set was used as the receiver and demodulator, except that bit synchronization and integrate-and-dump was carried out using the internal bit synchronizer in the codec. The principal conclusions

*Coding for Navy UHF Satellite Communications (Phase I), Final Report on Contract No. N00039-76-C-0384, Harris Corporation, Electronic Systems Division, April 1977.

of this testing program are as follows (numbers in parentheses indicate the location in the main text where the results are documented):

- In the case of underprivileged terminals (submarines and aircraft) where RFI is not a factor but link margin is a major concern, rate -1/2 coding can provide as much as 5 dB coding gain (reduction in required C/N_0 or enhanced margin) over uncoded operation for 4800 b/s information rates. For 2400 b/s rate, the achievable gain is reduced to approximately 3.5 dB because of modem effects. There may be a simple means of overcoming these effects and restoring full coding gain at 2400 b/s. (3.2.5)

- For all three code rates, coding provides simultaneously protection against bursts of erasures caused by periodic pulsed RFI blanked in the AN/WSC-3, and moderate coding gain (up to 4 dB), the amount of gain varying with the code rate. (3.2.2)

- Even for the highest currently envisioned transmission rate of 19.2 ks/s and the largest pulse width of 200 μsec, for which erasure bursts are five symbols long (including blanker pulse extension), use of pseudorandom interleaving does not provide significant performance improvement over the performance of coding alone. That is, the code alone is powerful enough to provide essentially all the RFI protection available from coding and pseudorandom interleaving. This conclusion applies even in the case of two independent RFI sources of 200 μsec pulse width and 5% duty cycle. Thus, unless channel rates substantially in excess of 19.2 ks/s or more severe RFI parameters are envisioned, use of pseudo-random interleaving is not warranted. (3.2.3)

- In addition to protecting against erasure bursts resulting from high power pulsed RFI sources, coding can provide substantial performance enhancement over uncoded operation in a very dense RFI environment, such as is typically encountered aboard surface ships. (3.2.6)

The performance results obtained using the RFI Simulator are corroborated, in part, by results obtained from testing on an actual satellite link using FLTSATCOM Channel 4. Within the accuracy with which C/N_0 can be established, the satellite link test data is in excellent agreement with the results obtained in the RFI Simulator test configuration.

Performance of the AN/WSC-3 is in some cases a limiting factor on actual achievement of the available coding performance. The reason for this is that in coded operation, the AN/WSC-3 must be operated at levels of E_s/N_0 substantially below the range over which it is specified to operate. Thus although

this unit meets its required performance specifications for uncoded operation, some modification may be desirable to insure efficient operation in a coded system.

In addition to these considerations, the presence of coding opens several areas of concern with regard to system timing. These include the provision of adequate preamble length to establish decoder synchronization and to allow demodulator acquisition at the depressed levels of C/N_0 which may be used, and the proper orchestration of information rate and channel rate clocks.

Although the results of Phase II of the study confirm the Phase I predictions and provide experimental evidence of potential performance enhancement through the use of coding, we maintain that a major system engineering effort remains to resolve these issues relating to operation with the existing communications equipment. These efforts must weigh the performance impact of these interface problems against the complexity of their solutions to determine the most cost-effective system configuration.

TABLE OF CONTENTS

TABLE OF CONTENTS
(Continued)

1.0 INTRODUCTION

Harris Corporation, Government Communication Systems Division, is pleased to submit this Final Report on Contract No. N00039-77-C-0259, the Navy UHF SATCOM Coding Study (Phase II). In the prior phase of this study, we investigated the shipboard UHF SATCOM environment, considered a broad class of error-correction coding techniques with potential application to this problem, and selected a candidate technique which promised to provide significant coding gain and simultaneous protection against the most troublesome forms of RFI occurring in the shipboard environment. This recommended technique employed convolutional codes and Viterbi decoding, with pseudorandom interleaving to disperse the burst effects of pulsed RFI.

The purpose of Phase II of the study was to confirm and extend the results of Phase I by experimental means. Specifically, our primary objectives in Phase II were:

- Implement a breadboard codec of the type recommended in Phase I.
- Carry out a comprehensive testing program with this codec, using the shipboard RFI simulator at the Naval Postgraduate School.
- Identify any performance limitations and interfacing constraints imposed by the requirement to interface with existing equipments.

These objectives have been carried out, and the results are documented in this Final Report.

Section 2.0 is concerned with the breadboard codec itself. This section contains a functional description of the unit, and performance data under conditions of ideal modulation and demodulation. The information in Section 2.0 is augmented by an Operating Guide, which is a separate volume submitted concurrently with this report. The Operating Guide contains detailed operating instructions and complete electrical schematics and layout diagrams.

Section 3.0 contains the results of the testing program carried out at the Naval Postgraduate School. The discussion here includes description of the tests and their purpose, test results, and major conclusions.

In Section 4.0, we address the relationship between the encoding/decoding equipment and its neighbors both on the baseband side and the channel

side. We identify a number of instances in which characteristics of these units limit achievable performance, or place constraints on system operation which require additional attention.

Finally, Section 5.0 contains our recommendation for additional investigation, at the system level, of the issues raised in the previous sections.

2.0 BREADBOARD CODEC DESCRIPTION

The breadboard encoder/decoder hardware which was implemented is generally as recommended in the Phase I Final Report [2-1], with several modifications which appeared desirable during the implementation phase. In this section, we present a functional description of the codec, as well as test data using ideal modem and channel characteristics, which verify proper operation and performance of this hardware. Complete description of the codec hardware and operating instructions are contained in the Operating Guide [2-2] submitted concurrently with this report.

2.1 Codec Functional Description

Figure 2.1-1 is a functional block diagram of the breadboard codec. The major components include a variable rate convolutional encoder and Viterbi decoder, a pseudorandom block interleaver and deinterleaver, a data source and comparator, and a bit synchronizer which accepts an NRZ-L baseband waveform and produces 3-bit soft decisions and channel rate clock. In addition to accepting such an analog waveform, the receive side of the codec can accept hard or soft decisions and channel rate clock from an external modem/bit synchronizer. The interleaver and deinterleaver can be enabled or bypassed by a front-panel switch. Code rate selection or bypassing the encoder and decoder is also accomplished via a front-panel switch. In addition, data may be differentially encoded prior to convolutional coding and differentially decoded following Viterbi decoding. The codec contains an internal PN data source and comparator, but can also interface to an external source and sink.

The principal components and their functions are described in more detail in the following paragraphs.

2.1.1 Data Source and Comparator

The internal data source is a length-127 PN sequence generated by a 7-stage maximal length linear feedback shift register. The comparator consists of an identical shift register which is manually synchronized to the received data and counts discrepancies between the received data and the regenerated PN sequence. Errors are indicated by pulses on an error count output which can be routed to a counter for BER measurements.

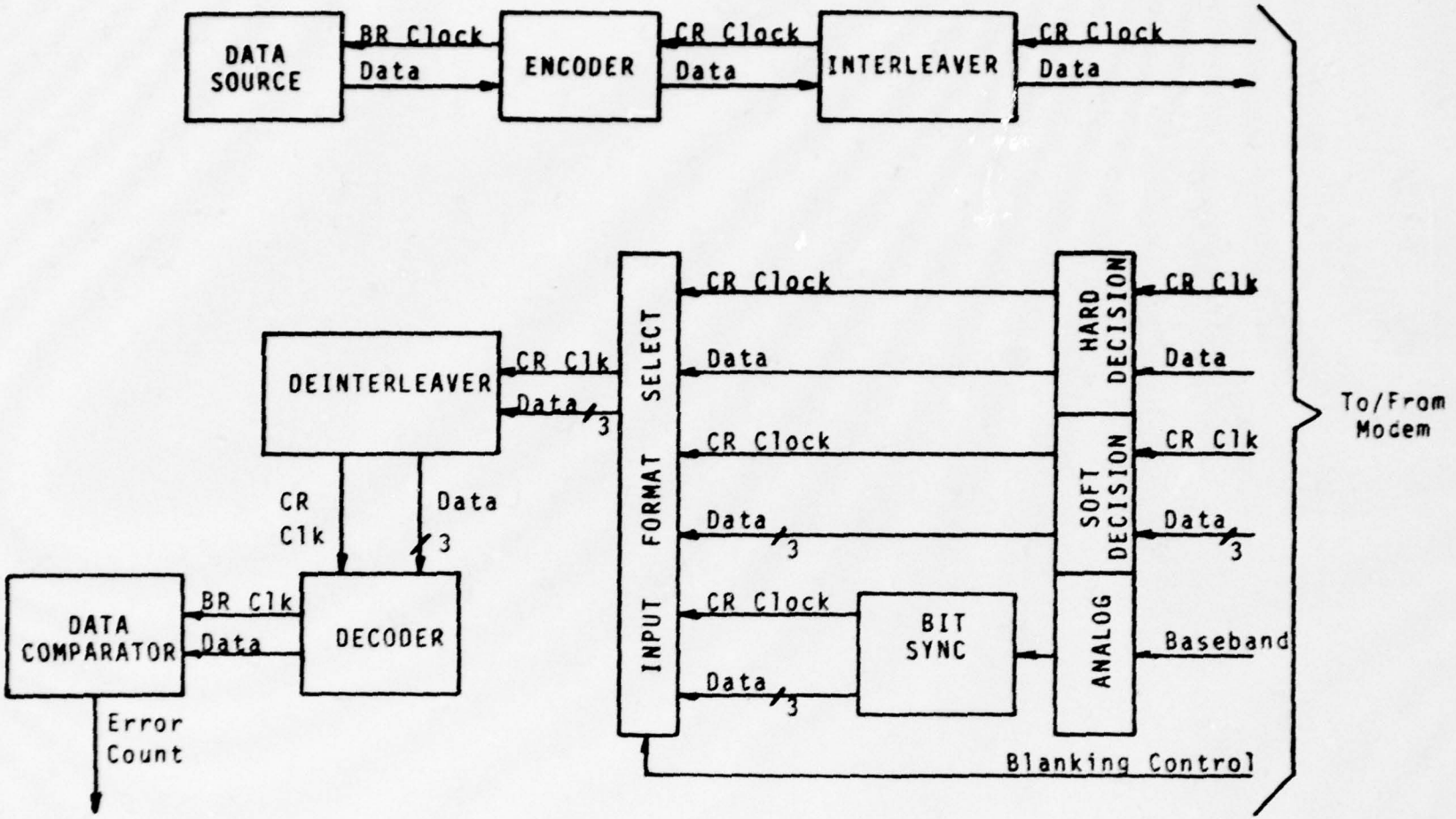

FIGURE 2.1-1. CODEC FUNCTIONAL BLOCK DIAGRAM

2.1.2 Convolutional Encoder and Decoder

Convolutional codes of rates 1/2, 2/3, and 3/4 are provided. The effective constraint lengths are k=9,10, and 11, respectively. The code generators and the first six terms of their weight structures are tabulated in Table 2.1.2-1. In this table, d indicates codeword weight and w_d indicates the total number of information 1s in all the codewords of weight d. These weight structures can be used to compute a union bound which accurately predicts performance in the range of BER of interest (see Appendix A of [2-1]).

The rate -2/3 and -3/4 codes are punctured rate -1/2 codes, which greatly simplifies the decoding operation, as discussed in [2-3]. Selection of these codes resulted from a rather extensive search for good code generators carried out under both phases of this study. The codes selected are the best transparent codes of their rates and constraint lengths we were able to find.

The use of transparent rate -2/3 and -3/4 codes was a departure from our originally proposed design. We initially recommended the best codes found of each rate without regard to whether or not they were transparent; in fact the recommended rate -1/2 code was transparent and the other two were non-transparent. However, we subsequently became concerned about the frequency of cycle slips in the AN/WSC-3 demodulator at the low signal-to-noise ratios at which we intended to operate. When a non-transparent code is used and a 180^{o} phase reversal occurs in the demodulator, loss of branch synchronization occurs, and the result is loss of data for typically several hundred bits while branch synchronization is reestablished. On the other hand, if the code is transparent and differential coding is used, a phase reversal does not cause loss of branch sync, but merely causes a burst of decoding errors on the order of a constraint length long. Thus the more conservative design approach is to use transparent codes. The sacrifice in performance incurred by using the transparent codes was found to be very slight.

The use of differential coding external to the convolutional coding also contributes some degradation due to the amplification of the error rate. Union bounds predict approximately 0.2 dB degradation in the absence of RFI and less than 0.4 dB degradation in the presence of RFI, when differential coding is selected.

The constraint lengths of the codes used in the codec are longer than commonly employed with Viterbi decoders. (The most common rate -1/2 code

Table 2.1.2-1.

Convolutional Codes and Weight Structures

			Weight Structure	
Rate	k	Generators	d	W_d
1/2	9	561	12	33
		753	13	0
			14	281
			15	0
			16	2197
			17	0
2/3	10	0755	8	61
		0427	9	380
		1342	10	1534
			11	7134
			12	31252
			13	113767
3/4	11	0631	6	10
		0557	7	324
		1622	8	1995
		2624	9	11080
			10	77182
			11	468328

has k=7; corresponding effective constraint lengths for rate -2/3 and -3/4 codes of equivalent complexity are 8 and 9, respectively.) In Phase I of this study we found that the increased constraint lengths provide substantially better performance in the presence of RFI, and because of the relatively low operating speeds of interest here, use of longer codes is feasible.

The Viterbi decoder is of a conventional design, generally as described in Section 5.1.5 and Appendix B of [2-1]. As noted there, the only significant departures from previous designs are the multiple rate capability (since punctured codes are used, the impact of multiple rates is minimal), longer constraint length codes, and increased decoding depth (found to be necessary since low-weight codewords in rate -2/3 and -3/4 codes tend to be longer than low-weight codewords in rate -1/2 codes).

2.1.3 Interleaver and Deinterleaver

The interleaver and deinterleaver perform a pseudorandom permutation and its inverse on the data transmitted and received over the channel, in order to disperse the effects of RFI bursts. At the interleaver, data to be transmitted is inserted in a 1008-location RAM in accordance with a pseudorandom addressing sequence which is stored in an addressing PROM. The data is read out sequentially from the RAM for transmission. Two 1008-location RAMs are actually employed in a ping-pong fashion, with one having data stored randomly while data is being output sequentially from the other.

The inverse permutation is accomplished by the deinterleaver, except that three bits of storage per transmitted symbol are required because of soft decisions. In order to properly synchronize the deinterleaver, frame synchronization bits are inserted periodically in the data. The deinterleaver contains frame synchronization circuitry which searches for the frame sync pattern until sync is established, then continues to monitor the pattern to verify that sync is not lost. We initially proposed to stuff the additional sync bits into the data stream, but later decided to simply override encoder output bits by frame sync bits. A sync pattern of 24 bits is spread over two consecutive blocks, so that one bit of every 84 is overridden. These overridden bits are treated as erasures by the decoder; these erasures degrade performance by 0.2 to 0.4 dB. The advantage of overriding rather than stuffing is that there is no additional overhead, and the transmitted and information

bit rates are precisely related by the inverse of the code rate whether interleaving is used or not. This simplifies the problem of providing bit rate and channel rate clocks.

Calculated frame synchronization performance parameters using this 24-bit sync word at the worst expected channel error rate are summarized in Table 2.1.3-1.

2.1.4 Bit Synchronizer

In order to have the capability for soft-decision decoding with the AN/WSC-3 demodulator, we proposed to access an internal test point within the AN/WSC-3 at which the Costas loop I channel (NRZ baseband) is available, and to perform an integrate-and-dump operation on this signal within the codec, with symbol timing provided from the AN/WSC-3 bit sync. In testing the AN/WSC-3 performance, however, we found evidence that the bit synchronizer performance is inadequate at the depressed levels of C/N_0 at which a coded system operates, although its performance is satisfactory at the specified (uncoded) operating point. This type of behavior is not uncommon in modems which are not designed for use in a coded system, and it can place a significant limitation on the amount of the theoretically available coding gain which can actually be achieved when coding equipment is backfitted into such systems.

Because of this problem, we elected to install a complete bit synchronizer, rather than just an integrate-and-dump circuit, in the codec. Interface to the AN/WSC-3 is still at the Costas loop I channel, but now symbol timing as well as a decision voltage is developed within the codec. The most cost-effective approach was to use a bit synchronizer of existing design which could be integrated into the codec with minimal design effort. The bit sync is an all-digital, "any rate" design which is tunable up to 100 ks/s, and is the design used in the MD-1030 PSK modem which Harris supplies to NRL. Although we expected to use only a small fixed set of symbol rates, the availability of the "any rate" design without development cost made it the appropriate choice for this function.

2.1.5 Receive Side Input Formats

In addition to an analog NRZ baseband input, the codec can accept either hard decision or 3-bit soft decision inputs, together with channel rate

Table 2.1.3-1.

Frame Synchronizer Probabilities

Event	Probability
Failure to find first occurrence of sync pattern	0.56
Falsely declaring occurrence of sync pattern	1.8×10^{-5}
Failure to recognize loss of sync	0.28
Falsely declaring loss of sync	5.8×10^{-8}

clock, from an external bit synchronizer. A rear panel switch allows selection of one of these three input options.

2.1.6 System Timing

The transmit and receive portions of Figure 2.1-1 operate asynchronously. On the transmit side, the fundamental timing signal is the channel rate (CR) clock, sometimes called the symbol rate clock, which governs the speed of data transmission by the modem over the channel. Figure 2.1-1 indicates CR clock supplied to the codec from the modem (or other source), but the codec also has the capability to generate a CR clock internally and supply it to the modem. In this case, a channel rate of 2.4, 4.8, 9.6 or 19.2 ks/s can be selected. When CR clock is supplied externally, the codec can accept any rate up to approximately 50 ks/s.

Bit rate (BR) clock is developed from CR clock by deleting pulses as necessary from the CR clock. Thus in the uncoded mode, BR clock is the same as CR clock, while with rate -1/2, -2/3, or -3/4 coding, every second, third, or fourth pulse, respectively, is deleted from the CR clock. Typical BR clocks are as illustrated in Figure 2.1.5-1.

On the receive side, fundamental timing is established by the CR clock developed in the internal bit sync when an analog input is used, or by the CR clock supplied to the codec by the modem when hard or soft decision input is used. When analog input is used, the bit sync is tuned to nominal CR using a front panel thumbwheel switch. Bit rate clock is developed from CR clock by deleting pulses, as discussed above.

2.1.7 Configuration Options

Table 2.1.7-1 summarizes the switch-selectable options built into the breadboard codec. Further details on operation of the codec are contained in [2-2].

2.2 Codec Physical Description

Figure 2.2-1 is a photograph of the breadboard codec showing front panel and some interior details. The circuitry consists of 13 wire-wrap digital logic cards, of which the card shown near the front is typical; one printed-circuit analog card of the same size containing an AGC circuit for analog inputs;

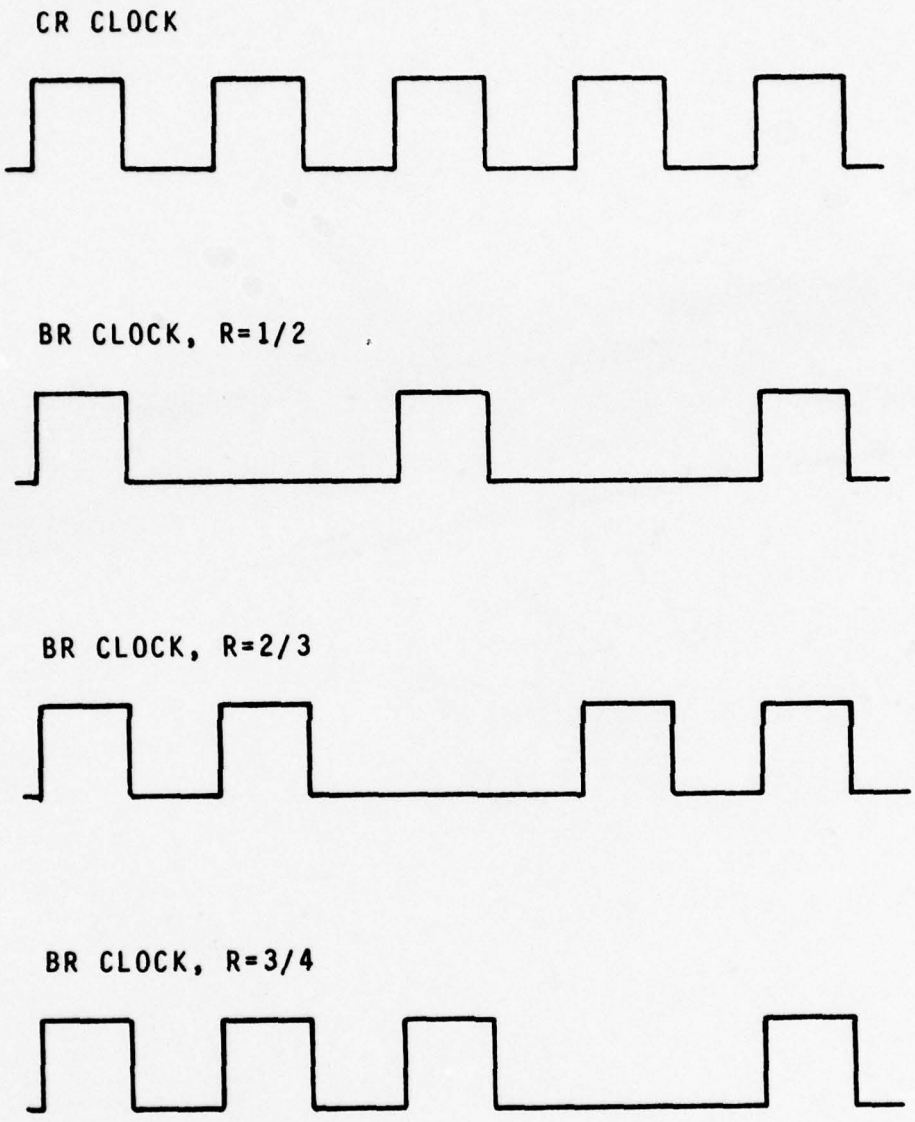

FIGURE 2.5.1-1. CLOCK RELATIONSHIPS

TABLE 2.1.7-1.

CODEC CONFIGURATION OPTIONS

Option	Choices	Means of Selection	Remarks
Differential Coding	ENABLE/DISABLE	Front panel switch	
Code	OFF, 1/2,2/3,3/4	Front panel switch	Off position bypasses convolutional encoding and decoding
Interleaver/ Deinterleaver	ENABLE/DISABLE	Front panel switch	
Data Source	INTERNAL/EXTERNAL	Front panel switch	Internal: internal PN data source and data comparator used External: external data source and data output used. Source and sink must be compatible with asymmetrical bit rate clocks.
External Blanker	ENABLE/DISABLE	Internal switch (normally DISABLE)	If enabled, externally supplied blanking signal will cause noncommittal decoder or deinterleaver inputs during blanking time.
Phase Resolve	ENABLE/DISABLE	Internal switch (normally DISABLE)	Applies only if interleaver is enabled. If enabled, 180^{o} phase ambiguity resolved by sync pattern prior to decoding.
Clock Source	INTERNAL/EXTERNAL	Internal switch (normally EXTERNAL)	Transmit side channel rate clock to or from modem. If internal, selectable symbol rates of $19200 \div 2^{n}$, n=0,1,2,3 are generated by internal clock.
Demod Data Source	ANALOG/SOFT/HARD	Rear panel switch	ANALOG - internal bit sync used SOFT - 3-bit digital (sign-magnitude format) HARD - 1-bit digital

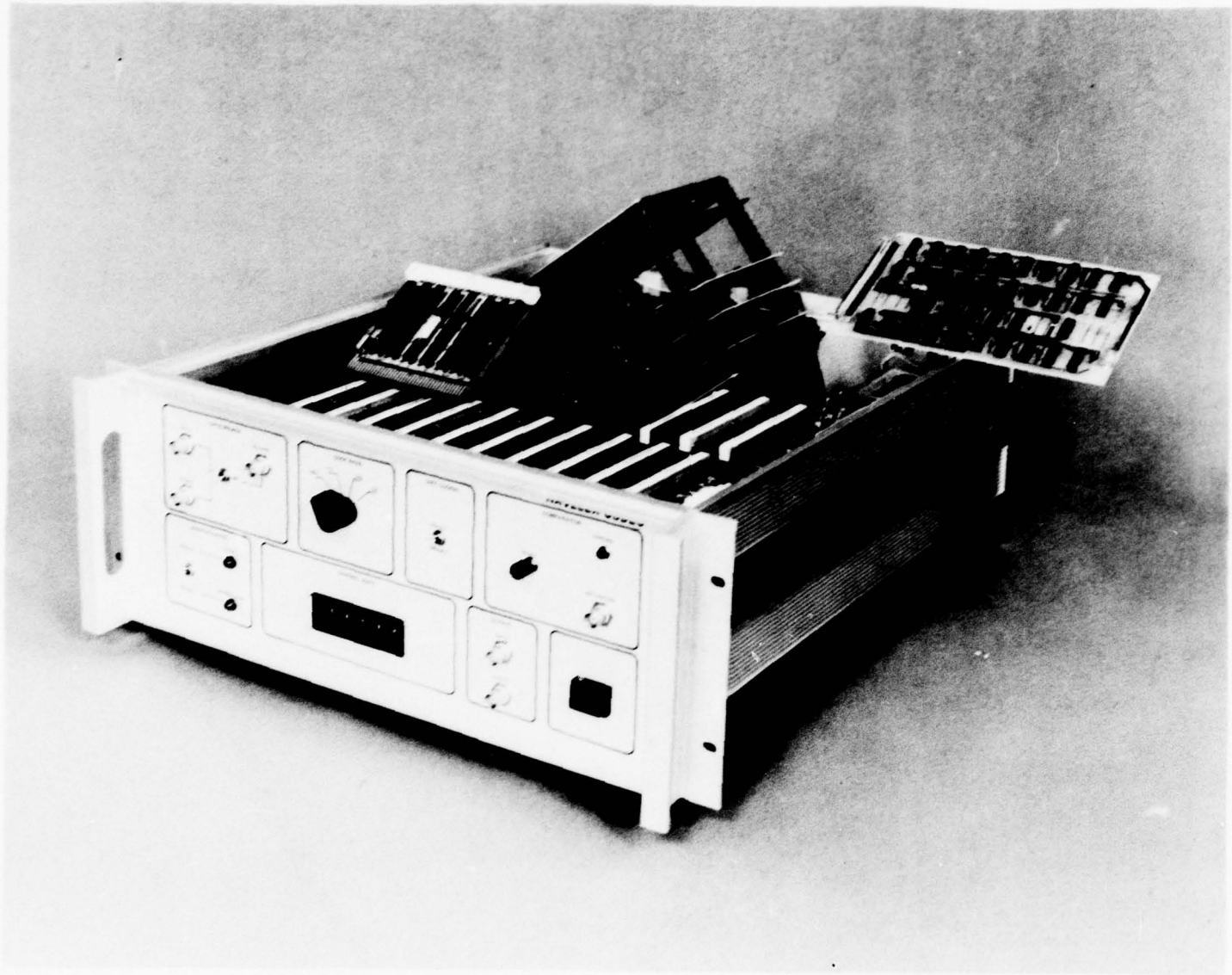

78-09886C

FIGURE 2.2-1. BREADBOARD CODEC

and five printed circuit cards comprising the bit sync, of which the card shown near the rear is typical. The bit sync cards are housed in a card rack which is hinged and can be tilted up as shown for card removal.

All interfaces to the modem are located on the rear panel.

Complete descriptions of all switches, indicators, and input/output ports, as well as complete electrical schematics, are contained in [2-2].

2.3 Baseline Performance

In order to verify performance of the bit synchronizer and encoder/decoder, performance was measured with these units alone, using an ideal PSK modulation scheme. To accomplish this, encoder output bits were used to modulate a 70 MHz carrier and wideband Gaussian noise was added. The resultant was then mixed with a correctly phased replica of the same 70 MHz LO to produce a noisy NRZ-L baseband waveform, which was input to the bit synchronizer.

Results of this test are shown in Figure 2.3-1. Note that uncoded performance tracks within 0.4 dB of theoretical performance over the entire range of interest, even to as low as 0 dB E_b/N_o. This high performance at low values of E_s/N_o is essential to achieve the full coding gain available.

Coded results are shown along with union bound predictions of performance. When the measured data is corrected for the 0.2 dB to 0.4 dB bit synchronizer degradation, agreement with the union bounds is excellent. This agreement is expected, since the union bound calculations take into account all implementation losses in the decoder.

Since the channel rate is held constant at 9600 s/s, the information rate (bit rate) for each of the cases shown is as follows:

Uncoded	9600 b/s
R=3/4	7200 b/s
R=2/3	6400 b/s
R=1/2	4800 b/s

These differences in bit rate are corrected for in Figure 2.3-1 by plotting performance versus E_b/N_o, or C/N_oR, where R is the information rate. Thus the separations between these curves and the uncoded curve represent performance enhancement relative to the fundamental parameter E_b/N_o. The actual coding gain for a fixed information rate may be slightly different because of small variations in performance with channel rate. For example, to determine coding gain with R=1/2, 4800 b/s, we should compare the R=1/2 curve of

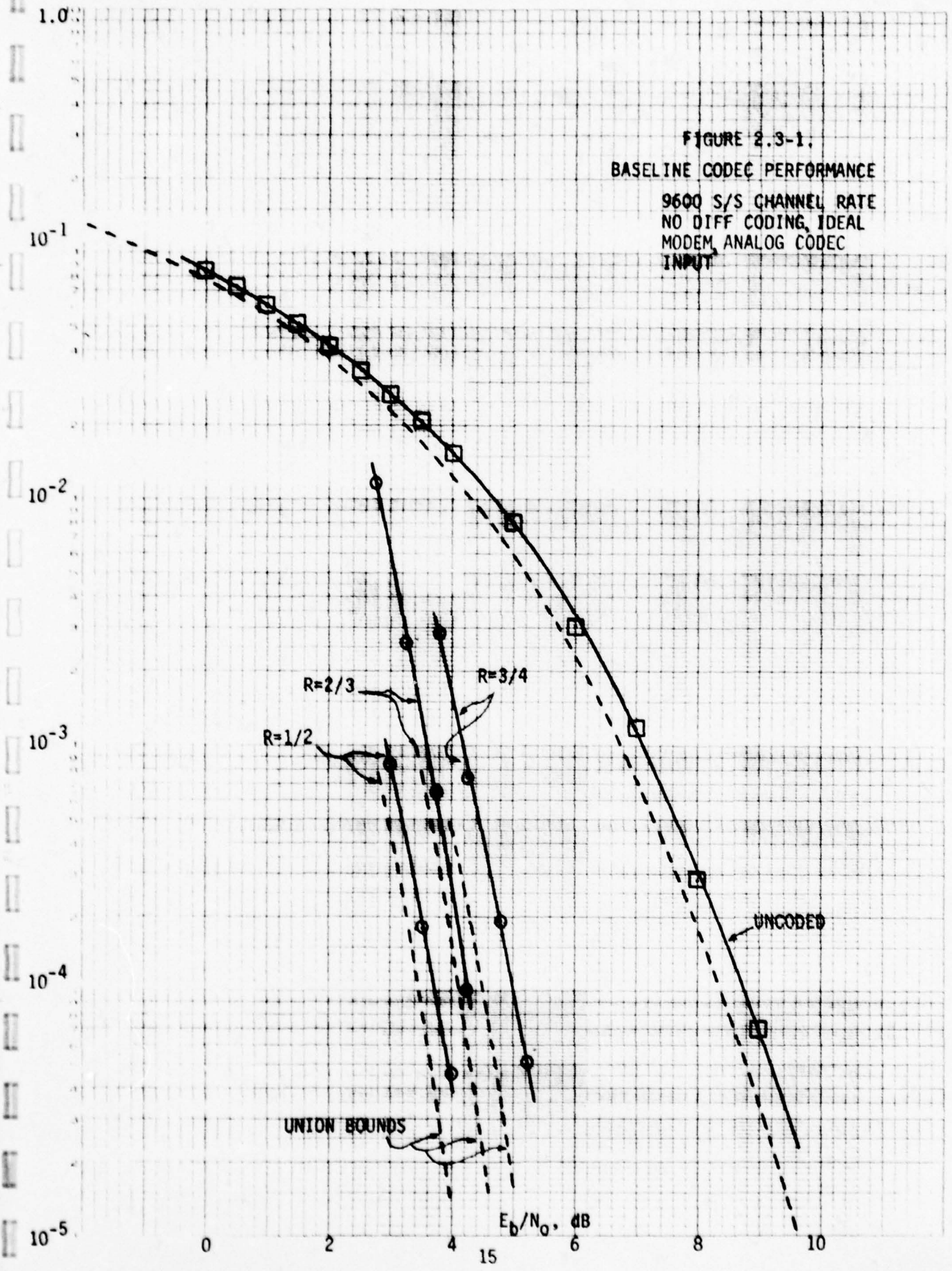

FIGURE 2.3-1.
BASELINE CODEC PERFORMANCE
9600 S/S CHANNEL RATE
NO DIFF CODING, IDEAL
MODEM, ANALOG CODEC
INPUT

Figure 2.3-1 with an uncoded curve of P_e versus E_b/N_o for 4800 b/s. This latter curve may be slightly different from the uncoded 9600 b/s curve shown in the figure.

This discrepancy is unavoidable in cases where variable code rates, but fixed channel rates are used, as is the case with most of the results to be presented in this report. It is not of serious concern, since channel rate sensitivities tend to be small. However, it should be recognized that in operating with modems capable of a discrete set of channel rates, such as the AN/WSC-3, choice of code rate has implications concerning the available information rates, as well as the required E_b/N_o. The conventional interpretation of coding gain considers information rate to be fixed, and both required E_b/N_o and channel rate to vary with choice of code rate (the classical bandwidth-power tradeoff). When the modem is the constraint, channel rate is fixed and thus required E_b/N_o and information rate vary with code rate.

In addition to the test with analog inputs, the encoder/decoder was tested with hard decision inputs by introducing statistically independent transmission errors into the encoder output sequence and routing this noisy sequence to the hard decision decoder input. Plots of decoder output rate P_e versus channel error rate p for all three code rates are shown in Figure 2.3-2. Also shown is a union bound prediction of P_e versus p for the rate -1/2 code. The performance slightly better than the union bound is not unexpected, since the union bound is an upper bound on output error rate, and includes all implementation losses in the decoder. We have not computed union bounds on hard decision performance for the other two codes, but the results of Figure 2.3-2 indicate performance on the order of 1.8 dB to 2 dB worse at $P_e=10^{-5}$ than the union bound prediction for soft decisions, which is the expected behavior.

Since performance of the decoder alone is insensitive to channel rate (up to a maximum determined by the logic speed), the hard decision data was taken at a channel rate of 48 ks/s. This accounts for the relative ease of obtaining valid data points in the neighborhood of $P_e=10^{-5}$.

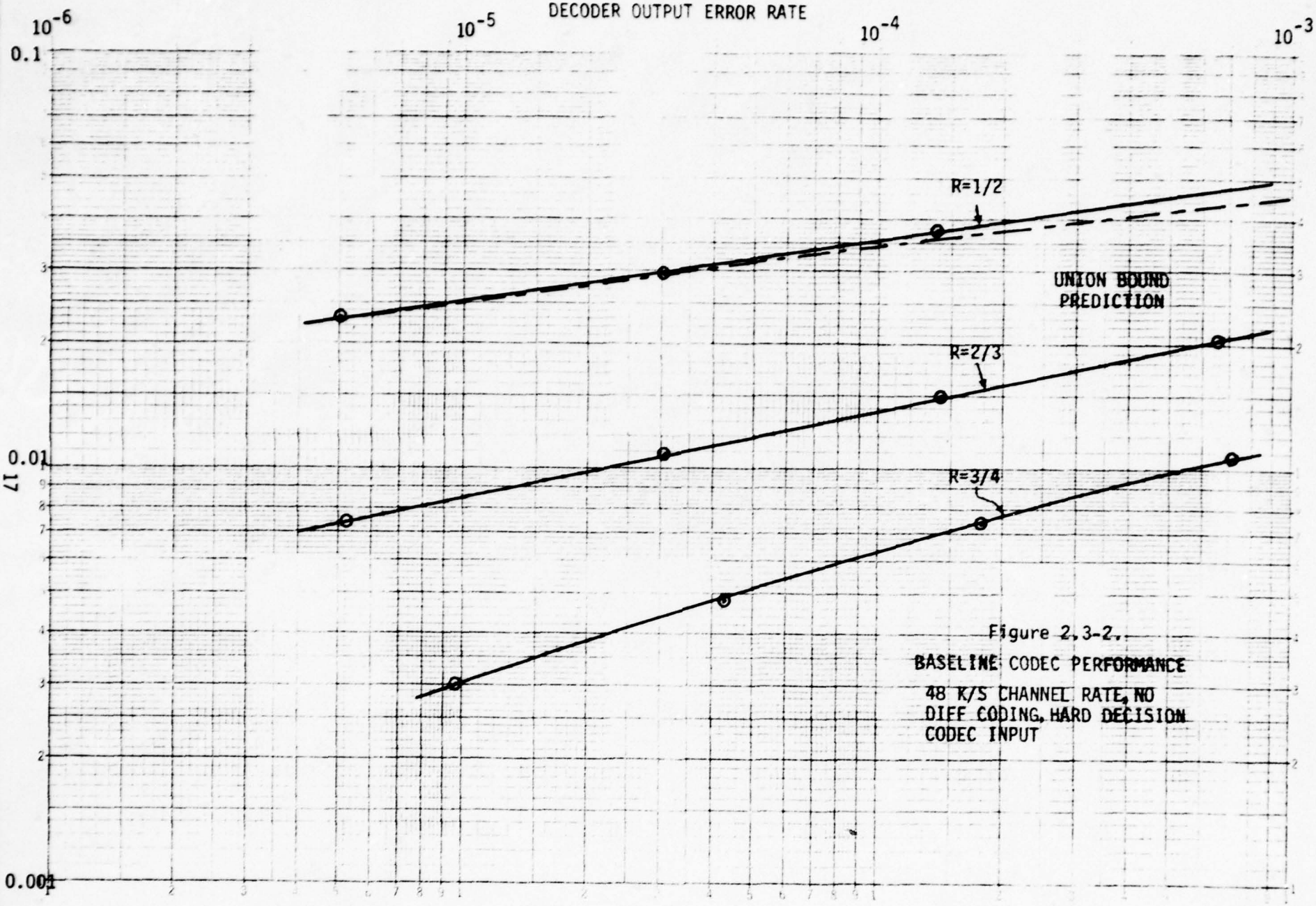

Figure 2.3-2.
BASELINE CODEC PERFORMANCE
48 K/S CHANNEL RATE, NO DIFF CODING, HARD DECISION CODEC INPUT

REFERENCES

2-1 Coding for Navy UHF Satellite Communications (Phase I), Final Report on Contract No. N00039-76-C-0384, Harris Corporation, Electronic Systems Division, April 1977.

2-2 Coding for Navy UHF Satellite Communications (Phase II), Codec Operating Guide, Harris Corporation, Government Communication Systems Division, August 1978.

2-3 J. B. Cain, G. C. Clark, Jr., and J. M. Geist, "Punctured R=(n-1)/n Convolutional Codes and Simplified Maximum Likelihood Decoding," IEEE Trans. Information Theory, to appear January 1979.

3.0 MONTEREY EXPERIMENTAL PROGRAM

The primary objective of Phase II of this study was to verify through experiment the analytical predictions of coded system performance which were obtained during Phase I. This objective was satisfied by a comprehensive testing program using the breadboard codec developed on this program and the RFI simulator test bed previously developed by the Naval Postgraduate School. This RFI simulator, the capabilities of which are discussed fully in [3-1], was assembled after an extensive study of the shipboard RFI environment [3-2], and provides an excellent test fixture for controlled, repeatable testing in a realistically modeled environment.

This section discusses the tests and results obtained with the RFI simulator, as well as results obtained during a four hour FLTSATCOM access, also using Naval Postgraduate School transmitting and receiving equipment.

It is a pleasure to acknowledge here the substantial contributions of Professor John E. Ohlson and his associates at NAVPGSCOL to the success of our testing program at Monterey. These contributions include not only the extensive previous research and engineering efforts which led to development of their tests facilities, but also a considerable amount of direct assistance and many valuable suggestions and comments during our use of these facilities.

3.1 Background and Narrative

The Monterey testing program was originally conceived to be a two-week program consisting of a series of tests designed to verify predicted performance against thermal noise and burst RFI, and to investigate performance against other forms of RFI for which analytical predictions of performance were not possible.

Testing began at NAVPGSCOL on 15 May 1978. Two problems were encountered in the codec hardware during testing. One problem occurred in the deinterleaver, and was diagnosed and fully repaired at Monterey. The other problem was of an intermittent nature and occurred in the bit synchronizer. We now believe that the bit sync difficulties were a combination of thermal problems on one card and a marginal timing condition on another card due to a mix of logic families. Ultimately, consistent, reliable performance was achieved using a particular combination of cards including some spare cards we had available.

Because of the time lost in correcting these hardware problems, the actual testing carried out in the two week period 15 May - 26 May 1978 was less exhaustive than originally planned. However, valuable data was collected on achievable coding gain and burst RFI protection with all code rates, with and without interleaving.

The breadboard codec was returned to the Harris plant at the end of this testing period. Questionable parts were changed out and the codec was then operated continuously for several days without difficulty.

Since no further hardware problems occurred in this in-plant testing, the codec was taken again to NAVPGSCOL for an additional week of testing 26-30 June 1978. During this week additional test data was obtained with the RFI simulator, and some testing was conducted on an actual satellite link using FLTSATCOM Channel 4. The codec performed properly during this week of testing and was left at NAVPGSCOL at the conclusion of the testing program.

The following paragraphs discuss the specific tests carried out at Monterey and the results obtained. Complete descriptions, procedures, and test data are recorded in [3-3].

3.2 RFI-Simulator Tests

The test setup for these tests is generally as illustrated in Figure 3.2-1. The PSK modulator, synthesizer, power divider, combining unit, RFI sources, and attenuators are physically part of the RFI simulator equipment. The AM-6691 preamplifier is the preamplifier used in a surface ship installation, and is housed in a deck box along with a diplexer. The noise figure of this amplifier has been accurately determined, and the attenuation along the path from the power divider to the preamplifier input is precisely known. Thus by varying the level of the PSK demodulator output and noting the power meter reading, C/N_0 can be set accurately. (The gain of the preamplifier isolates the noise figure of the AN/WSC-3 from the system noise figure.)

As discussed in Section 2.1.4, connection to the AN/WSC-3 is made at the Costas loop I-channel within the PSK demodulator, identified as "I&D Data" in the AN/WSC-3 documentation [3-4]. This signal is the NRZ baseband, which is input to the codec bit sync. Physically, the connection is accomplished by connecting the center and outer conductors of a length of coaxial cable to test point A1J6 on module A1A7 and to ground, respectively. The cable is routed through an

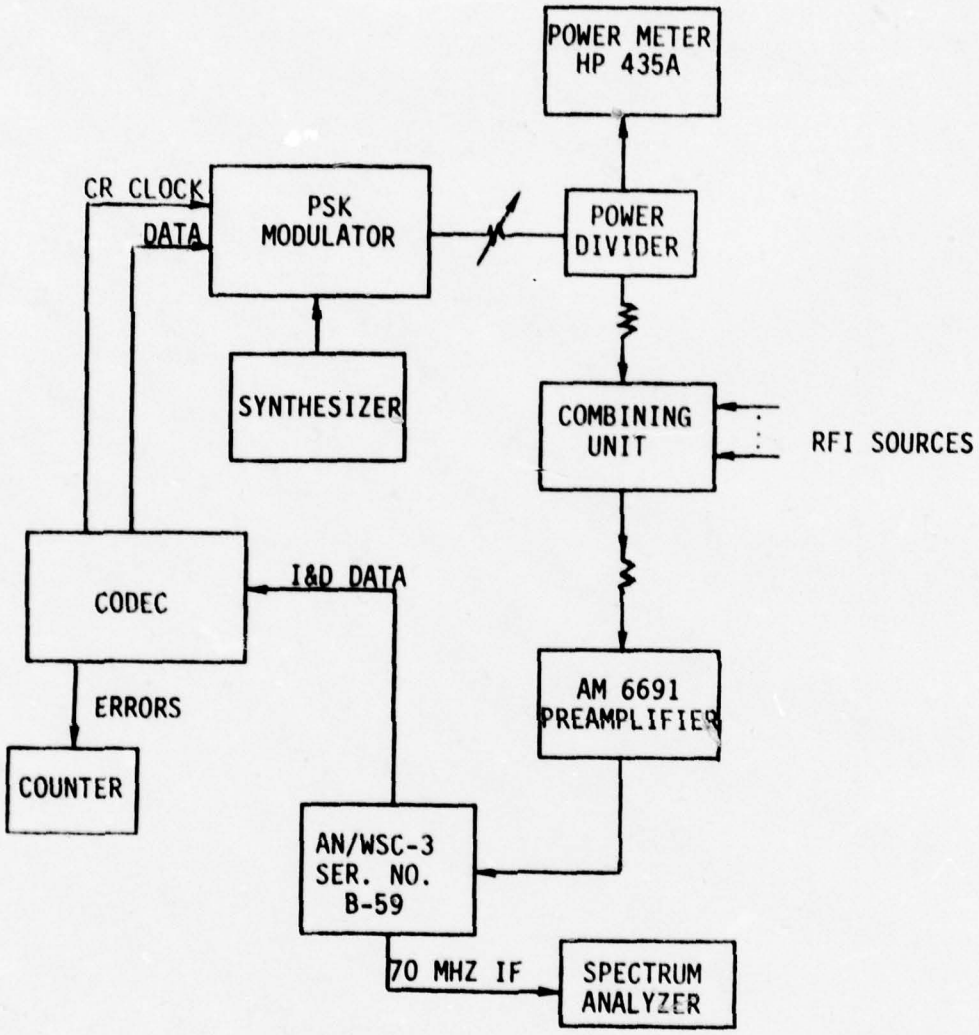

FIGURE 3.2-1. SIMULATOR TEST CONFIGURATION

existing hole in the rear of the AN/WSC-3 cabinet, so that EMI integrity is not degraded. We have found that this means of accessing the baseband is satisfactory for test purposes.

All data reported here was taken using the internal PN data source and comparator in the codec. Unless specifically noted otherwise, all data shown is without differential coding, whether convolutional coding is used or not. Under normal conditions, performance with differential coding can be inferred with reasonable accuracy from performance without. Generally, we preferred to take data without differential coding, since its use can disguise the occurrence of carrier cycle slips in the modem, and we wanted to be aware of their occurrence. Exceptions to this general procedure include some cases in which we specifically desired to accurately model an actual communication link (in which differential coding normally would be used), and some cases in which cycle slipping was so frequent that it was impossible to take data without using differential coding. In all cases in which differential coding is used, it is used prior to any convolutional coding; i.e., in the codec rather than in the PSK modulator.

Except where specifically noted otherwise, all data was taken with a channel rate of 9600 s/s. Because of the relatively low information rates used, unreasonably long times would be required to measure error rates in the range of 10^{-5} reliably. Thus most of the data to be presented is valid at error rates on the order of 10^{-4} and higher.

Excellent repeatability was obtained with the test setup of Figure 3.2-1, even between data taken on the two different visits to Monterey. For this reason, the test results presented below are given in a logical order, without regard to the actual sequence of tests performed. However, the actual dates of the tests are indicated.

3.2.1 Monterey Baseline (27 June 1978)

Baseline performance with and without coding in the presence of thermal noise only was measured for comparison with the baseline shown in Figure 2.3-1. The predominant source of any differences between these two baselines is loss in the RF and modem equipment, which are ideal in the baseline of Figure 2.3-1. (Although both test setups were carefully calibrated, there may also be small calibration differences between the two.)

Figure 3.2.1-1 illustrates uncoded performance, and includes the uncoded baseline data of Figure 2.3-1. This data shows an increased degradation from theory of approximately 1.0 dB over the degradation due to bit sync above.

Figures 3.2.1-2, -3, and -4 show measured performance for rate -3/4, -2/3, and -1/2 codes, respectively, for both the Monterey baseline and the ideal modem baseline. Note that the additional degradation to coded performance is greater than to uncoded performance, increases as code rate decreases, and for each code rate, increases as E_b/N_o decreases. This excess degradation is primarily attributable to phase jitter in the carrier tracking loop in the AN/WSC-3 PSK demodulator, which increases as E_s/N_o decreases, and which generally has a more serious effect on coded performance than on uncoded performance.

3.2.2 Performance With Burst RFI (24-25 May 1978)

The worst-case interferer among the pulsed RFI sources of concern has 200 μsec pulse width and a duty cycle of approximately 5%. At 9600 s/s channel rate, this pulse is slightly less than two symbols long. However, at the 19.2 ks/s channel rate envisioned for future modems, the RFI pulse is nearly four symbols long, and including the effect of 50 μsec pulse extension in the blanker, the pulse is approximately five symbols long. Since the maximum channel rate with the current model AN/WSC-3 is 9600 s/s, we simulated the worst-case effect at 19.2 ks/s by using 9600 s/s channel rate and doubling the length of the RFI burst.

Two approaches were employed to evaluate performance in the burst RFI environment. In the first method, a high-power Gaussian noise pulsed signal of specified pulse width and PRF was inserted into the combining unit. As shown by Ohlson et. al. [3-2, 3-5], this is a reasonable model of the effects of these pulsed RFI sources. In this case, the AN/WSC-3 blanking circuit is triggered, and under ideal operation would suppress the NRZ baseband voltage for the duration of the pulse so that the 3-bit soft decisions made by the bit synchronizer would contain 00 magnitude bits. These soft decisions are handled as noncommittal or blanked symbols by the decoder.

The second method, which was intended to eliminate any non-ideal performance of the blanking circuit, uses the external blanking input to the codec and causes blanking at the decoder or deinterleaver input by setting the magnitude bits to 00 regardless of the bit sync output. In this method, no RFI

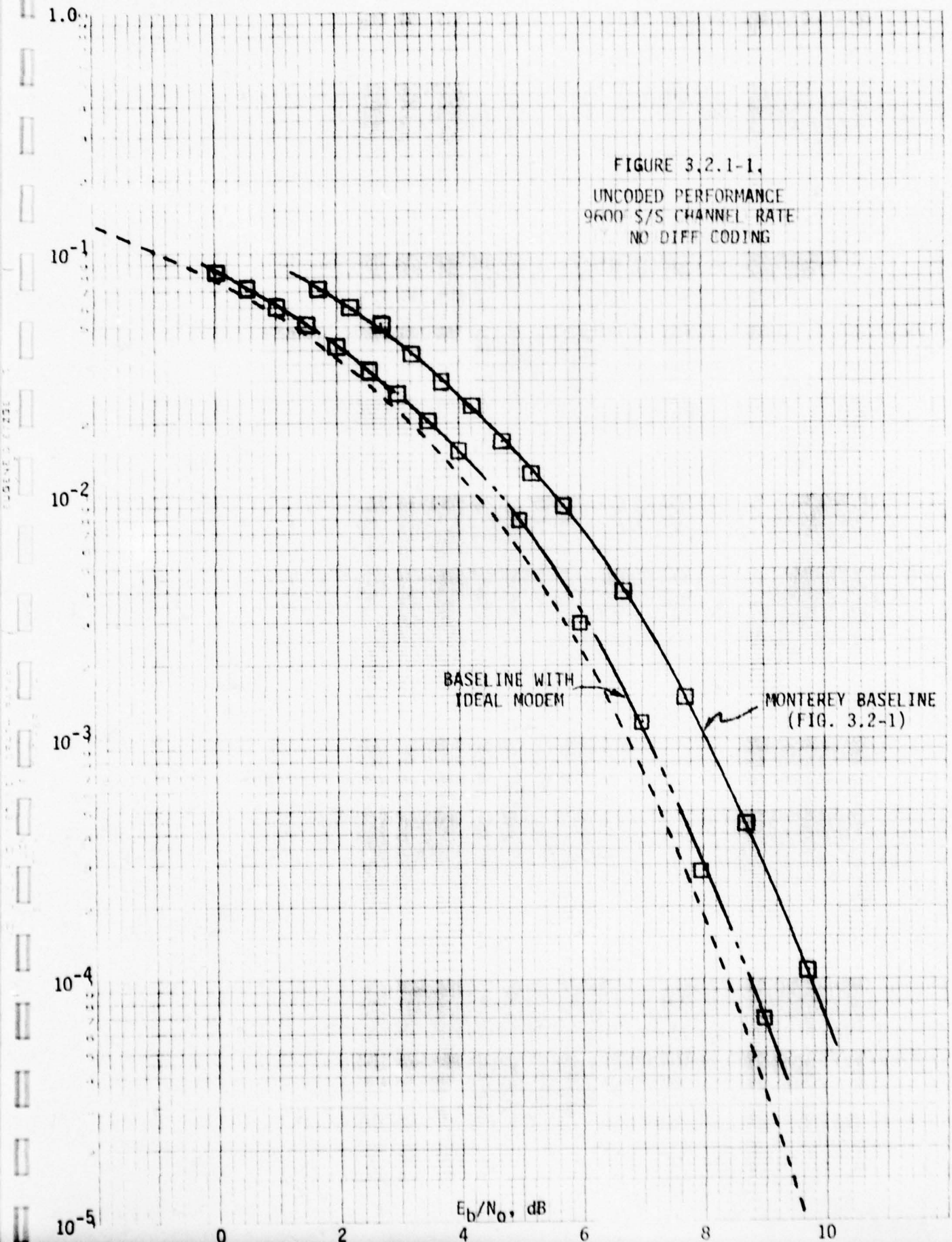

FIGURE 3.2.1-1.
UNCODED PERFORMANCE
9600 S/S CHANNEL RATE
NO DIFF CODING

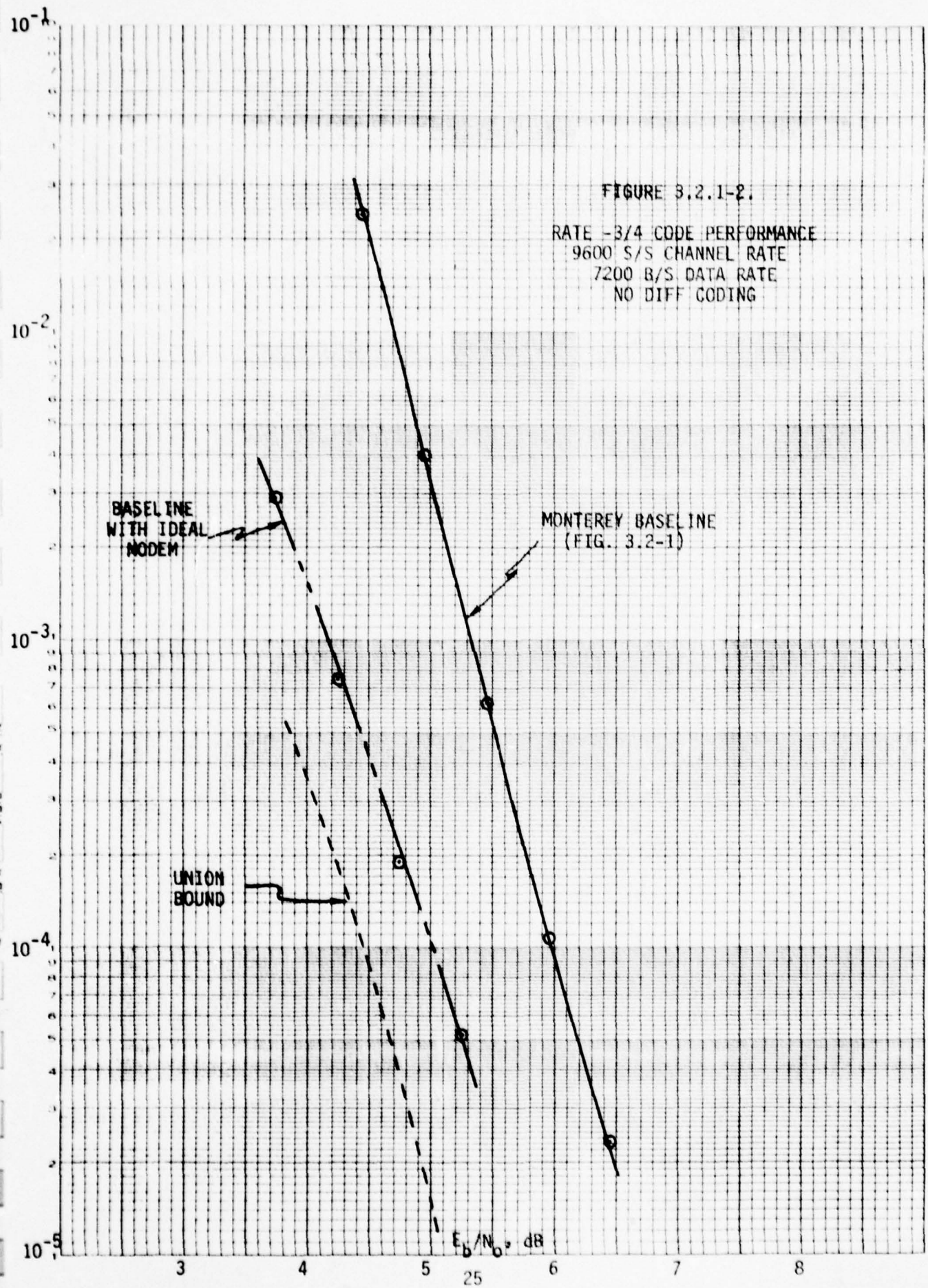

FIGURE 3.2.1-2.

RATE -3/4 CODE PERFORMANCE
9600 S/S CHANNEL RATE
7200 B/S DATA RATE
NO DIFF CODING

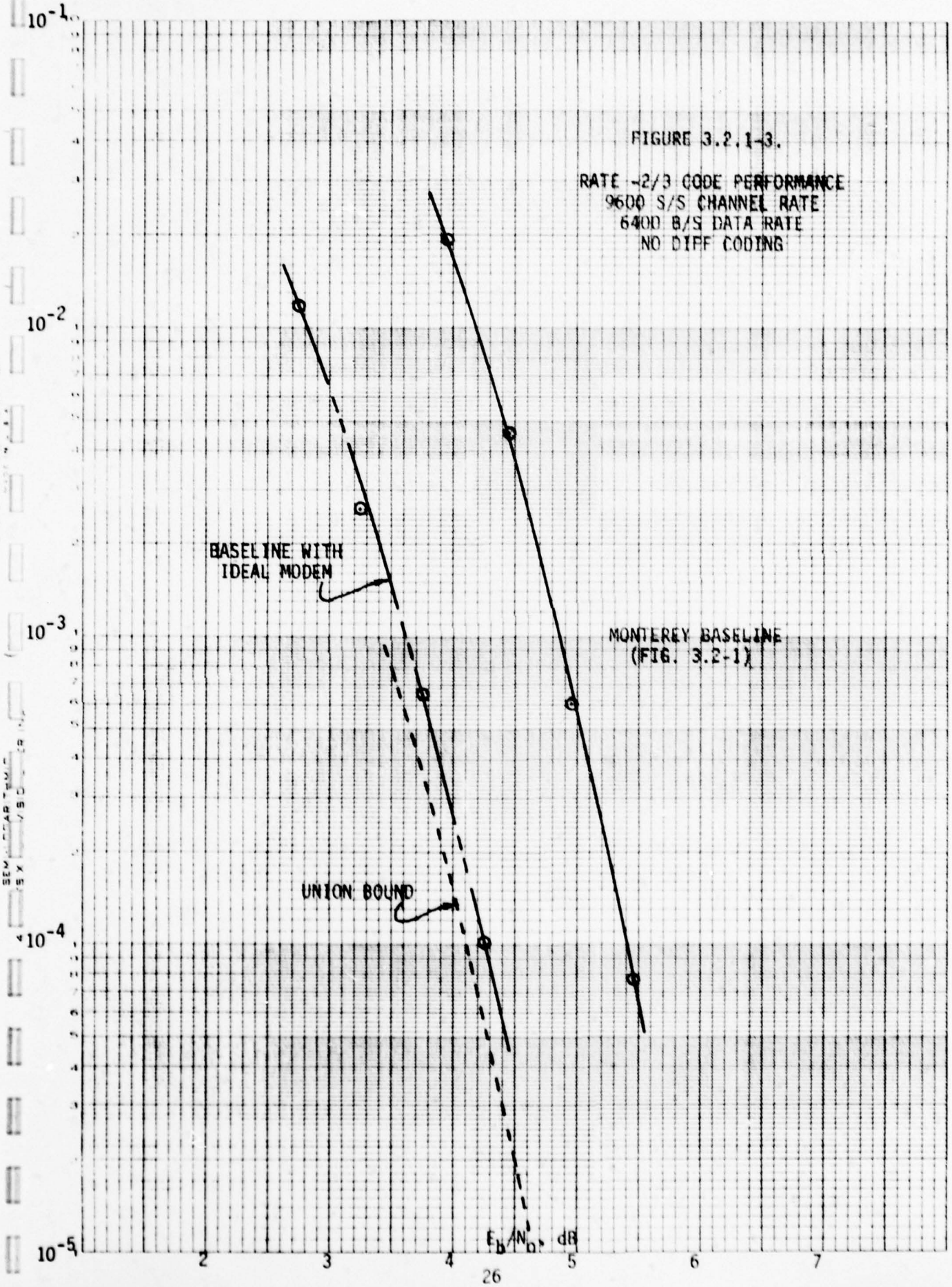

FIGURE 3.2.1-3.

RATE -2/3 CODE PERFORMANCE
9600 S/S CHANNEL RATE
6400 B/S DATA RATE
NO DIFF CODING

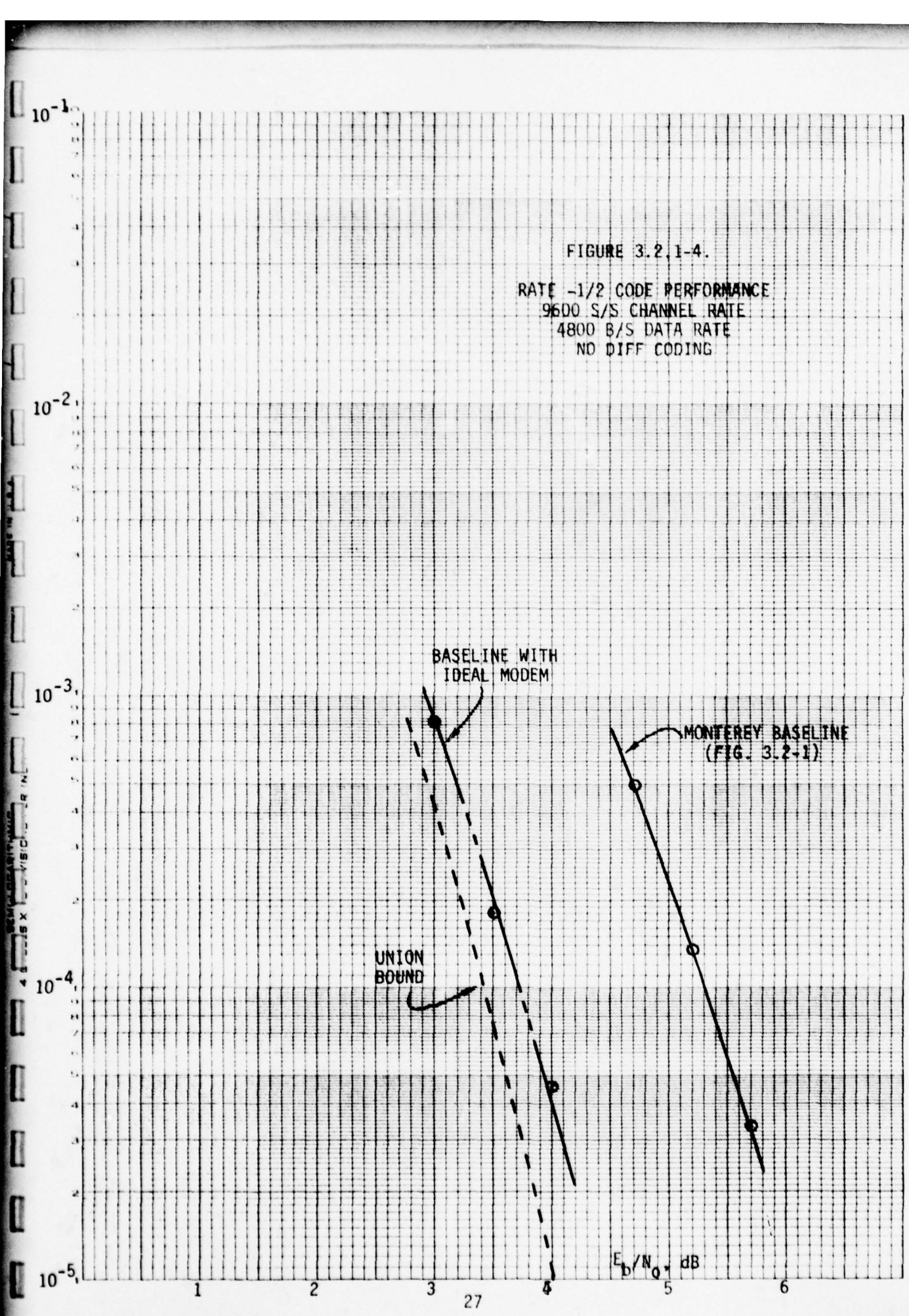

FIGURE 3.2.1-4.

RATE -1/2 CODE PERFORMANCE
9600 S/S CHANNEL RATE
4800 B/S DATA RATE
NO DIFF CODING

is actually input to the combining unit. The purpose of this method is simply to determine performance in the presence of burst erasures under ideal circumstances, for verification of analytically predicted performance.

Test data was taken with all three code rates, with and without interleaving. With the ideal blanking method, the pulse width and PRF was adjusted to blank exactly five of every 100 symbols, for a 5% duty cycle. With the real RFI added in at the combining unit, pulse width was set to 400 μsec and PRF to 125 Hz, for a nominal 5% duty cycle, although pulse extension increases the effective duty cycle. Data was taken for a single such RFI source as well as for two asynchronous sources, yielding a nominal 10% duty cycle. The peak noise level of these pulses was set approximately 30 dB above the thermal noise flow, which was verified to be sufficient to trigger the blanker.

The test results are illustrated in Figures 3.2.2-1, -2, and -3, along with a baseline curve for each code taken without RFI. (These baselines are consistent with, but not identical to, the baselines presented in Section 3.2.1.) The performance with ideal blanking and interleaving is consistent with the predictions from Phase I [3-6]. However, this data cannot be compared directly with the data using the AN/WSC-3 blanker, for several reasons: the effective duty cycles are different; the actual RFI causes fractional symbol blanking, while the ideal blanks on a total symbol basis; and there are non-ideal effects in the AN/WSC-3 blanker.

A surprising conclusion from this data is that interleaving contributes negligible performance improvement, and may actually degrade performance. For short bursts, it is clear that interleaving is not required, but the bursts of concern here are five symbols long, and our intuition had convinced us that interleaving would provide substantial performance improvement. Since it is difficult and time consuming to correctly calculate the required weight structures which would be necessary to evaluate union bounds on performance degradation due to bursts of this length, we did not do so in Phase I. However, Trumpis and McAdam [3-7] have evaluated performance by an approximate technique, and for bursts of length 5, their predictions of degradation are even more pessimistic. In view of these results and our intuitive feelings about the sensitivity of Viterbi decoders to burst events, we found the measured performance very surprising. After obtaining these test results, we did carry out the appropriate weight search and union bound calculations and confirmed that the measured performance is in accordance with what would be predicted (See Appendix A).

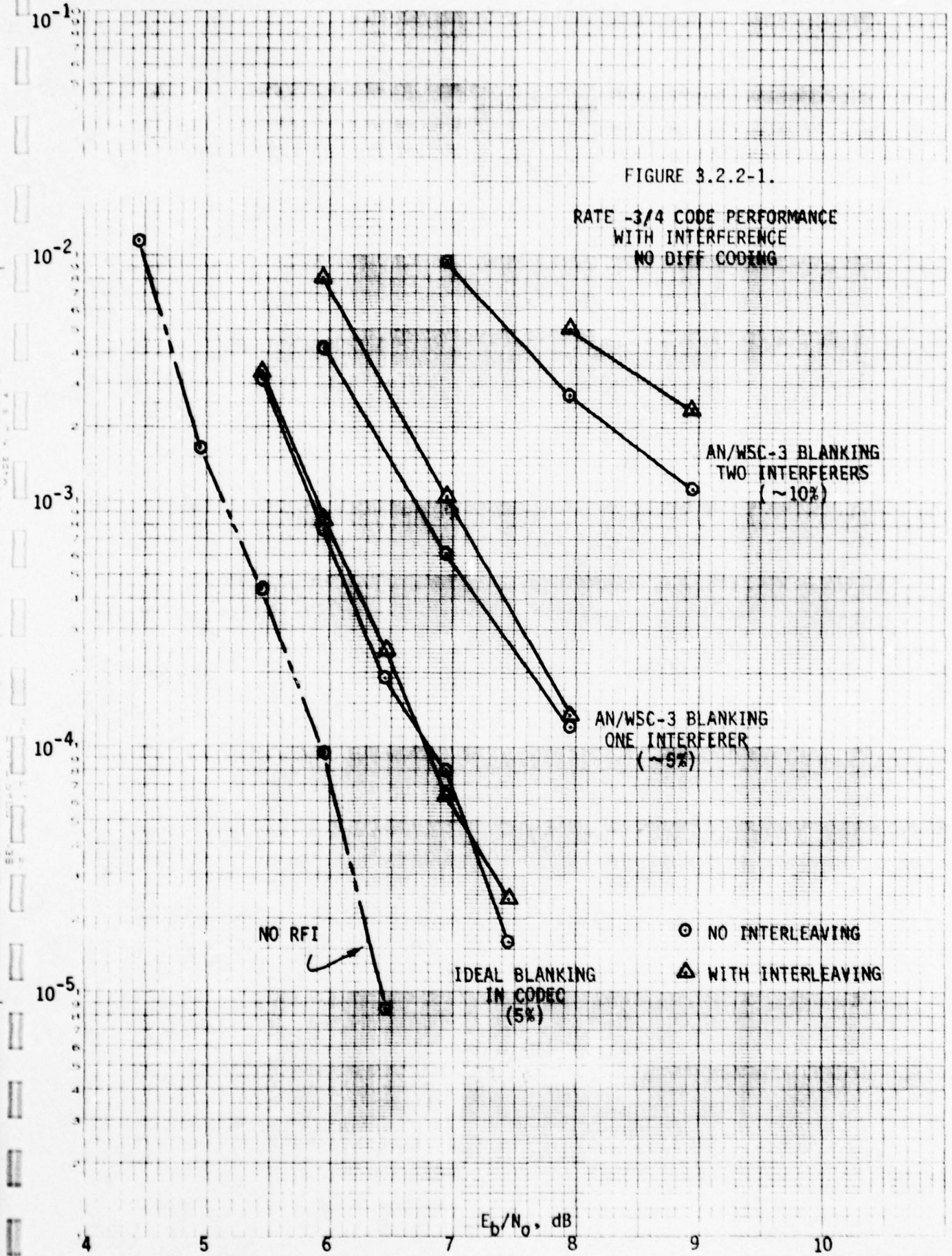

FIGURE 3.2.2-1.

RATE -3/4 CODE PERFORMANCE
WITH INTERFERENCE
NO DIFF CODING

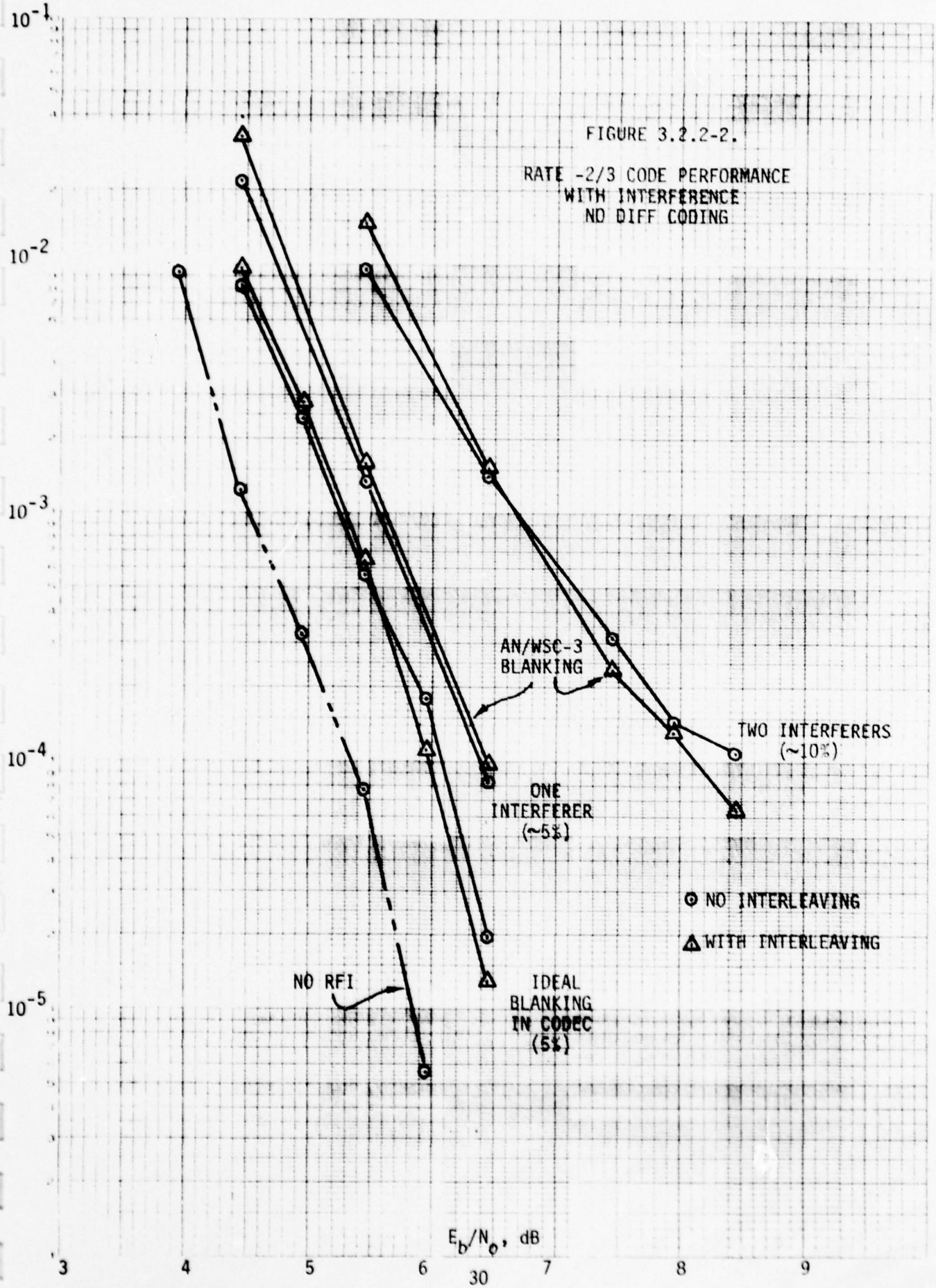

FIGURE 3.2.2-2.

RATE -2/3 CODE PERFORMANCE WITH INTERFERENCE ND DIFF CODING

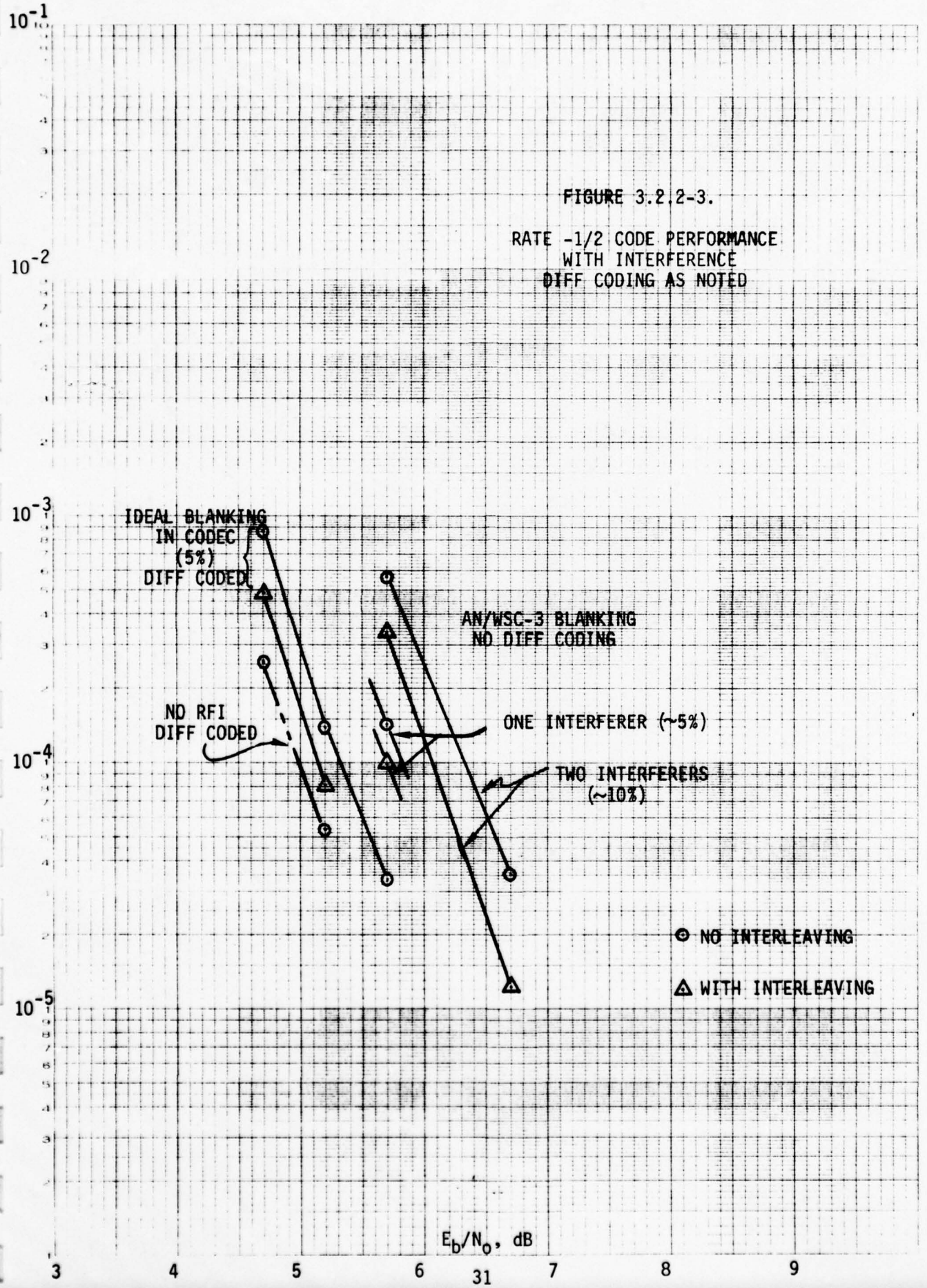

FIGURE 3.2.2-3.

RATE -1/2 CODE PERFORMANCE
WITH INTERFERENCE
DIFF CODING AS NOTED

These results indicate that for bursts of the lengths of concern here, interleaving is not required.

3.2.3 Sensitivity to Burst Length (27 June 1978)

This test was carried out in order to further investigate performance with and without interleaving, as a function of the length of the erasure burst. In order to eliminate blanker effects, erasure bursts were inserted at the decoder (or deinterleaver) input using the external blanking input, with no RFI actually present at RF. Only the rate -3/4 code was considered, and only at a single value of E_b/N_o=5.9 dB, which yielded output error rate of $P_e \approx 10^{-4}$ in the absence of erasures. The increase in error rate was evaluated as a function of erasure burst length in symbols.

Two PRF conditions were used. In the first, PRF was reduced as pulse width was increased, to maintain a constant erasure duty cycle of 5%. In the second, PRF was held constant at 96 Hz, corresponding to a period of 100 symbols, so that duty cycle increases linearly with burst length.

Results are as illustrated in Figure 3.2.3-1. Note that in the case of constant duty cycle, performance is relatively constant independent of burst length when interleaving is used (as it should be), but that performance may be better or worse without interleaving, depending on burst length. For bursts on the order of six symbols or longer it is desirable to interleave. This crossover point varies with the code rate. The test data reported in Section 3.2.2 shows that with rate -1/2, performance is better with interleaving at burst length 5, so that the crossover is at less than 5 symbols. There may also be some sensitivity to signal-to-noise ratio in the location of this crossover point.

When the PRF is fixed and duty cycle increases with symbol rate, the performance is seen to be uniformly superior when no interleaving is used.

Since this experiment was ancillary to the main objective of testing, time constraints did not justify more detailed testing. However, the behavior noted here is interesting and merits further analytical or experimental investigation.

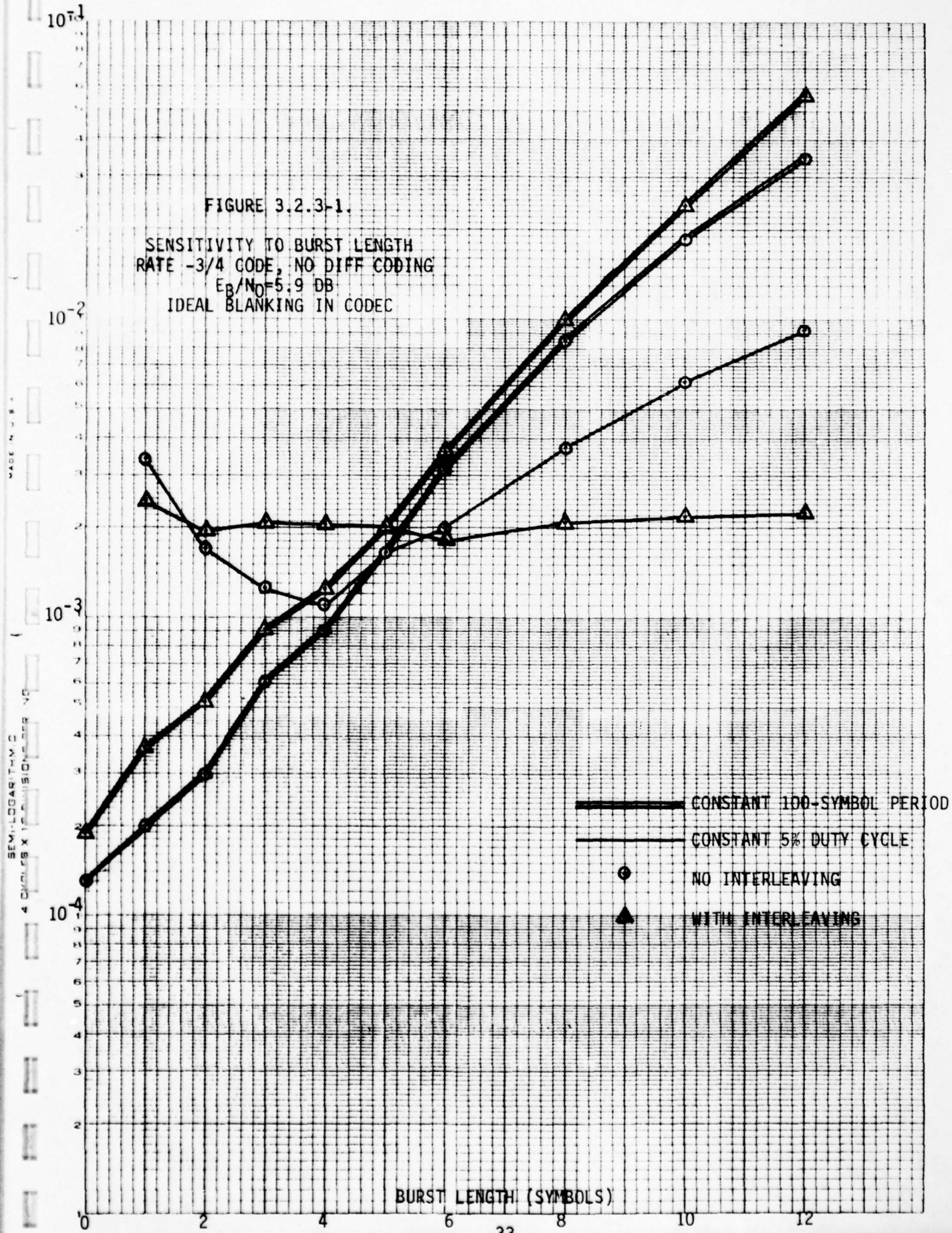

FIGURE 3.2.3-1.

SENSITIVITY TO BURST LENGTH
RATE -3/4 CODE, NO DIFF CODING
E_B/N_O=5.9 DB
IDEAL BLANKING IN CODEC

3.2.4 Sensitivity to RFI Level (28 June 1978)

The AN/WSC-3 blanking circuitry relies on the RFI pulse power levels being large in comparison with the desired signal plus noise in the blanking bandwidth, so that rapid increase in power can be used as the criterion for blanking. For RFI levels too small (but still in excess of signal plus noise), the blanking threshold may not be exceeded, and all RFI effects passed along to the demodulator and decoder. At the other extreme, for very high power RFI pulses, there are apparent ringing effects which reduce the effectiveness of the blanking circuit. Thus the performance is at least to some extent a function of RFI pulse level when the AN/WSC-3 blanking circuit is used to blank the pulses. This behavior has also been noted by Carlson and Ohlson [3-5] for uncoded data.

This test was intended to evaluate the sensitivity of performance to RFI level variation with coded data. As in the previous test, only the rate -3/4 code was used, and only at a single E_b/N_o, namely 6.9 dB, which is sufficient to achieve an error rate less than 10^{-5} in the absence of RFI. An RFI pulse width of 450 μsec and 125 Hz PRF was employed.

Figure 3.2.4-1 shows error rate as a function of excess noise level during the pulse, with and without interleaving. Excess noise level of 7 dB was measured using a spectrum analyzer on the AN/WSC-3 70 MHz IF output, detuned from the signal frequency, and was varied using non-precision attenuators. (Excess noise level could not be measured with the spectrum analyzer over the entire range because of saturation in an amplifier used in front of the spectrum analyzer.) Thus there is some inaccuracy in the abcissas of the points in Figure 3.2.4-1.

The effect of varying RFI level on blanker performance is illustrated by the oscilloscope photographs of Figure 3.2.4-2. In each photograph, the upper trace is the gate which turns on the RFI pulse and the lower trace is the NRZ baseband waveform delivered to the codec. Horizontal scale is 100 μsec per division. (The camera exposure time is not constant for all four exposures, so the number of sweeps in the photographs is not the same.) In exposure (a), the noise level is 7 dB higher during the pulse than in the absence of the pulse, which is insufficient to consistently trigger the blanker, so there is considerable activity in the baseband signal during the pulse time. In (b), excess RFI is 17 dB above N_o, and the blanking circuit functions properly. In (c), the excess RFI is 37 dB. In (d), the excess RFI is 49 dB, and blanking is incomplete. Cases (b)

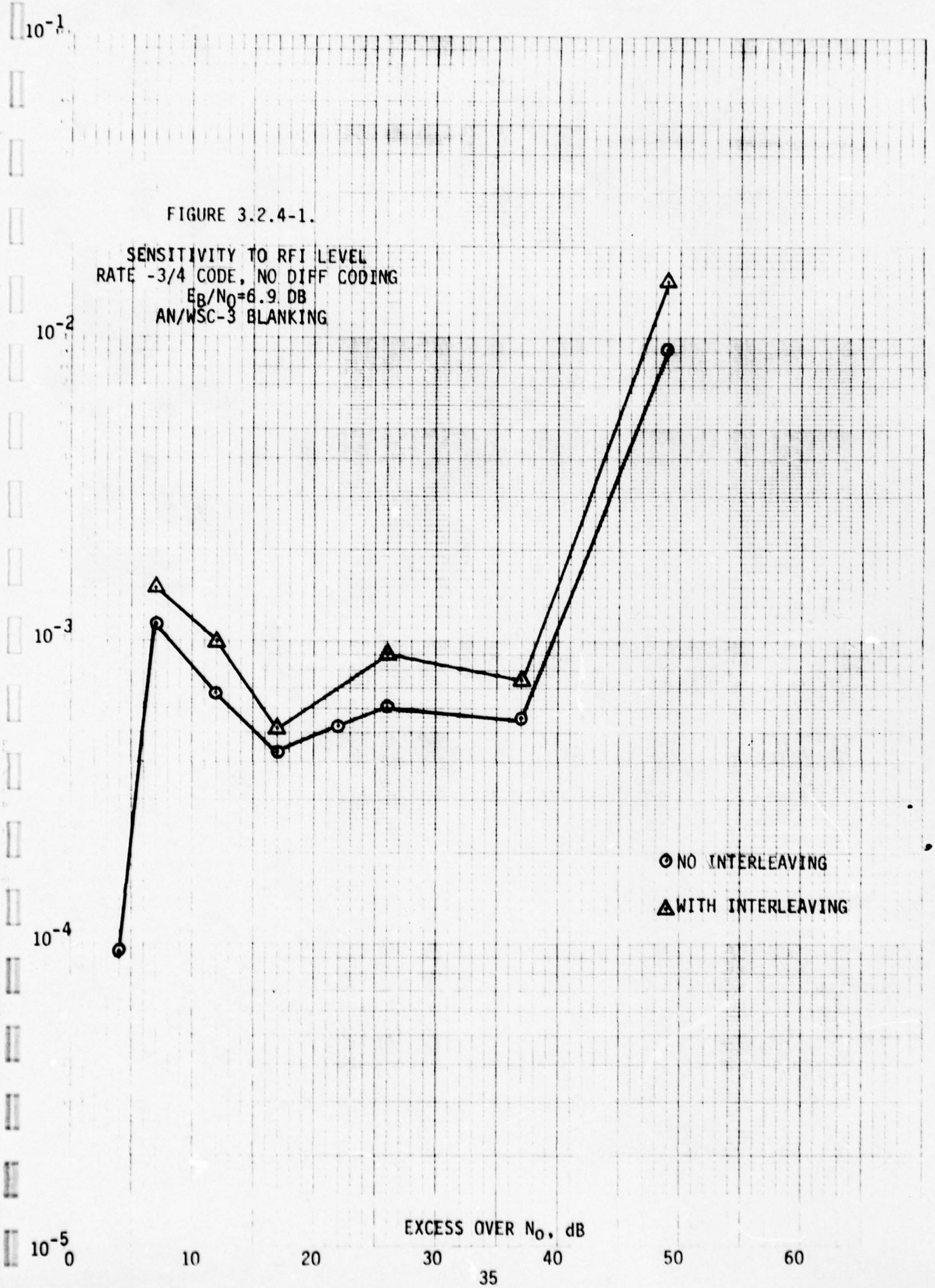

FIGURE 3.2.4-1.

SENSITIVITY TO RFI LEVEL
RATE -3/4 CODE, NO DIFF CODING
E_B/N_O=6.9 DB
AN/WSC-3 BLANKING

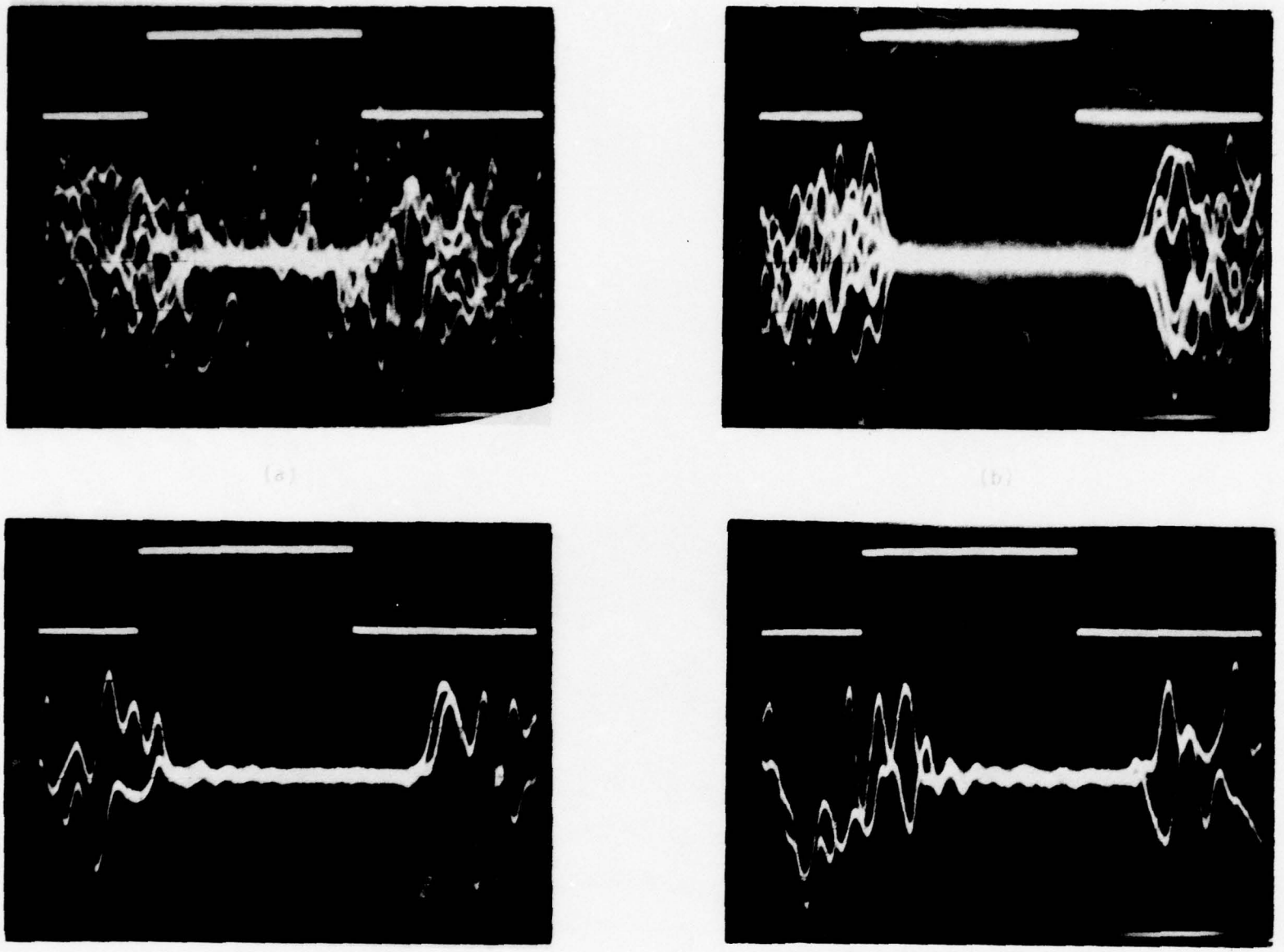

FIGURE 3.2.4-2. BASEBAND NRZ WAVEFORM DURING BLANKING

and (c), in which the blanking circuit performs properly, are in the range of minimum error rate in Figure 3.2.4-1, while in (a) and (d), error rate is higher because of the incompleteness of the blanking.

The operation of the blanking circuit is controllable to some extent by setting the blanking threshold. Appendix B contains some analysis of expected performance as a function of blanker threshold for a simplistic, but reasonable, model of the blanking process.

3.2.5 Coding Gain For Underprivileged Terminals (26 May 1978)

One of the most important potential applications for coding is to provide coding gain, i.e., additional E_b/N_o margin, in links to underprivileged terminals such as aircraft and submarines. These links currently operate at 2400 b/s information rate, but the baseband equipments have the capacity to increase to 4800 b/s. In these links, RFI is not normally a problem, but the poor G/T of the terminals jeopardizes successful data transmission on the downlink from the satellite to the terminal, and makes coding gain desirable.

The purpose of this test was to evaluate the amount of actual coding gain available at 2400 b/s and 4800 b/s information rate using the AN/WSC-3 receiver and soft decision decoding. (Since aircraft do not use AN/WSC-3 transceivers, the results do not directly apply to these links, but they are directly applicable to the submarine link.) The only code rate consistent with these data rates and AN/WSC-3 channel rates is rate -1/2, so only this code was used. In addition, all data taken used differential coding, since this is the normal transmission mode currently used, and since with rate -1/2 coding the occurrence of cycle slips in the demodulator is so frequent that it is difficult to take data without differential coding. (This general problem is discussed further in Section 4.1.)

Figure 3.2.5-1 shows BER performance for 4800 b/s information rate versus E_b/N_o. The coded data has a channel rate of 9600 s/s, so that the demodulator and bit sync are tuned to 9600 s/s. However, E_b/N_o is signal-to-noise ratio in the data rate bandwidth of 4800 Hz, so comparison between the two curves is fair. The codec bit sync is used in the uncoded as well as the coded results.

Figure 3.2.5-2 illustrates the same data for 2400 b/s. Note that the available coding gain in this case is significantly reduced from that shown

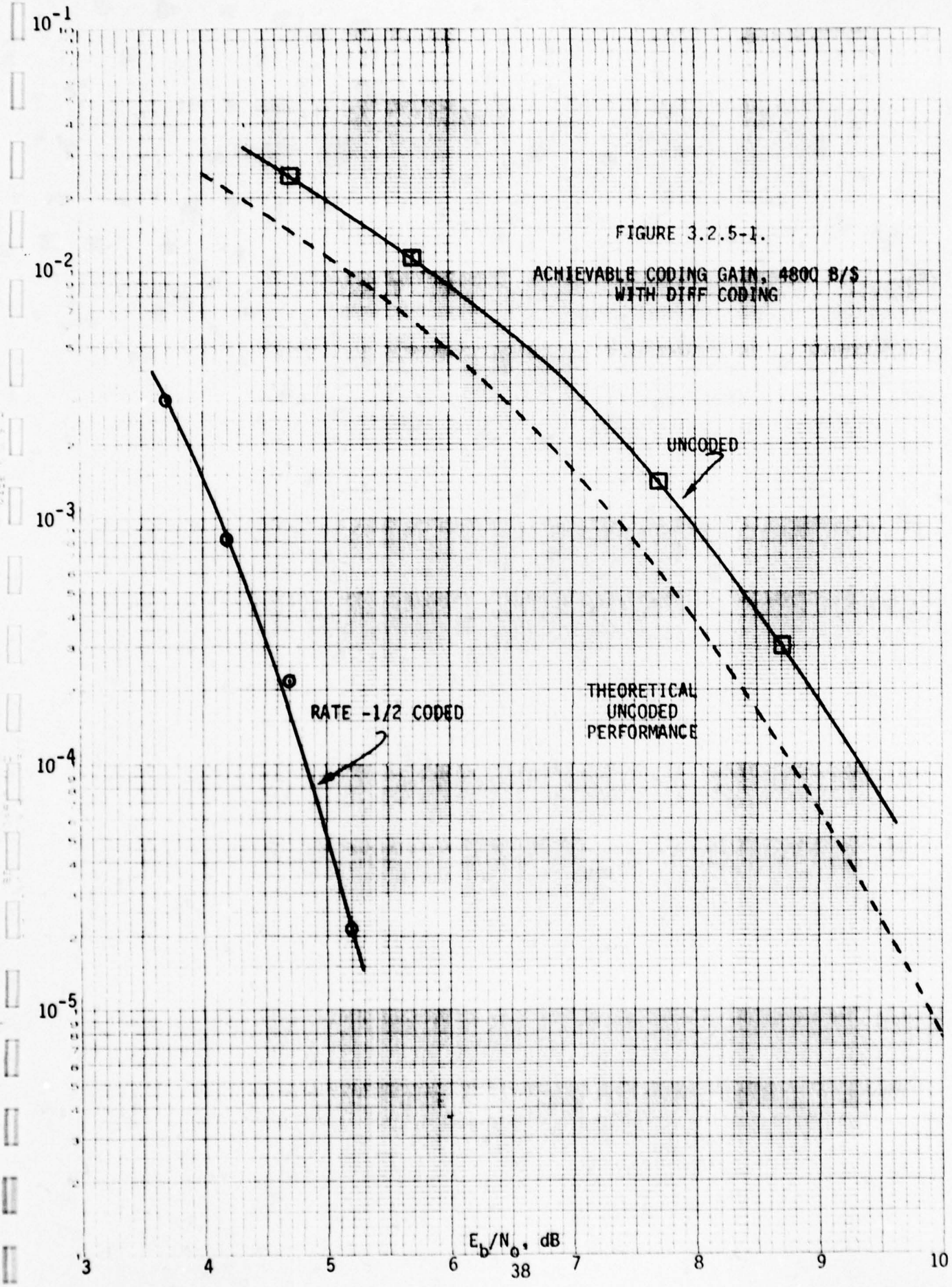

FIGURE 3.2.5-1.

ACHIEVABLE CODING GAIN, 4800 B/S
WITH DIFF CODING

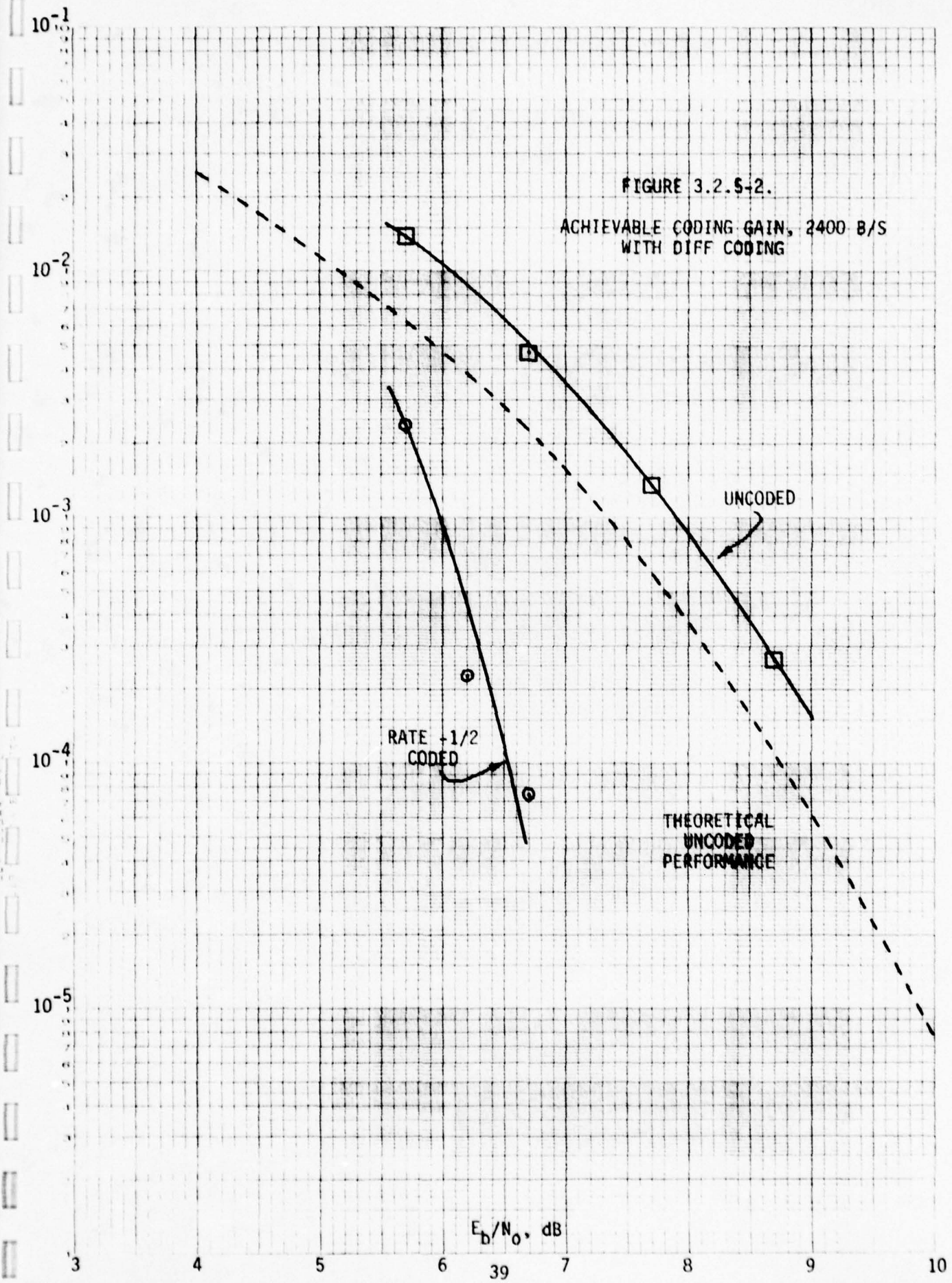

FIGURE 3.2.5-2.

ACHIEVABLE CODING GAIN, 2400 B/S
WITH DIFF CODING

at 4800 b/s. The reason for this appears to be that for the same E_b/N_o, the C/N_o as seen by the demodulator is 3 dB lower when the information rate is 2400 b/s than when it is 4800 b/s. Thus effects such as phase jitter on the recovered carrier and carrier cycle slip rate are significantly worse.

3.2.6 Emulation of Shipboard RFI Environment (29 June 1978)

Communications to surface ships are adversely affected by a number of sources of RFI, as discussed by Ohlson and Landry [3-2]. These include not only the major source of concern in this study, namely pulsed RFI from radars, but also machinery noise and harmonics and intermodulation products of other communication signals. This test was intended to provide an example of performance enhancement through coding in a 4800 b/s data link with a typical set of miscellaneous RFI sources, each of a level sufficient to significantly degrade performance if operating alone. As in the previous test, only rate -1/2 coding was employed and all data was differentially coded. The RFI sources and their significant parameters are tabulated in Table 3.2.6-1. Carrier frequency of the desired signal was 260 MHz.

With the exception of E5, the interfering signal levels were set to degrade uncoded performance by approximately an order of magnitude in error rate by each acting alone. To do this, E_b/N_o was set to 9.2 dB and error rate 1.85×10^{-4} was measured. Then each of the sources (except E5) was inserted individually and adjusted until BER was increased by approximately a factor of 10. The actual BER elevations achieved are listed in Table 3.2.6-2. Since the pulse width of E5 is approximately one bit at 4800 b/s, this emitter will establish an error rate floor when present, so its level cannot be set as above. Instead, the level was chosen as 30 dB above the thermal noise floor, which insures proper operation of the AN/WSC-3 blanker.

Bit error rate was measured as desired signal level varied, with all RFI sources except E5 active. The results are shown in Figure 3.2.6-1 for coded and uncoded data. Figure 3.2.6-2 is a similar figure showing performance with the pulsed RFI source E5 active as well as the other sources. Coded data was taken both with and without interleaving; the interleaver is seen to provide slight but not significant improvement. Finally, Figure 3.2.6-3 compares coded performance under conditions of no RFI, all RFI except radar, and all RFI including radar.

TABLE 3.2.6-1.

RFI SOURCES

Source*	Type	Parameters
E1	Cochannel interferer	4800 b/s PSK 2^{20}-1 PN data source f_c = 260 MHz + 100 Hz
E2	Intermodulation product	19.2 kb/s PSK 2^{20}-1 PN data source f_c = 260 MHz - 33 Hz
E4	UHF AM signal (densensitization)	AN/SRC-20 radio modulated by local broadcast station f_c = 268.3 MHz
E5	Pulsed RFI	Pulse width = 200 μsec PRF = 250 Hz Level = 30 dB above N_o
E9	Impulsive noise	Pulse width = 5 μsec Poisson arrival times with 1 kHz average frequency

*These designations refer to sources on the RFI simulator.

TABLE 3.2.6-2.

INDIVIDUAL DEGRADATIONS TO UNCODED BER

Source	Measured BER
None	1.85×10^{-4}
E1 only	1.28×10^{-3}
E2 only	1.77×10^{-3}
E4 only	1.83×10^{-3}
E9 only	2.21×10^{-3}

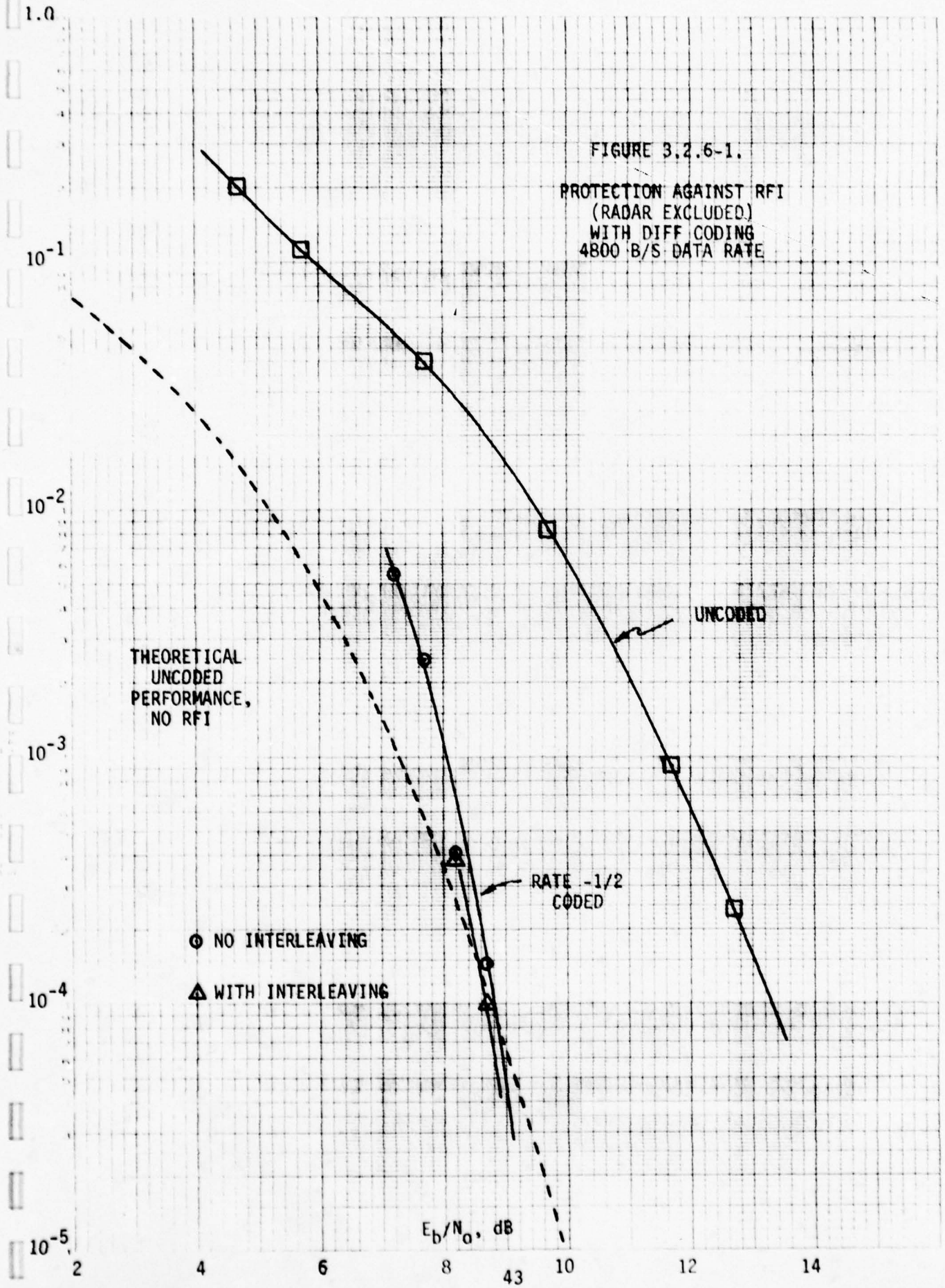

FIGURE 3.2.6-1.

PROTECTION AGAINST RFI
(RADAR EXCLUDED)
WITH DIFF CODING
4800 B/S DATA RATE

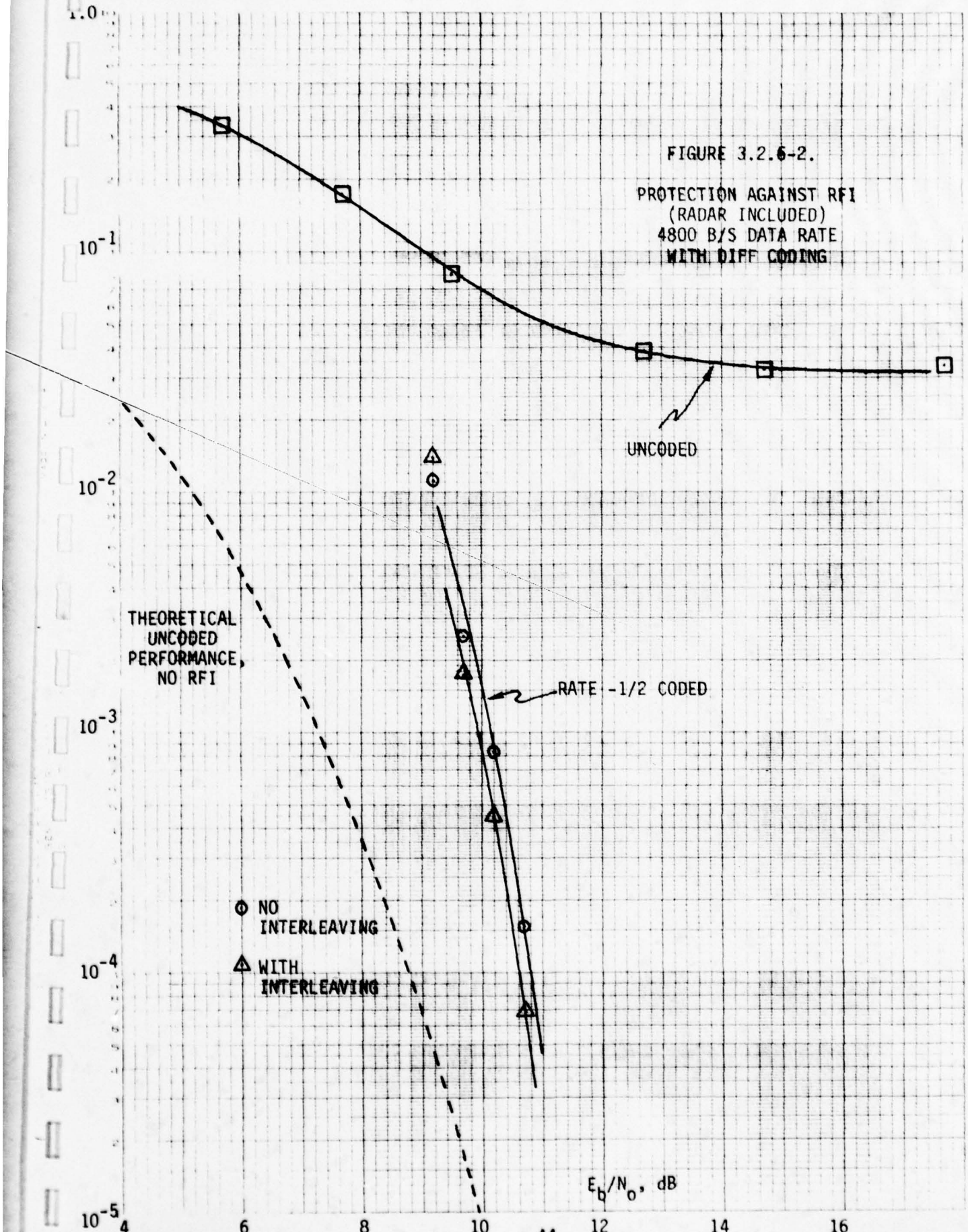

FIGURE 3.2.6-2.

PROTECTION AGAINST RFI
(RADAR INCLUDED)
4800 B/S DATA RATE
WITH DIFF CODING

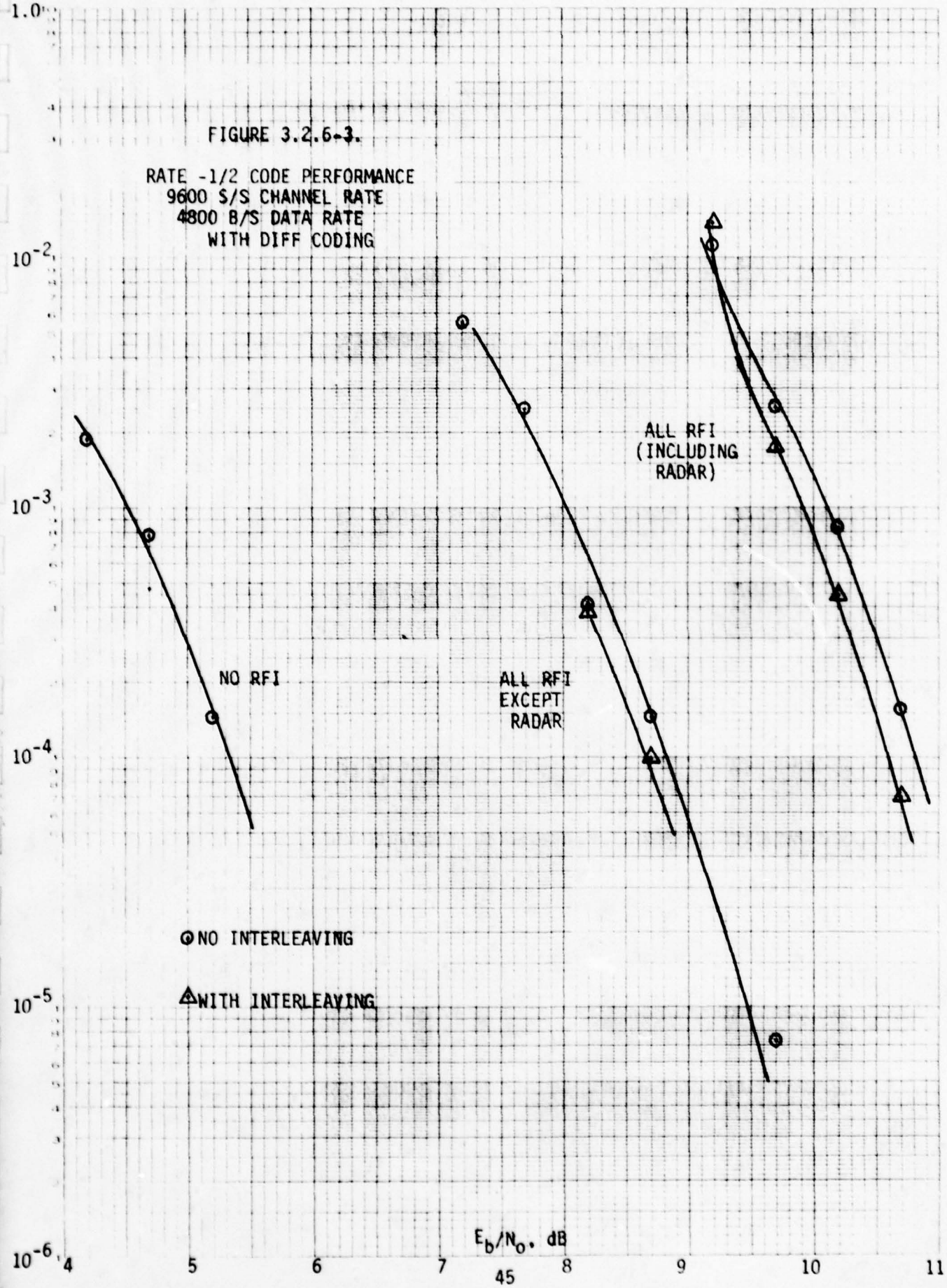
1.0
10^{-2}
10^{-3}
10^{-4}
10^{-5}
10^{-6}
RATE -1/2 CODE PERFORMANCE
9600 S/S CHANNEL RATE
4800 B/S DATA RATE
WITH DIFF CODING
NO RFI
ALL RFI EXCEPT RADAR
ALL RFI (INCLUDING RADAR)
NO INTERLEAVING
WITH INTERLEAVING
E_b/N_o, dB
4
5
6
7
8
9
10
11

FIGURE 3.2.6-3.

It must be recognized that this data pertains to a specific set of RFI sources. Although these interferers represent a "typical" shipboard environment, actual performance may vary significantly as the interferers and their parameters change. Nonetheless, these results demonstrate the potential performance enhancement coding can provide against not only burst interferers, but other types of interference as well.

3.3 Satellite Link Tests

By arrangement with Naval Telecommunications Command, an access of FLTSATCOM Channel 4 was authorized in the time period 1500-1900Z on 29 June 1978 for purposes of testing the codec over an actual satellite link. The equipment configuration for this test, illustrated in Figure 3.3-1, included an additional AN/WSC-3 used as a transmitter, and an OE-82 antenna and AM-6691 deck box located on the roof of Spanagel Hall at NAVPGSCOL. The deck box on the roof, which is identical to that used in the simulator tests, contains a diplexer and preamplifier. However, the preamplifier was bypassed and the preamplifier in the laboratory deck box used instead, so that variable attenuation could be inserted ahead of the preamplifier in order to vary the receiving terminal G/T. Transmitter EIRP was controlled using the power control knob on the transmit AN/WSC-3 and monitoring power on a power meter. Details of the calibration of EIRP and G/T are contained in Appendix C.

In order to use the access time efficiently, we elected to perform separate uplink and downlink tests. In the uplink test, the receive terminal G/T was set at the best achievable value and BER measured as a function of uplink EIRP. In the downlink test, EIRP was maximum and BER measured as G/T varied. Since the links of major concern are downlink-limited, the downlink test was performed first, and as much uplink testing as possible was accomplished in the time remaining after completion of the downlink test.

3.3.1 Downlink Test

In the downlink test, transmitter EIRP was set at the maximum value of 27 dBW. The power spectrum of the resulting downlink (with 9600 s/s channel rate), as determined by the NAVPGSCOL SATCOM Signal Analyzer, is illustrated in Figure 3.3.1-1.

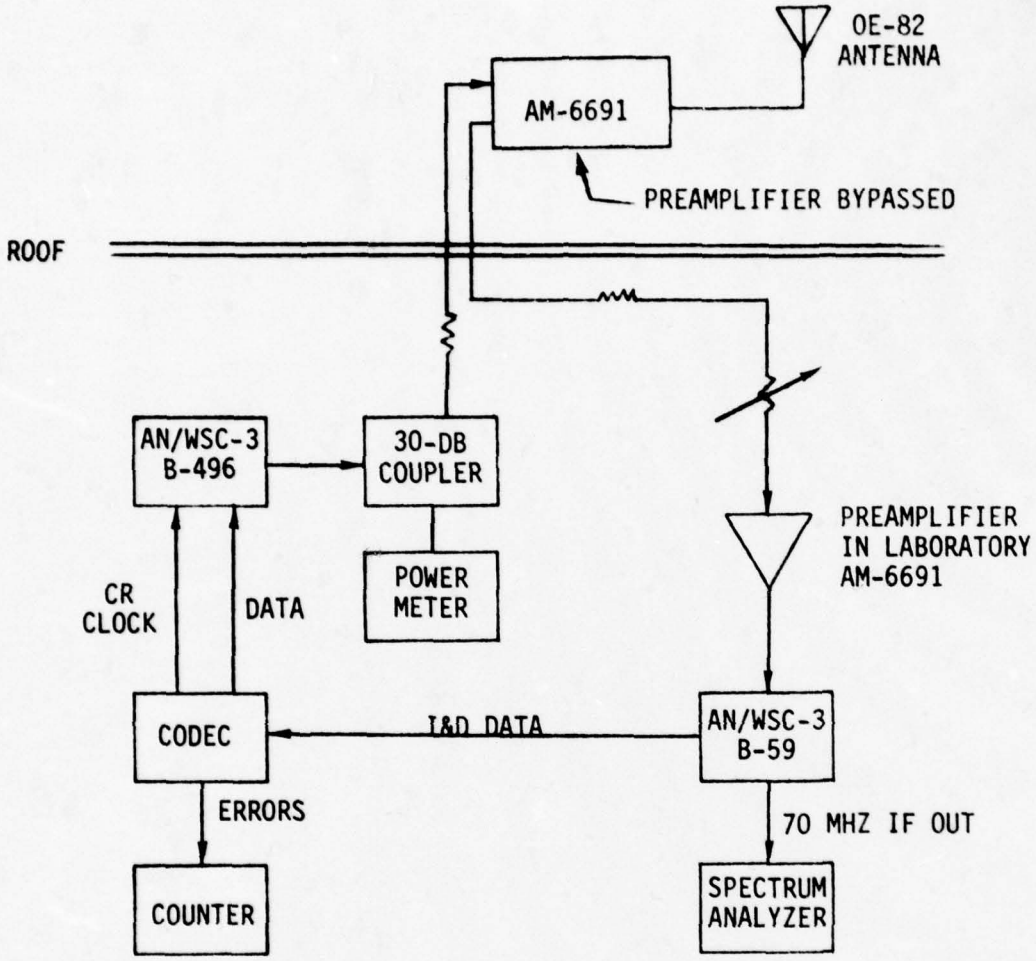

FIGURE 3.3-1. EQUIPMENT CONFIGURATION FOR SATELLITE LINK TESTS

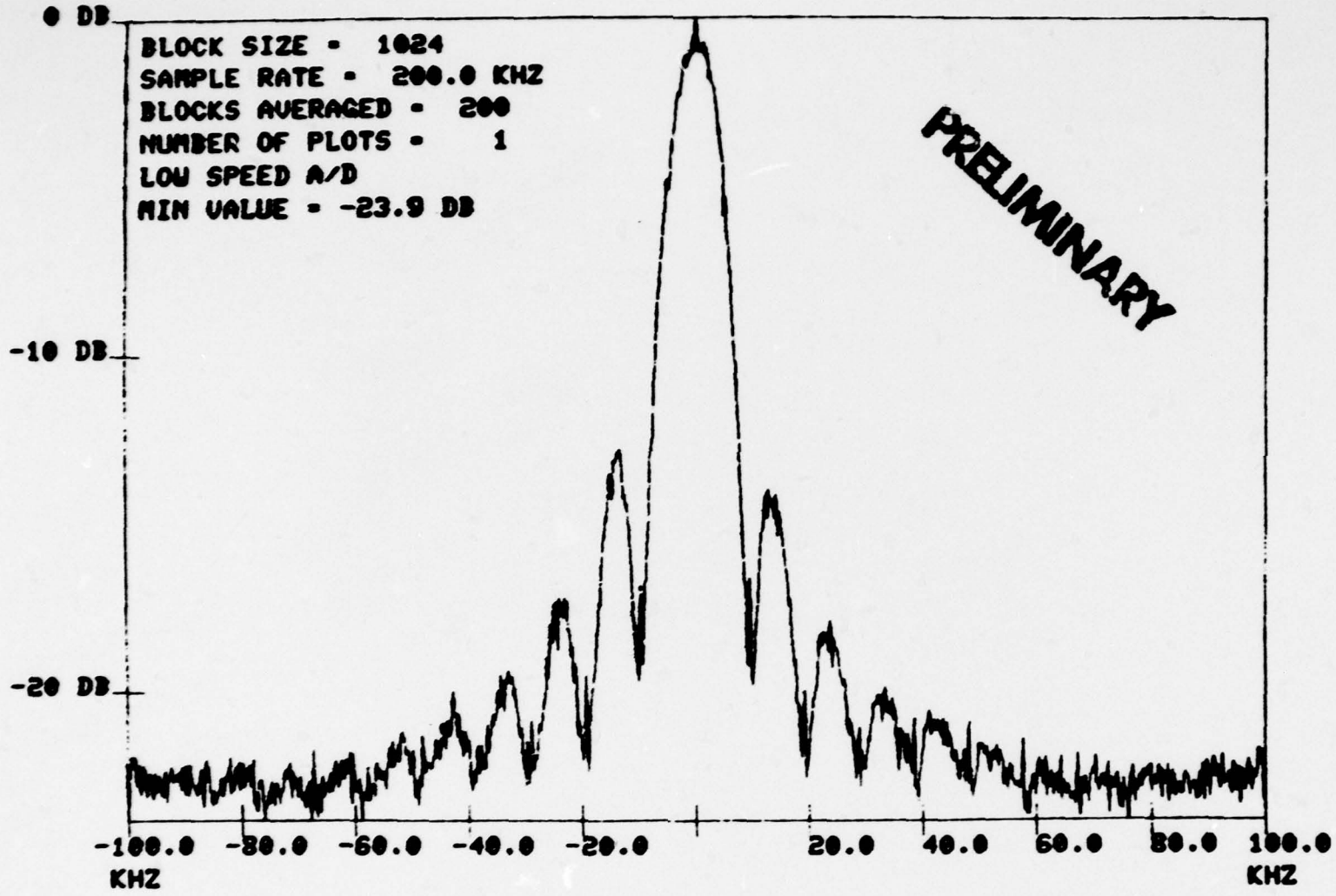

FIGURE 3.3.1-1. POWER SPECTRUM OF FLTSATCOM CHANNEL 4 DOWNLINK
(Courtesy of J. E. Ohlson)

In order to avoid the time-consuming difficulties we normally encountered in taking data at low C/N_0 due to cycle slips, we elected to take all data using differential coding, although an uncoded baseline without differential coding was also taken where possible. Data was taken at all three code rates for a channel rate of 9600 s/s. In addition, rate -1/2 data at 4800 s/s and uncoded data at 4800 b/s and 2400 b/s were taken in order to evaluate coding gain for 2400 b/s and 4800 b/s links, as was done in the test described in Section 3.2.5.

Figure 3.3.1-2 shows measured BER versus receiving terminal G/T for channel rate 9600 s/s, for uncoded data and all three code rates, all with differential coding. Note that this data is plotted versus G/T (or equivalently, C/N_0) and that differences in data rate in the three cases are not taken into account. Thus direct comparison of the performance based on separation of the curves does not truly compare communication efficiency of the four alternatives (uncoded, rate -1/2, -2/3, -3/4), as would be the case if performance were plotted versus E_b/N_0.

Measurement with the spectrum analyzer indicates that at the best G/T of -19.2 dB/K, E_s/N_0 at 9600 s/s is 31 dB. Within the accuracy of this measurement, the data of Figure 3.3.1-2 agrees closely with the data obtained using the simulator, and as reported in Section 3.2.1.

Figure 3.3.1-3 shows potential coding gain for a 4800 b/s link with rate -1/2 coding over an uncoded link, both with differential coding. Since the data rate is the same for both curves, separation between them is a valid measure of communication efficiency, and can be interpreted as the amount of downlink margin provided by coding. Figure 3.1.3-4 shows similar data for 2400 b/s information rate. The data in these two figures agrees closely with that presented in Section 3.2.5 for these cases.

3.3.2 Uplink Test

In the uplink test, the receiver G/T was set at the maximum achievable level of -19.2 dB/K and EIRP varied with the power control knob of the transmitting AN/WSC-3. The goal in the test was to measure performance for the same sets of conditions addressed in the downlink test. However, the uplink test had to be carried out in the last 40 minutes of the scheduled access, and only the 9600 s/s channel rate data could be taken. These results are illustrated in Figure 3.3.2-1.

FIGURE 3.3.1-2.

FLTSATCOM DOWNLINK PERFORMANCE
9600 S/S CHANNEL RATE
ALL DATA DIFF CODED

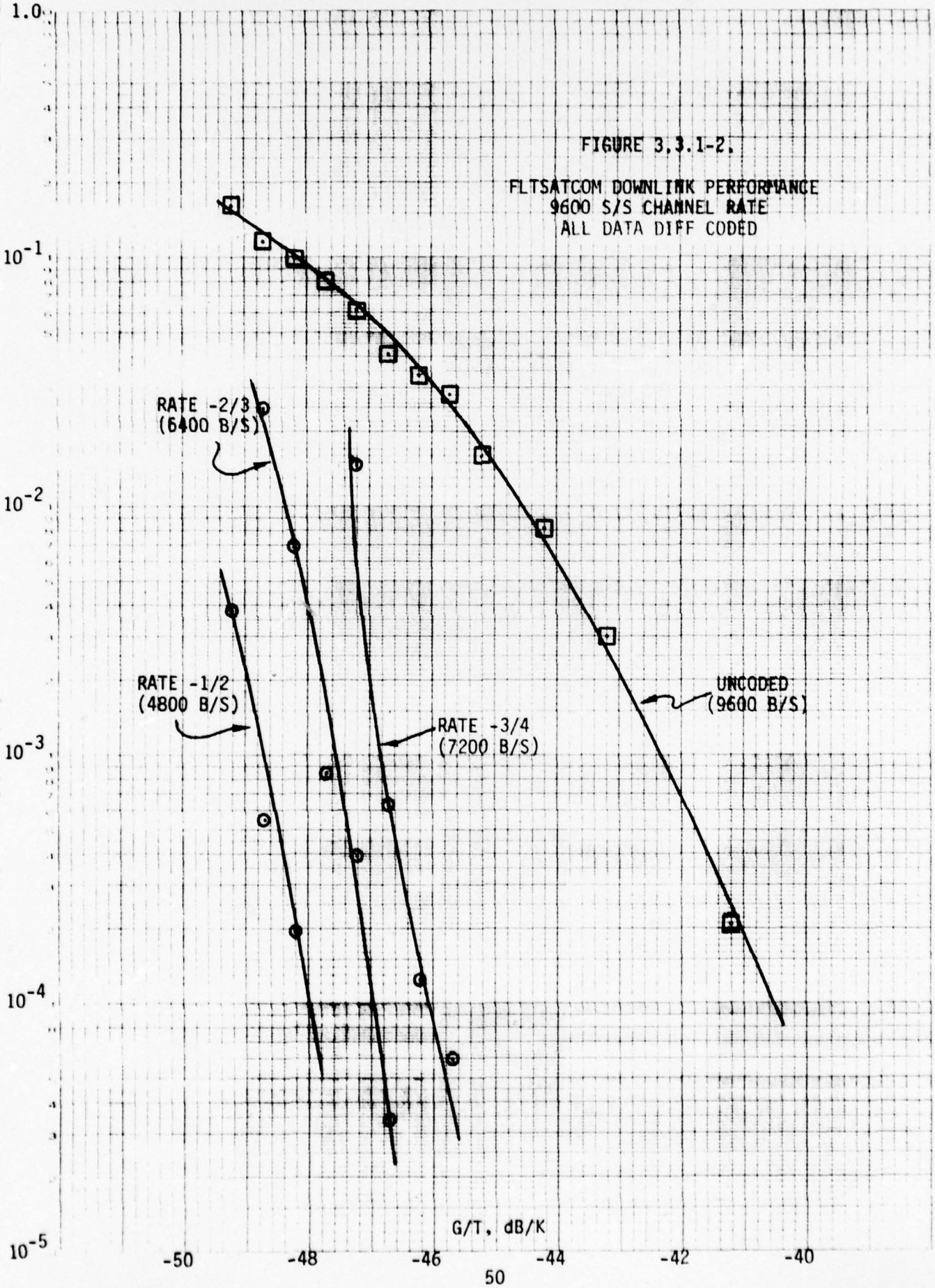

FIGURE 3.3.1-3.

DOWNLINK CODING GAIN
4800 B/S DATA RATE
WITH DIFF CODING

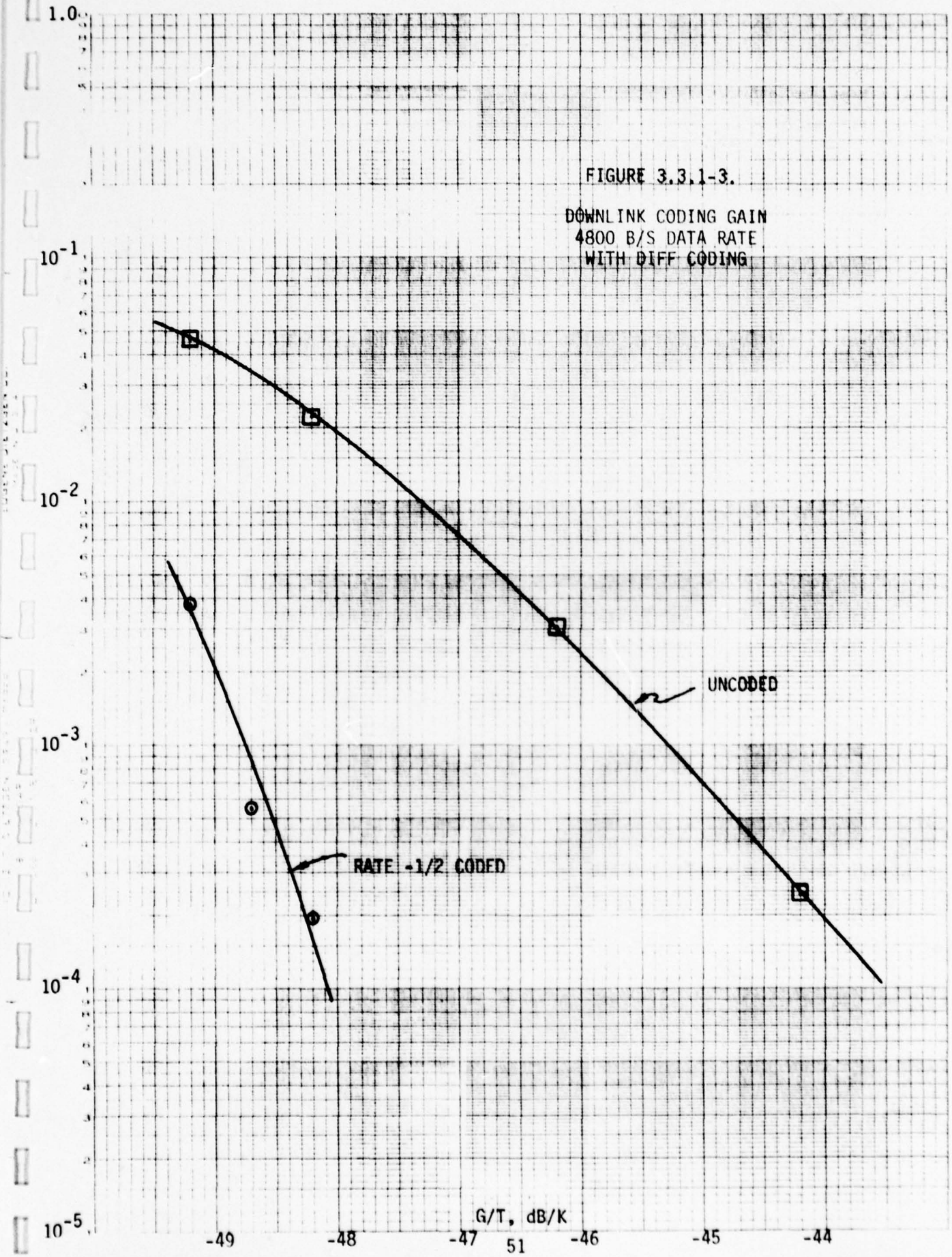

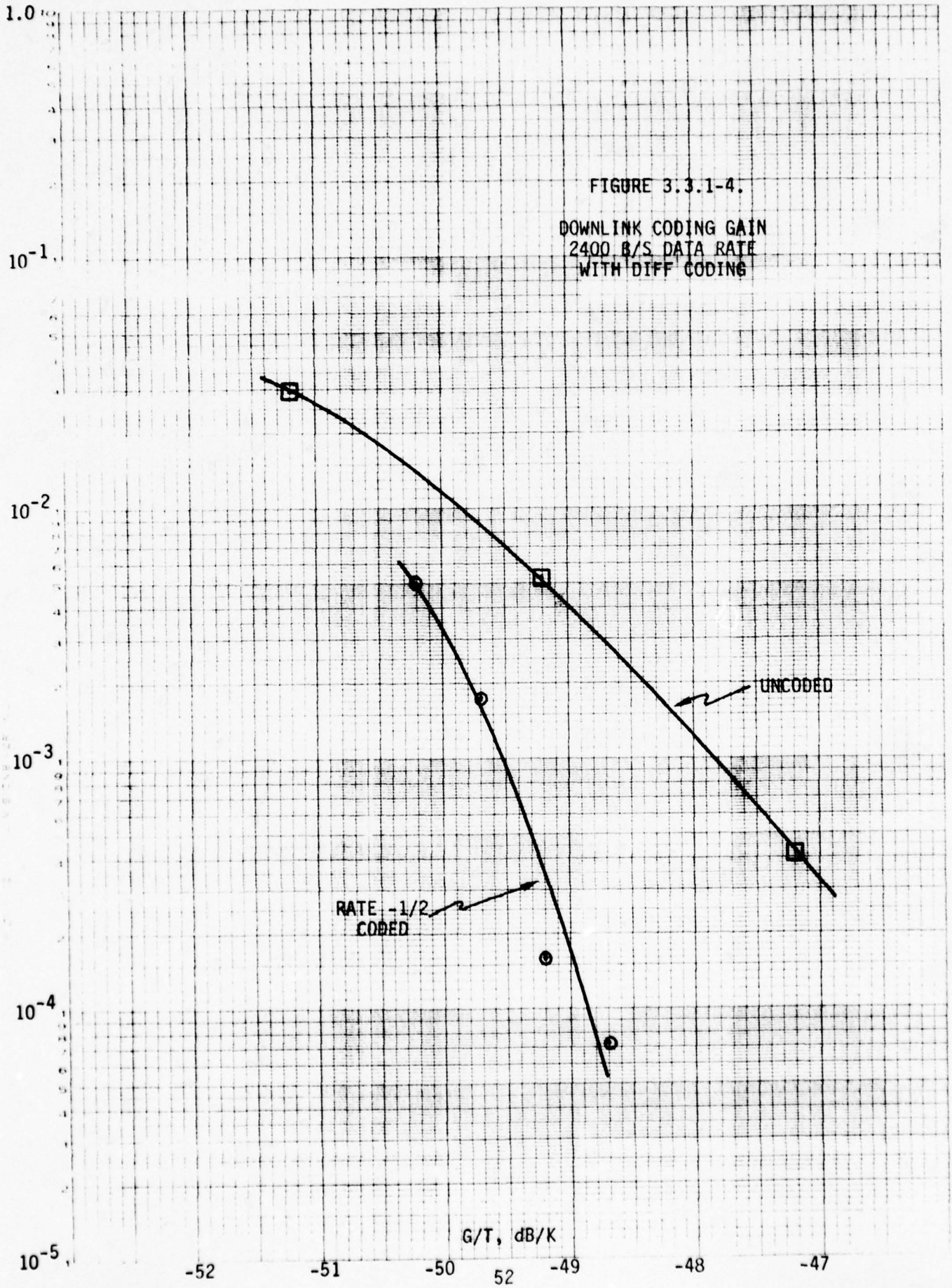

FIGURE 3.3.1-4.

DOWNLINK CODING GAIN
2400 B/S DATA RATE
WITH DIFF CODING

Because of the short available time, data points were taken with short run times, reducing the statistical significance of these results. Some data collected was later discovered to be inconsistent or otherwise questionable. For example, two BER measurements with the rate -2/3 code were made, but the values are so inconsistent as to be meaningless, and they have not been presented. The same is true of one data point with the rate -3/4 code. In reviewing the test records, we have been unable to determine the cause of these problems. After the end of our scheduled access we noted some other activity in the channel. It is possible that this activity could have been present during our testing, but a more likely explanation is that we simply did not have time to be as careful in taking the data as we were in previous tests, and could not recognize and recheck questionable data at the time. In any event, the difficulties noted here justify our decision to give priority to the more important case of the downlink test.

3.4 Summary of Test Results

The preceding pages contain a substantial amount of performance data showing the quantitative improvement provided by coding. We summarize here what we believe to be the major conclusions which can be drawn from these test results, indicating for each the paragraph where the data supporting the conclusion can be found.

- Coding at rates up to 3/4 can provide protection against a single 200 μsec, 5% duty cycle interferer at channel rates up to 19.2 kb/s, provided that the pulses are blanked. For protection against two such interferers, rate -2/3 or less is required. For these rates, interleaving provides negligible or minimal improvement. (3.2.2)

- Rate -1/2 coding can provide up to 4.5 dB of gain required E_b/N_o at $P_e=10^{-4}$ (and more at $P_e=10^{-5}$) over uncoded performance for links with 4800 b/s data rate. For 2400 b/s links, the available gain drops to approximately 3 dB at 10^{-4}, the reduction in gain being attributable to modem performance degradation (3.2.5)

- Coding provides simultaneous gain in E_b/N_o and RFI protection against a broad variety of non-pulsed RFI sources representative of a shipboard environment. (3.2.6)

FIGURE 3.3.2-1.

FLTSATCOM UPLINK PERFORMANCE
9600 B/S CHANNEL RATE

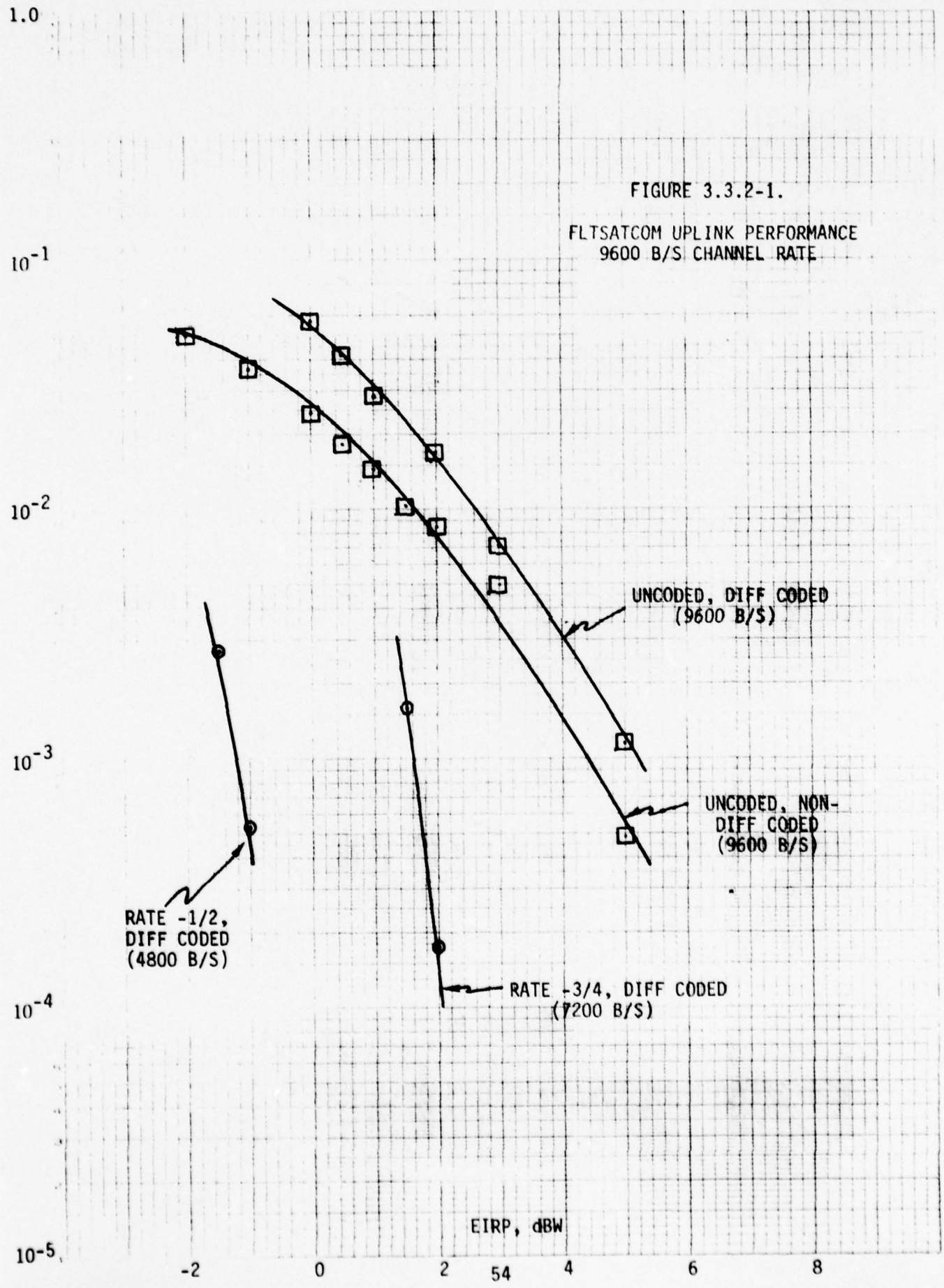

- Available coding performance which is actually achievable is limited by performance of the AN/WSC-3 demodulator at the low levels of C/N_0 at which it must operate to achieve this gain. (3.2.1 and others)

Finally we note that while these claims are based primarily on performance tests using the RFI simulator as a test bed, they are corroborated in large measure by the results obtained by testing on an actual FLTSATCOM link (3.3).

REFERENCES

3-1. E. S. Brick and J. E. Ohlson, A Simulator for Shipboard RFI in Satellite Communications, NAVPGSCOL Report NPS-620L76109, October 1976.

3-2. J. E. Ohlson and T. C. Landry, Shipboard RFI in UHF Satellite Communications, NAVPGSCOL Report NPS-620L76103, October 1976 (CONFIDENTIAL).

3-3. Harris Corporation, Government Communication Systems Division, Technical Record Book No. 7102.

3-4. Technical Manual, Satellite Communication Set AN/WSC-3 (3 volumes), NAVELEX 0967-LP-545-4050, -4060, -4070.

3-5 R. F. Carlson and J. E. Ohlson, Performance of the AN/WSC-3 and AN/SSR-1 Satellite Communications Units in the Presence of Pulsed Radar Noise, NAVPGSCOL Report NPS-620L76122, December 1976 (CONFIDENTIAL).

3-6 Coding for Navy UHF Satellite Communications (Phase I), Final Report on Contract No. N00039-76-C-0384, Harris Corporation, Electronic Systems Division, April 1977.

3-7. B. D. Trumpis and P. L. McAdam, "Performance of Convolutional Codes on Burst Noise Channels," NTC 77 Conference Record, paper 36:3, November 1977.

4.0 INTERFACING CONSIDERATIONS

An important practical constraint which must be satisfied by any coding equipment which might be adopted is that it be capable of operating with existing communications equipment, without substantial modifications to such equipment. During the course of this study, we have noted a number of cases in which characteristics of the existing equipment reduce the system performance improvement potentially available through the use of coding; some of these cases have been discussed in the previous sections. In addition, we have seen instances where the presence of coding calls for reexamination, at the system level, of the communication equipment configuration, and possibly modifications to this equipment in order to improve overall system performance. In this section, we summarize these interfacing considerations for the most important configuration of interest, namely when the coding equipment is interfaced between the AN/WSC-3 Satellite Communication Set and the ON-143 Interconnecting Group. This is the common terminal configuration for surface ships and submarines. Most of the principles discussed here also apply to aircraft terminals, but we have not investigated the specific hardware characteristics of aircraft installations.

4.1 AN/WSC-3 Performance

The PSK demodulator and bit synchronizer in the AN/WSC-3 is designed for operation in an uncoded mode, and thus with relatively high signal to noise ratio in the channel rate bandwidth (E_s/N_o). In fact, the lowest E_s/N_o at which any defined performance is required by the specification [4-1] is 8.5 dB. The AN/WSC-3 meets its specified performance requirements. However, modems which operate with coding typically operate with much lower values of E_s/N_o. For example, if a rate -1/2 code is used and provides 5 dB of coding gain, the modem operates with 8 dB less E_s/N_o than if it were providing the same performance at the same information rate in uncoded operation. A modem can exhibit acceptable performance at large E_s/N_o yet be unacceptable for use with coding because of degradation at lower values of E_s/N_o.

Using two Government-furnished AN/WSC-3 units, we tested performance of the demodulator and bit synchronizer at low signal-to-noise ratios in order to determine whether performance of the AN/WSC-3 placed any serious limitation on the achievable coding performance. These investigations revealed that the

AN/WSC-3 bit synchronizer, and to a lesser extent the carrier recovery loop, do not perform well enough at low SNR to provide as much coding gain as is theoretically available. The primary problems are the following:

(1) Higher bit slippage rate than can be tolerated in a coded system.

(2) 180^{o} cycle slips in the recovered carrier.

(3) False declarations of loss of lock, with consequent output muting and initiation of the acquisition sequence.

For our testing purposes, we overcame (3) by a jumper connection which forces the acquisition circuitry to always indicate lock. This is an unacceptable long-term solution, but it appears that by adjusting the detection threshold, this problem could be resolved without modification to the equipment. We believe that (2) could be overcome or significantly mitigated by narrowing the carrier recovery loop bandwidth. We made no attempt to do so, because it was undesirable to make circuit modifications to the GFE, and because (2) has the least adverse effect on coding gain. The most serious problem is the bit slip problem, both because the onset of slips occurs at an unacceptably high signal-to-noise ratio, and because there appears to be no simple approach to solving the problem. In our experiments, since we intended to access the NRZ baseband and perform an integrate-and-dump operation in the codec anyway in order to produce soft decisions, a relatively simple solution was to derive the bit timing as well, using an approach known to perform adequately at low SNR. For the long term, however, the only options appear to be to replace the current AN/WSC-3 bit synchronizer by one capable of high performance at low SNR (which, incidentally, might as well produce soft decisions for the decoder), or to perform the bit sync operation in the codec. In the latter case, a desirable modification to the AN/WSC-3 would be to make the NRZ baseband available at an output port.

Figure 4.1-1 shows measured bit slip and cycle slip data for the AN/WSC-3 at 9600 b/s symbol rate. (The apparent flattening of the cycle slip

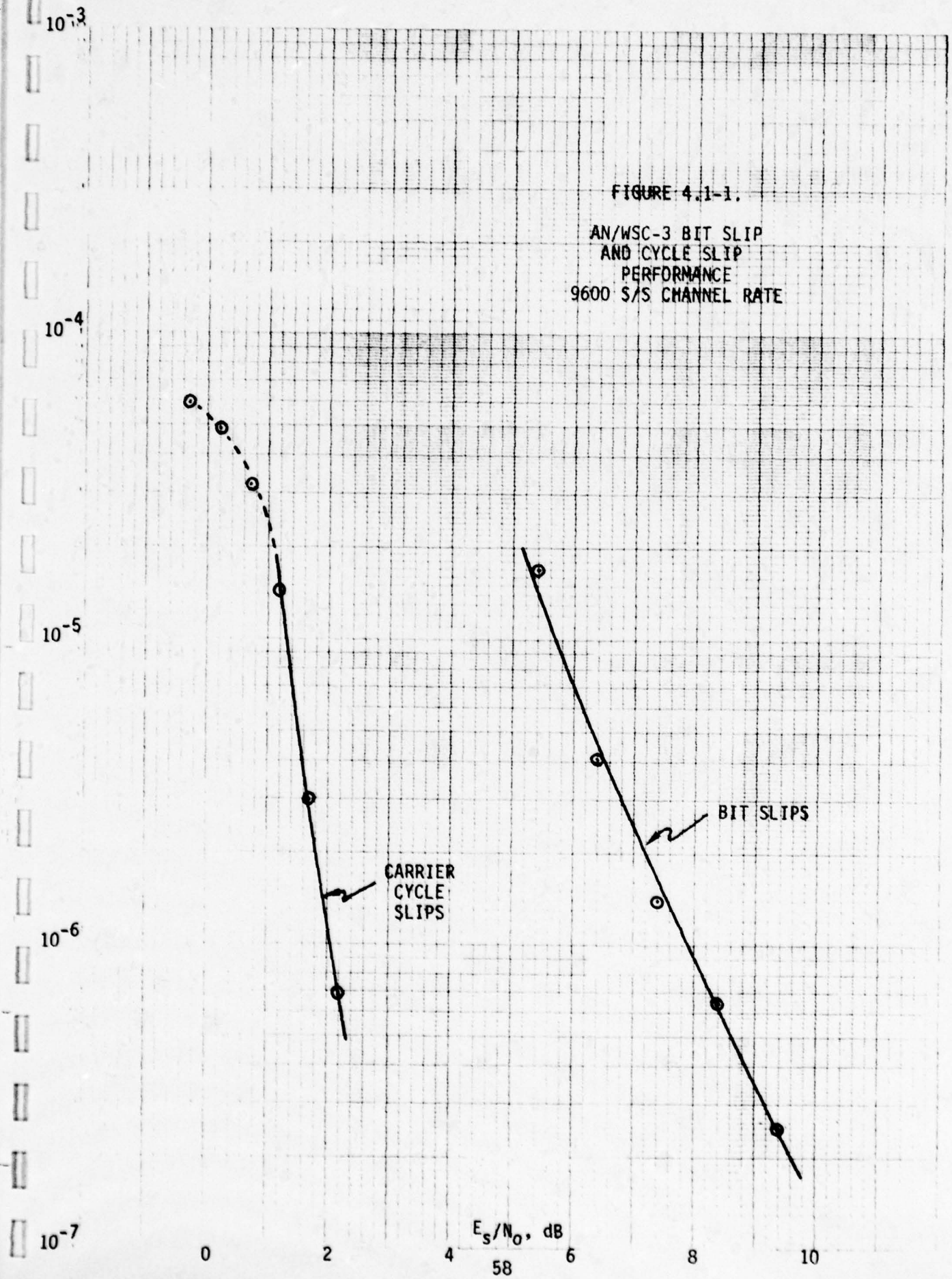

FIGURE 4.1-1.

AN/WSC-3 BIT SLIP AND CYCLE SLIP PERFORMANCE 9600 S/S CHANNEL RATE

rate curve for E_s/N_o less than 1 dB is not real, but is a consequence of the slip rate measurement technique used.*)

Note that the bit slip probability is low in comparison with bit error rate at the same E_s/N_o, so that for uncoded data the effect of bit slips is not significant (although the impact of loss of bit count integrity in long encrypted data records could be serious). With coding, however, not only is the output bit error rate at any given E_s/N_o much less than the raw channel error rate, but also the effect of a bit slip is much more serious since it causes a loss of branch synchronization and typically several hundred bits will be lost before branch sync is reestablished. Thus the bit slip performance shown in Figure 4.1-1, while adequate for the uncoded conditions for which the AN/WSC-3 is designed, is wholly inadequate for use in a coded system if any significant amount of real coding gain is desired.

The carrier cycle slip performance of the AN/WSC-3 is a much less serious problem, not only because the onset of cycle slips occurs at a substantially lower value of E_s/N_o, but also because the effect of a cycle slip is less serious than the effect of a bit slip. When transparent codes are used and the data is differentially coded, a 180^o phase reversal does not cause loss of branch sync, but merely causes the decoder to make errors for a few constraint lengths.

Since frequent cycle slips occur only at E_s/N_o values less than approximately 2 dB (with symbol rate 9600 b/s), their effect was found to be significant only when the rate -1/2 code used. For rate -2/3, the lowest value of E_b/N_o for which decoder branch sync could be maintained was approximately 4 dB, for which E_s/N_o=2.25 dB. Cycle slips do limit the achievable coding gain with rate -1/2 coding. In addition, it is important to note that

*The technique used is as follows: With an actual channel error rate p, a data comparator will count errors at rate 9600p when the recovered carrier phase agrees with the transmitted phase, and at rate 9600(1-p) when the recovered phase is antipodal. To measure cycle slip rates, the error rate (using the codec bit sync) was counted over 10 msec intervals using a frequency counter, and the counter output supplied to a strip chart recorder with full scale calibrations at 0 and 9600 Hz. In a several hundred second run, the number of transitions between the two nominal frequencies was counted by inspection of the recorder output. For high slip rates, slips close together are hard to resolve visually, and in addition the response time of the recorder can affect the results at high slip rates. This technique is accurate at slip rates of less than 10^{-5}, however.

the data of Figure 4.1-1 applies only to 9600 s/s channel rate. We did not measure slip rates at other channel rates, but the results discussed in Section 3.2.5 show that the available coding gain is significantly reduced when a channel rate of 4800 s/s is used. The most likely explanation for this behavior is a higher threshold E_s/N_0 for cycle slips, as would be the case if loop bandwidth is not switched when channel rate changes from 9600 s/s to 4800 s/s.

As we noted above, the performance limitations attributable to carrier cycle slips can probably be avoided, if necessary, by narrowing the loop bandwidths. However, system level considerations such as oscillator stabilities, frequency dynamics, and acquisition time must also be considered in deciding whether or not to carry out such a modification.

Another aspect of the AN/WSC-3 operation which affects coded performance is the RFI blanking circuit. Appendix B summarizes a study of the effects of blanking threshold variation which we carried out early in this program. This analysis explains the peaking of error rate around 10 dB excess noise level shown in Figure 3.2.4-1 and provides some rationale for the choice of threshold setting when coding is used. However, this analysis is based on a somewhat simplistic model, and setting of blanking threshold would be better accomplished by experiment. In any case, sensitivity of performance to variations in threshold setting near the optimum value is slight. A more serious concern is the effect of extremely high-level pulses shown in Figure 3.2.4-1, due to the failure of the blanking circuit to completely suppress the baseband signal during these pulses. If such high-level pulses actually occur, an improved approach to blanking would be to use the AN/WSC-3 blanking trigger to carry out blanking at the input to the decoder, rather than relying on a zero input voltage to the soft decision integrate-and-dump circuit. A desirable modification to the AN/WSC-3 would be to make this blanking indicator, presently available at an internal test point, available at an output port. It would also be necessary to time-align the blanking by compensating for any delays in the demodulator, bit synchronizer, and decoder input circuitry. Since these delays are fixed, the time alignment could be performed digitally within the codec, once the delays are determined.

4.2 System Timing

In standard shipboard installation, overall timing on the transmit side is under the control of the ON-143 Interconnecting Group. At the beginning of a transmission, this unit keys the AN/WSC-3 to begin transmission of a preamble, waits a prescribed interval of time sufficient for the receive terminal to acquire carrier and bit synchronization, and then begins supplying a bit rate clock to the source, encryption device, and modem. With coding in the system, an additional level of synchronization is required, namely, branch synchronization. This can be established in either of two ways. The usual manner is to allow branch sync circuitry to search for valid synchronization, based on some criterion which distinguishes between valid codewords and random data. This approach normally requires several hundred bits to reliably establish synchronization. Another approach is to insert a known pattern at the end of the preamble which, when recognized by a detector at the receiving terminal, indicates the beginning of encoded data. With this method, it is still desirable to have branch sync circuitry present so that in the event of a bit slip, branch sync can be reacquired.

Currently the preamble contains no pattern which could be used to establish start-of-data to a resolution of one symbol, and the wait interval between initial keying of the transmitter and clocking of the data is inadequate to allow the additional level of synchronization to be established by the usual branch sync search technique. Equally serious, this wait interval may not be long enough to allow carrier and channel rate clock acquisition at the reduced levels of C/N_0 which would be used with coding.

These considerations indicate the necessity of a careful study of transmit side timing, at the system level. It is likely that hardware modifications to the ON-143 Interconnecting Group may be necessary in order to properly orchestrate the timing.

Another aspect of timing which requires some consideration is the relationship between bit rate clock and channel rate clock when coding is used. Current data sources of interest have data rates of the form 75×2^n. The AN/WSC-3 provides channel rates of the same form. Thus the only code rate which simultaneously satisfies the currently used data rate and channel rates is rate -1/2. However, the portion of the AN/WSC-3 which is most affected by choice of channel rate is the bit synchronizer, and since there is good reason for changing this bit synchronizer in a coded system anyway, it may be a simple matter to allow

channel rates consistent with data rates $75x2^n$ and code rates 2/3 and 3/4, if these rates are desirable. If such code rates are used, circuits for generating uniform channel-rate clocks at 4/3 and 3/2 times the data rate must be developed. (These circuits will be substantially more complex than would be required with rate -1/2.) In our tests, this difficulty was avoided by always using a uniform channel rate clock as the master timing source, and developing data rate clocks by deleting pulses. In the actual systems, however, the master clock is the data rate clock provided by the ON-143.

REFERENCES

4-1 Military Specification MIL-C-28838 (EC), Communication Sets, AN/WSC-3, Satellite and AM-LOS Versions, Naval Electronic Systems Command, 4 May 1977.

5.0 CONCLUSIONS

The results presented in this report satisfy the primary objective of Phase II of this study, which was to provide experimental evidence of the performance enhancement which coding can provide. Our results verify, in the main, the Phase I predictions of performance against thermal noise and pulsed RFI, and quantify the limitations placed on this performance by existing equipment. In addition, these results provide evidence of the protection afforded by coding against other forms of RFI than periodic high-level pulses. In our judgement, the analytical results of Phase I and the experimental results of Phase II, taken together, provide answers to all the significant technical questions about coding performance in Navy UHF SATCOM links that can be answered at the functional level of the coding equipment itself.

In order to complete an assessment of the practical usefulness of coding in these links, it is now necessary to address a number of system-level problems such as those discussed in Section 4.0, as well as some not yet considered. Specifically, we recommend the following tasks:

- Careful reexamination of the requirements for coding, in order to determine *which links actually require* gain against thermal noise and how much gain is required, which links require RFI protection, and whether there is a real requirement for simultaneous coding gain and RFI protection.

- In the light of these specific requirements, address the problems arising from interfacing with the AN/WSC-3 and ON-143 which are discussed in Section 4.0, and determine the most realistic and cost-effective solutions to these interfacing problems for the specific applications identified.

- Address the platform limitations on size, weight, and power consumption which must be considered in any new equipment to be installed.

- Based on all the above information, select those applications in which coding is a viable and cost-effective technique for satisfying a real communication requirement, and define functional, physical, and performance characteristics for both coding equipment and for necessary modifications to other equipment to provide a workable system.

APPENDIX A

SENSITIVITY TO BURST RFI

The usual analytical tool for predicting performance of convolutional coding is the union bound, which uses the weight structure of the code and evaluates the probability of each possible error event and its contribution to net error rate. In applying the union bound when erasures are present, it is necessary to derive the weight structure as modified by the erasures. For the case of random erasures, the modified weight structure, averaged over the ensemble of erasure events, is easily derived from the unmodified weight structure without further searching. Thus union bounds for random erasures are easily calculated.

For periodic burst erasures, the modified weight structure can only be determined by carrying out a complete weight search for every possible phase of the RFI bursts. Thus for a 100-symbol RFI period, a complete weight search routine must be executed 100 times. Since each such weight search can take several minutes, we did not carry out this calculation in Phase I, especially since intuition suggested strongly that for bursts of five symbols, performance should degrade sharply without interleaving.

In the face of experimental results to the contrary, we did carry out complete weight searching and correctly calculated the union bounds for periodic bursts of length 5 and period 100. These bounds are presented in Figures A-1, A-2, and A-3. For simplicity, these bounds are for ideal decoder operation and infinitely fine demodulator output quantization. Union bounds presented elsewhere in this report reflect decoder implementation losses and three-bit quantization.

The bounds shown generally agree with the experimental results, showing that random interleaving provides no significant performance improvement.

It is interesting to compare these results with those of Trumpis and McAdam [A-1]. In order to avoid calculating the modified weight structure by averaging over all phases of the RFI, they observed that an erasure burst of length b in any given position could reduce the distance between codewords by between 0 and b positions. By assuming that ones in codewords are binomially distributed, they are able to calculate a modified average weight structure without additional searching. They assume that a contribution to distance

between codewords appears in any given position with probability 1/2. In fact, however, we find that, especially in the high-rate codes, low-weight codewords tend to be long, so that ones occur much less frequently than with probability 1/2, so that their results are pessimistic, sometimes by a significant amount. For example, Figure 20 of [A-1] shows required E_b/N_o of 6.6 dB for $P_e=10^{-5}$ with 5% random erasures, (which is consistent with Figure A-1, since our code is slightly longer), while Figure 26 shows required E_b/N_o of 10.9 dB for 5% duty cycle bursts of length 4 symbols. Thus they predict a sacrifice of 4.3 dB for burst of length 4, while Figure A-1 indicates the loss is only 0.2 dB even for length-5 bursts.

REFERENCE

A-1. B. D. Trumpis and P. L. McAdam, "Performance of Convolutional Codes on Burst Noise Channels," NTC Conference Record, paper 36:3, November 1977.

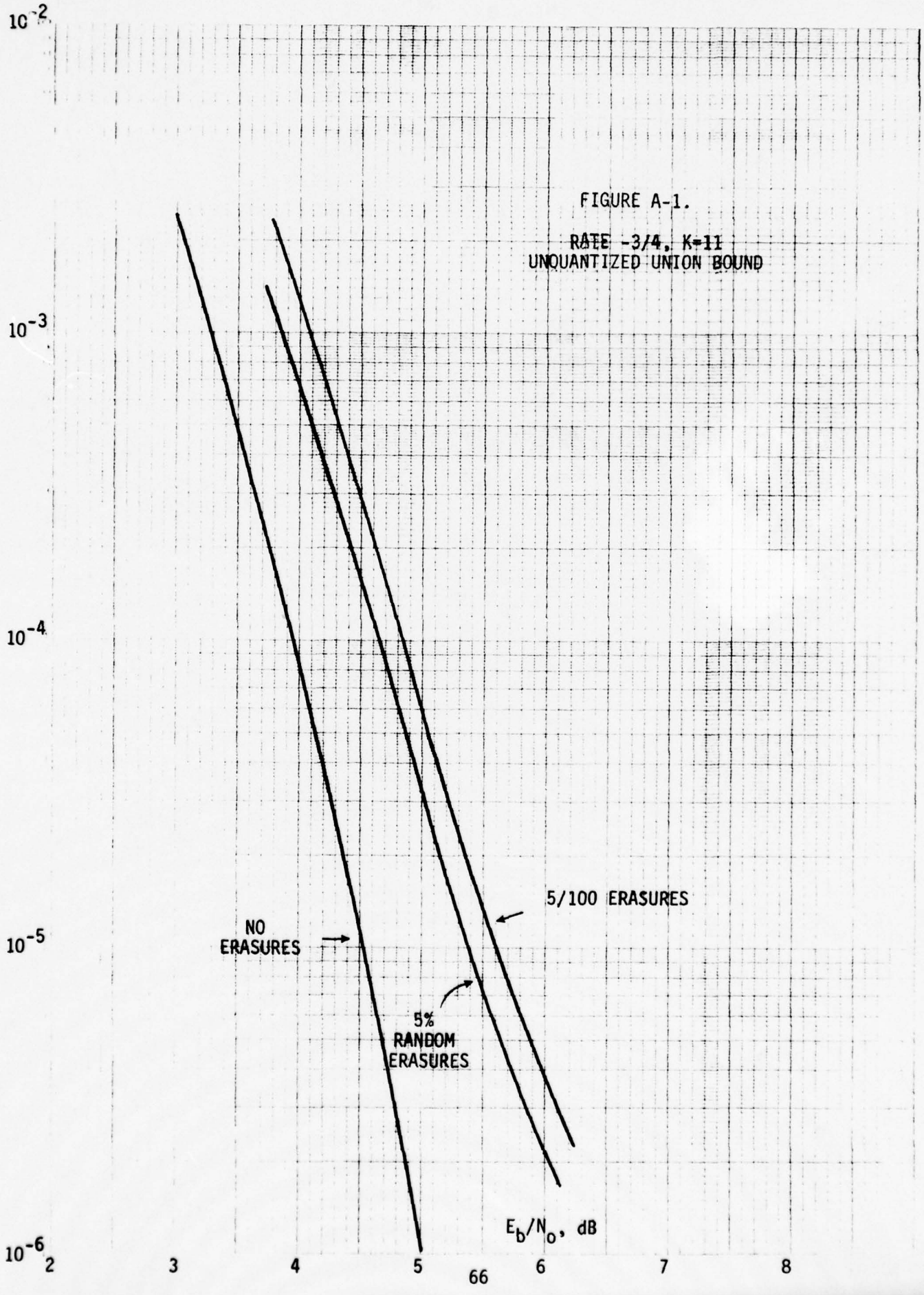

FIGURE A-1.

RATE -3/4, K=11
UNQUANTIZED UNION BOUND

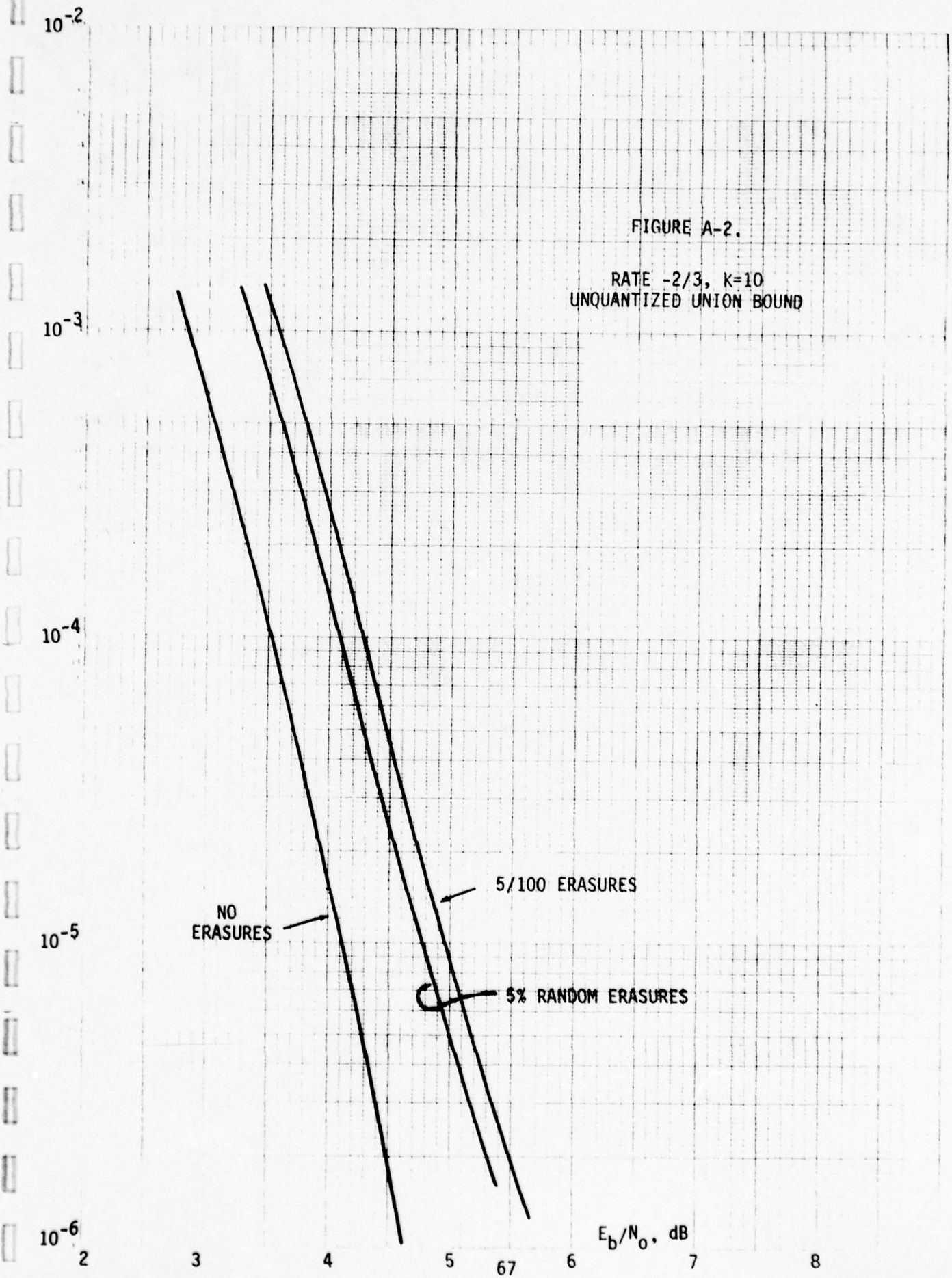

FIGURE A-2.

RATE -2/3, K=10
UNQUANTIZED UNION BOUND

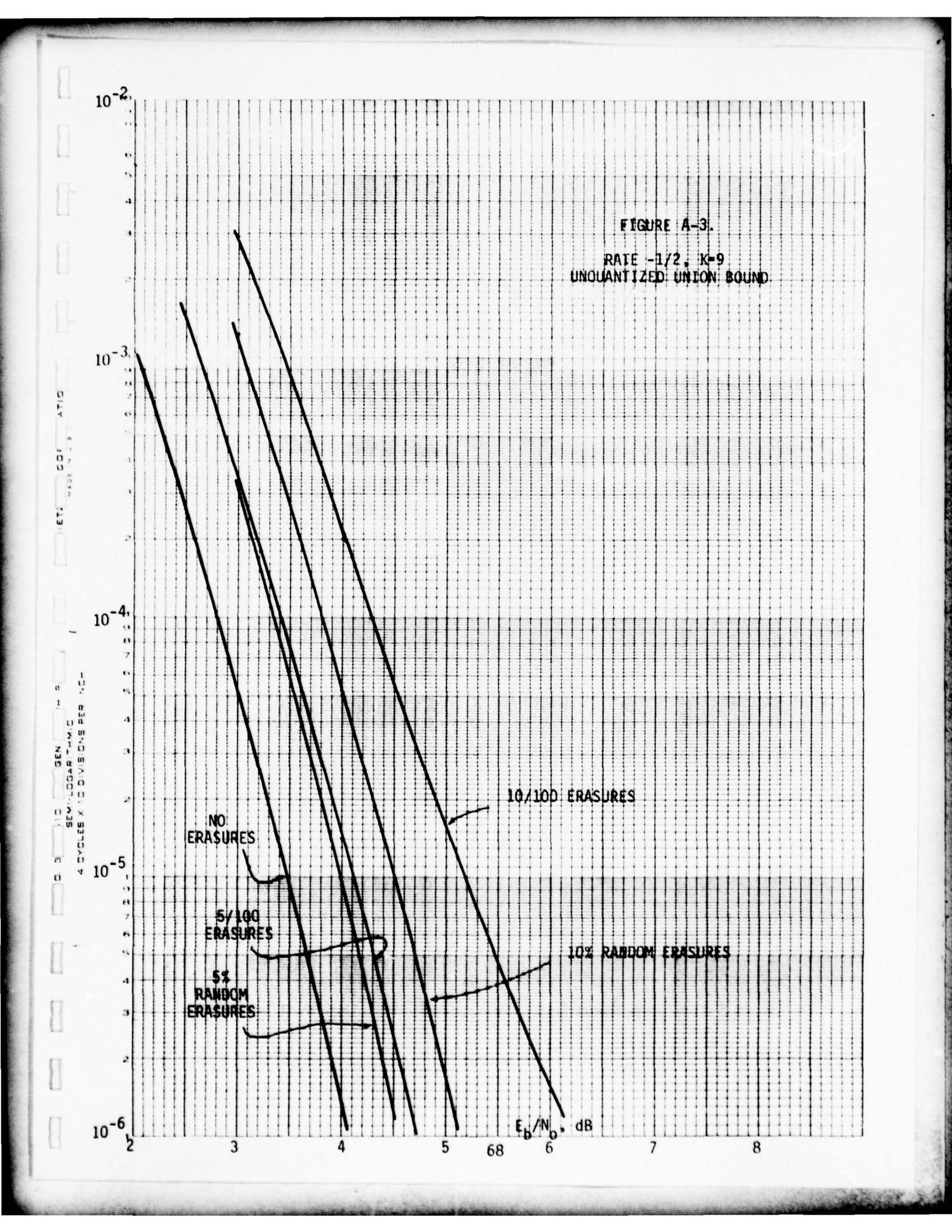
FIGURE A-3.
RATE -1/2, K=9
UNQUANTIZED UNION BOUND
10^{-2}
10^{-3}
10^{-4}
10^{-5}
10^{-6}
10/100 ERASURES
NO ERASURES
5/100 ERASURES
10% RANDOM ERASURES
5% RANDOM ERASURES
E_b/N_o, dB
2
3
4
5
6
7
8

APPENDIX B

CHOICE OF BLANKER THRESHOLD

Modems which operate in an environment with large RFI pulses typically utilize blankers to prevent extended ringing of the IF filter. The blanking threshold is set high enough to make the probability of the blanker being triggered by front-end noise small, but not so high as to allow very large RFI pulses to ring the IF filters. With this compromise some lower level RFI may get through the blanker and degrade performance.

The use of error correction coding offers the potential of correcting both the errors caused by lower level RFI that gets through the blanker and any bit erasures that occur when the blanker is on. Since errors and erasures have considerably different effects on decoder performance and the blanking threshold affects the mix of these two events, this implies that proper choice of blanking threshold is very important in optimizing performance. Typically, for a given choice of blanking threshold, the worst-case performance will be observed for RFI levels that are slightly below the blanking threshold. The purpose of this analysis was to characterize decoder performance for various levels of RFI relative to the blanker threshold and to allow selection of a blanker threshold that minimizes the worst-case error rate over all RFI levels. The system model used has some approximations to facilitate the analysis, but we believe that the results demonstrate typical behavior closely enough to give us significant insight into the problem.

Figure 1 shows a model of a modem with the blanking identical to the approach used in the AN/WSC-3. Signal plus noise level is monitored in a fairly wide bandwidth IF filter (B_1 H_z). In the WSC-3, this bandwidth is 200 KHz. Output level of this filter is nominally kept at a constant level by the AGC. The output of this filter is compared with a constant threshold to provide the blanking signal. A significant increase in signal plus noise is required in order to trigger the threshold detector. The second IF filter (B_2 H_z) is only 40 KHz wide in the WSC-3 and could ring for long periods of time due to RFI pulses if the blanker were not used. After the RFI pulse disappears, it will take about 50 μsec for the modem to recover from the effects of the blanking and for a valid input to the matched filter to appear.

One quantity of interest in computing performance is the blanker threshold crossing probability. The filter B_1 has a wide bandwidth and for a coded system the signal to noise ratio in this bandwidth will be extremely small. Therefore, to facilitate the calculations, we assume that the threshold detector is operating on noise only. We will also assume that the detector measures noise power using a square-law envelope detector.

With a Gaussian input with variance $N = N_o B_1$ the density function of the output is exponential, i.e.,

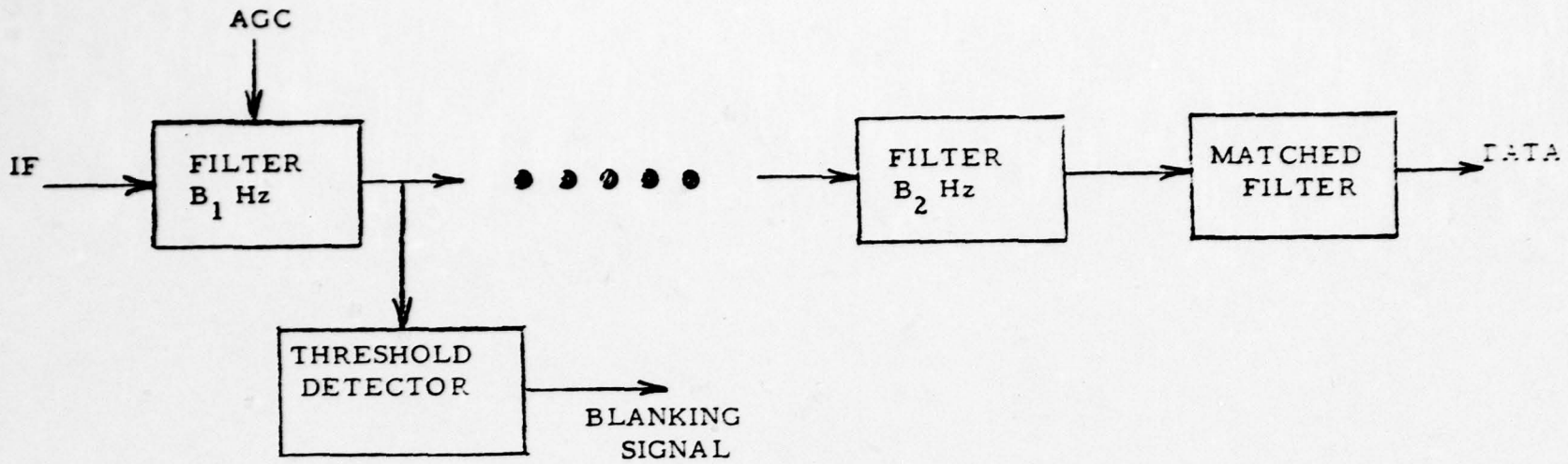

FIGURE 1: MODEL OF MODEM WITH BLANKING.

$$P(y) = \frac{e^{-y/2N.}}{2N} , \qquad (1)$$

which has a mean $\bar{y} = 2N$. Then the threshold crossing probability (for a threshold at X) is

$$Pr(y>X) = \int_x^{\infty} \frac{e}{2N}^{-y/2N} dy$$

$$= \exp \left\{ -X/2N \right\}$$

$$= \exp \left[-10^{T/10} \right] , \qquad (2)$$

where T is the threshold in dB above the mean.
Thus,

$$T = 10 \log_{10}(X/2N). \qquad (3)$$

We are interested in two probabilities – the threshold crossing probabilities with noise alone and with RFI plus noise. For noise alone this probability is simply

$$P_n = \exp \left[-10^{T/10} \right]. \qquad (4)$$

When interference is present, we will model the interference plus noise voltage at the IF filter output as a Gaussian process with variance I dB above the variance of the noise alone. We call I the RFI excess noise. While this assumption is not entirely accurate, there is experimental evidence that the RFI does contain a strong Gaussian component, and we believe that significant insight can be gained from the results. In this case the blanker threshold is now only (T-I) dB above the mean of the RFI plus noise. Then the level crossing probability is

$$p_i = \exp\left[-10^{-(T-1)/10}\right]. \qquad (5)$$

The level crossing probability for noise alone from (4) is shown in Figure 2 as a function of threshold, T. Values for the case of noise plus RFI may be obtained from this curve by using (T-1) rather than T as the abscissa. Note that for $T < 7$ dB the probability of falsely triggering the blanker on noise alone will be 10^{-2} or higher. Due to the blanker extension of 50 μsec, this would cause an increase in erasure rate at the decoder input large enough to degrade performance.

The effect of the pulse extension will be modelled as a Markov chain. The IF filter output has B_1 independent samples per second. For an RFI pulse extension of τ seconds, the number of samples the RFI pulse is extended by is

$$m = \lceil B_1/\tau \rceil \quad , \qquad (6)$$

where $\lceil x \rceil$ denotes the smallest integer $\geq x$. A Markov chain model of the blanker is shown in Figure 3. State o represents the time the blanker is <u>off</u> while States 1 through m represent the time the blanker is <u>on</u>. The quantity p is the threshold crossing probability. Note that m consecutive samples must fall below the threshold after a crossing to allow the blanker to be turned off (τ seconds). Using this model, the fraction of time the blanker is triggered is found to be

$$\pi_{on} = 1 - \frac{(1-p)^m}{1+p} \, . \qquad (7)$$

In the AN/W SC-3 $B_1 = 200$ KHz and $\tau = 50$ μsec giving m=10. The fraction of time the blanker is triggered can be computed as π_n for noise alone and as π_i for noise plus interference using (4) and (5), respectively, for p.

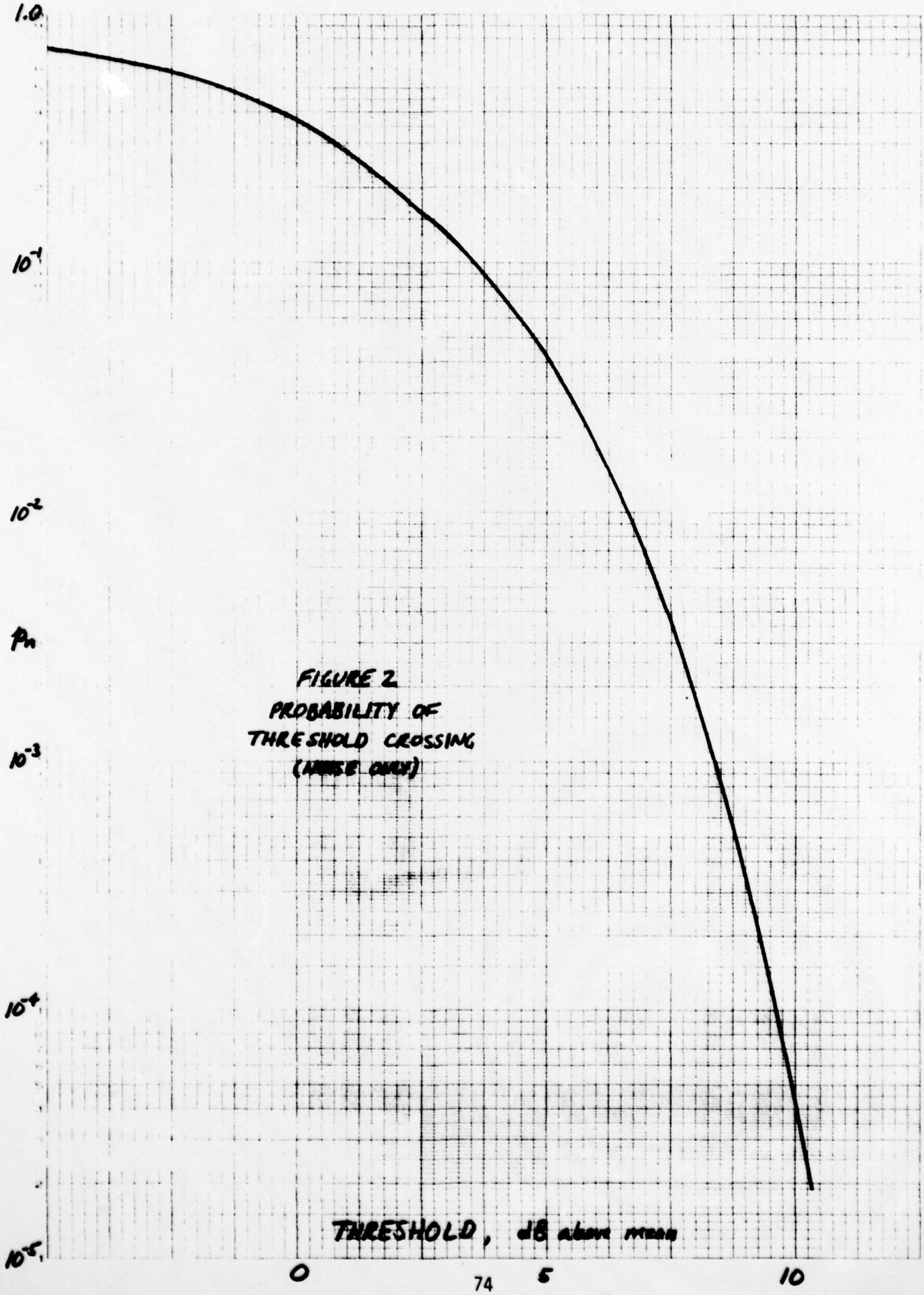

FIGURE 2
PROBABILITY OF
THRESHOLD CROSSING
(NOISE ONLY)

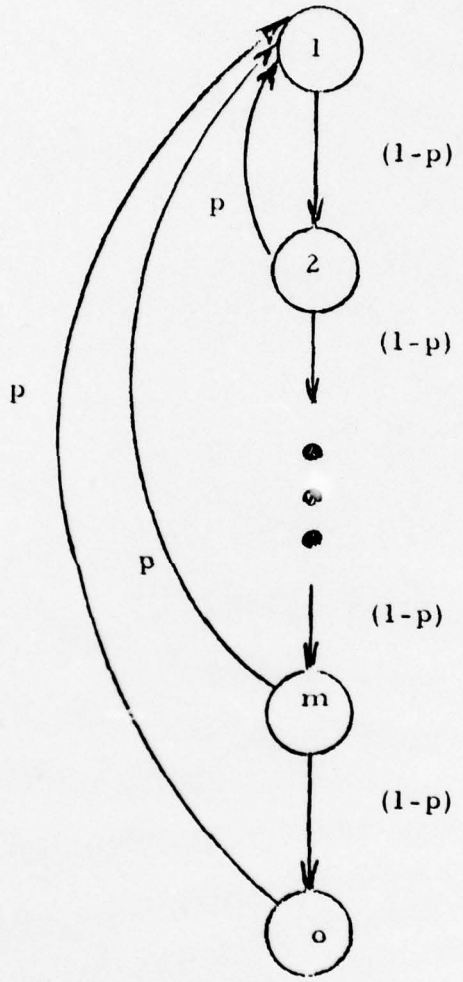

FIGURE 3: MARKOV CHAIN MODEL OF BLANKER

For the pulsed RFI problem one must also calculate the probability that after an RFI pulse there is extension of the blanking into the region where noise alone is present. The average amount of pulse extension into the RFI-free region (in discrete samples) is

$$N_e = \sum_{i=o}^{m-1} (m-i)p(1-p)^i$$

$$= \frac{-1+(m+1)p + (1-p)^{m+1}}{p} \qquad (8)$$

Then for RFI pulses with pulse length τ_r and duty cycle δ the average extension of the RFI duty cycle is

$$\delta_e = \frac{N_e}{m} \quad \frac{\tau}{\tau_r} \delta, \qquad (9)$$

for $\tau \leq \tau_r$. In the WSC-3, $\tau/\tau_r = 0.25$ for the 200 usec RFI pulse.

The coded system performance can then be computed using the union bound with a set of average 8-level transition probabilities. The applicable transition probabilities are

$$P_{nom}(j) = f(j, Es/No), \qquad (10)$$

the nominal transition probabilities (with no interference and no blanker threshold crossing),

$$P_{deg}(j) = f(j, Es/No-1), \qquad (11)$$

the degraded probabilities with interference, and

$$P_b(j) = (0, 0, 0, 0.5, 0.5, 0, 0, 0), \qquad (12)$$

the blanked probabilities which canhave occurrences only in the

two middle regions. Then using the previously calculated probabilities for the blanker being on both with and without RFI and the blanker extension into the RFI-free region, the average transition probabilities are

$$P_a(j) = (1-\delta-\delta_e)\left[(1-\pi_n)P_{nom}(j) + \pi_n P_b(j)\right]$$

$$+ \delta\left[(1-\pi_i)P_{deg}(j) + \pi_i P_b(j)\right]$$

$$+ \delta_e P_b(j) . \qquad (13)$$

Then using these transition probabilities and the code weight structure performance may be estimated using a union bound. In applying the average transition probabilities in the union bound, we are implicitly making the assumption that RFI with and without blanking always occurs coincident with entire bit interval.

The union bound was used to compute error rate for a $R = 1/2$, $k = 9$ code at $E_s/N_o = 1$ dB with RFI duty cycle $\delta = 0.05$. The results are shown in Figure 4. Here the error rate is shown as a function of noise plus interference level for several values of threshold. The effect of improper placement of the blanker threshold is demonstrated. At small values of threshold (<8 db) there is a significant increase in erasure rate caused by false triggering of the blanker on noise alone. When the threshold is placed too high (> 12 dB)

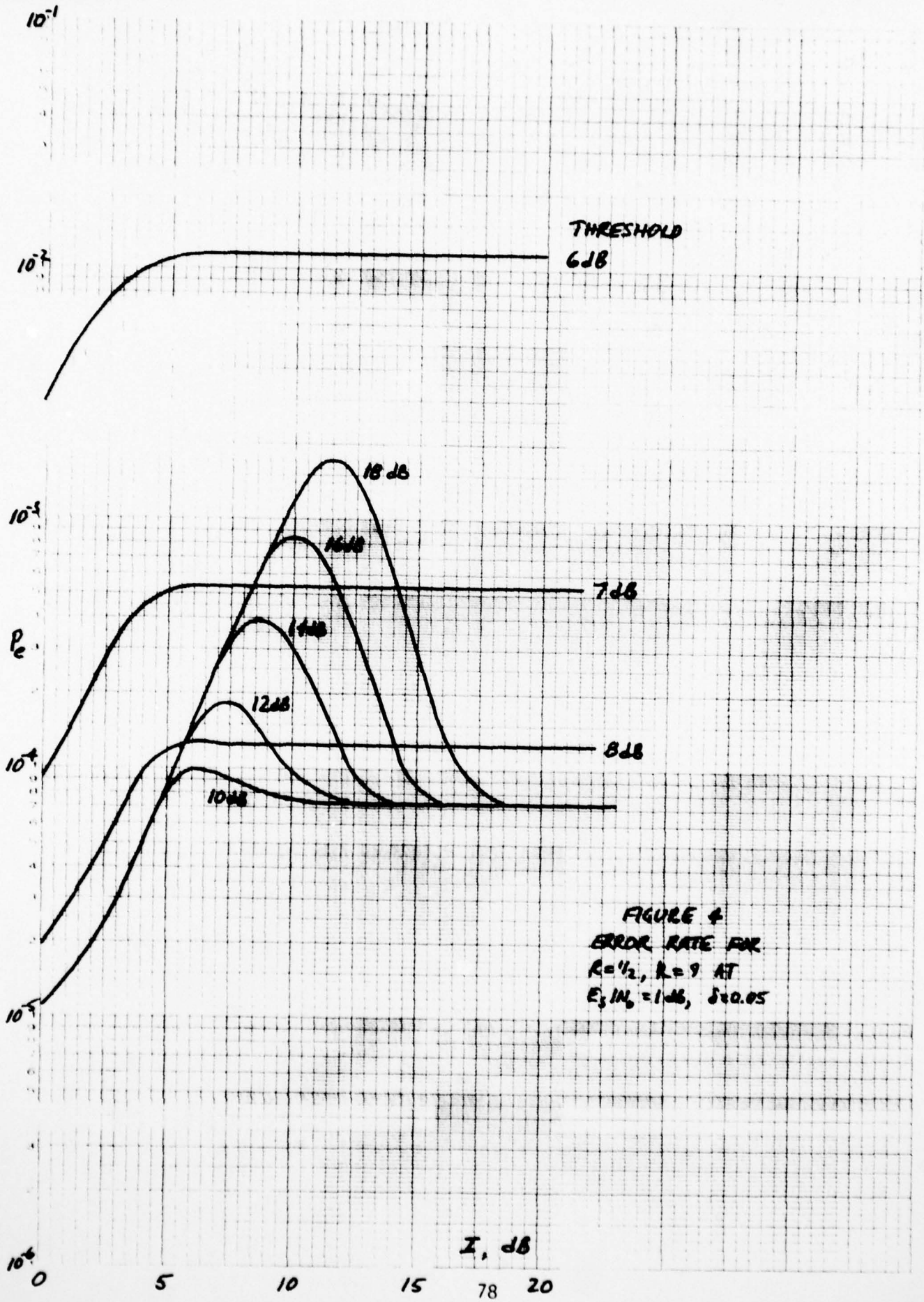

FIGURE 4
ERROR RATE FOR
$R = 1/2$, $K = 9$ AT
$E_s/N_o = 1$ dB, $\delta = 0.05$

one observes an error rate peak at some value of I several dB below the threshold. In this case the blanker is not triggering often enough when RFI is actually present. These curves are presented in another manner in Figure 5. Here the error rate is shown as a function of blanker threshold for several values of interference level, I. Fortunately the error rate reaches a minimum at about T = 10 dB for all values of I. Thus, one achieves best performance by selecting the blanker threshold at 10 dB.

Similar curves were obtained for the R = 3/4, k = 11 code. These results also indicate an optimum threshold setting at approximately 10 dB.

In both cases, RFI levels slightly below the blanking threshold cause a slight elevation in the error rate, and thus a peformance degradation with respect to the fully-blanked case. In the case of the R = 1/2 code, this degradation is only about 0.1 dB. For the R = 3/4 code, the degradation is approximately 0.5 dB (because of the smaller slope of the R = 3/4 error rate curve).

These results show that by proper choice of threshold, acceptable decoder performance can be insured at all levels of RFI.

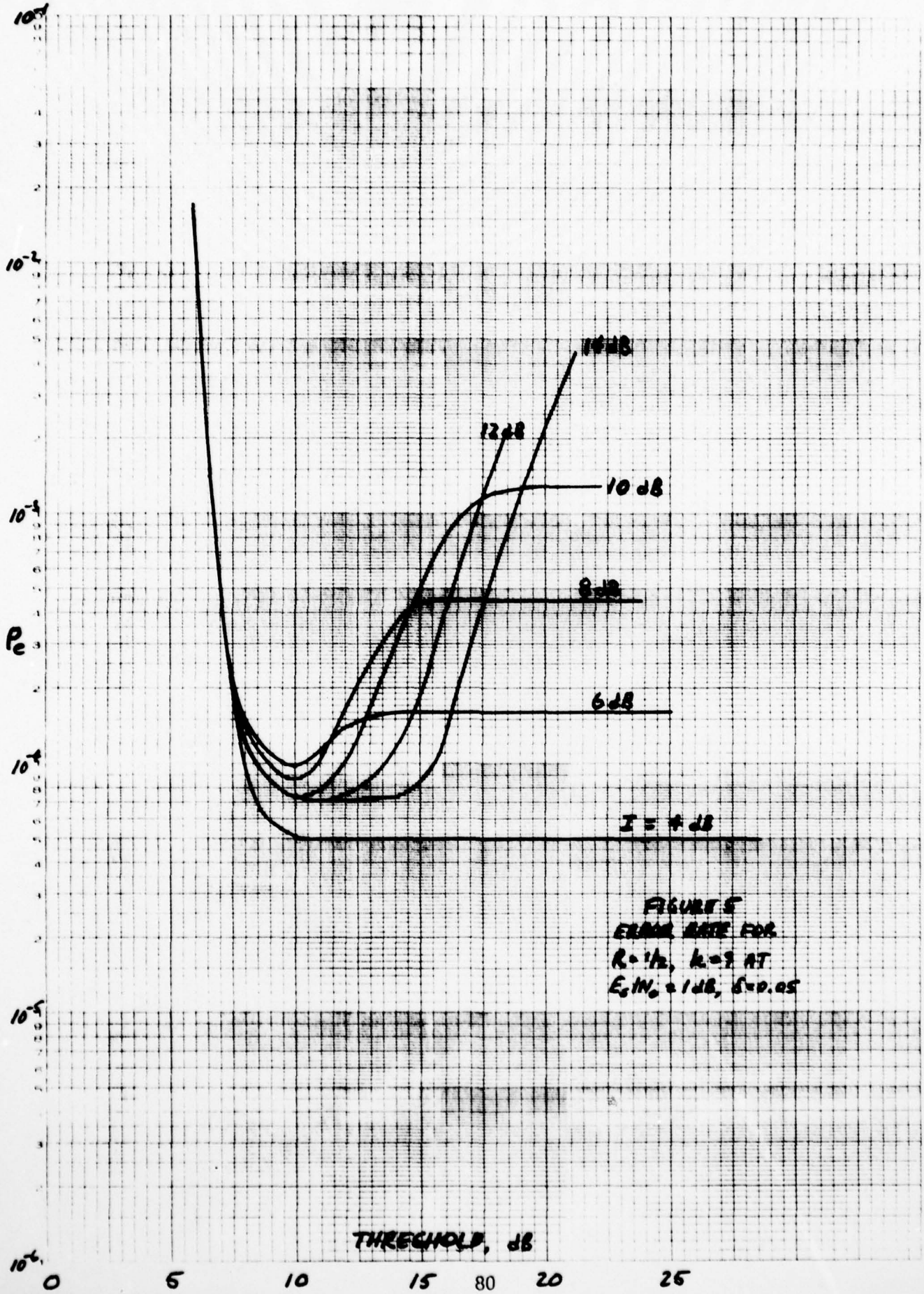

FIGURE 5
ERROR RATE FOR
$R = 1/2$, $k = 7$ AT
$E_s/N_o = 1$ dB, $\delta = 0.05$

APPENDIX C

EIRP AND G/T CALIBRATION FOR SATELLITE TESTS

Figure C-1 illustrates in detail the configuration of equipment used during the FLTSATCOM Channel 4 access discussed in Section 3.3. All values indicated on Figure C-1 were supplied by J. E. Ohlson and are the results of careful measurement.

On the receive side, the 27 dB gain of the preamplifier isolates the AN/WSC-3 noise figure, so that the system noise figure reference to the antenna output is

$$NF_{syst} = 2.2 + 0.3 + L + 0.3 + 2.0 + 0.8 = 5.6 + L \quad dB$$

where L is the total attenuation inserted by the two variable attenuators. The system noise temperature is thus

$$T_{syst} = 290(10^{.56}\ 10^{.1L} - 1) \quad K \ .$$

The antenna noise temperature is approximately 290 K, so that the operating temperature is

$$T_{op} = 290\ 10^{.56}\ 10^{.1L} = 1053 \times 10^{.1L} \ K \ .$$

Receiving terminal G/T is therefore

$$G/T = 11 - 10 \log T_{op}$$

$$= -19.2 - L \qquad dB/K \ .$$

On the transmit side, the test output of the 30 dB coupler is 29.9 dB below the primary output. Thus the power delivered to the antenna is 29.9-0.8-2.1-1.0=26 dB greater than the power meter reading. Including the effect of antenna gain, EIRP is given by

$$\text{EIRP} = 37 + \text{Power meter reading} \quad \text{dBW}$$

or more conveniently,

$$\text{EIRP (dBW)} = 7 + \text{Power meter reading (dBm)} .$$

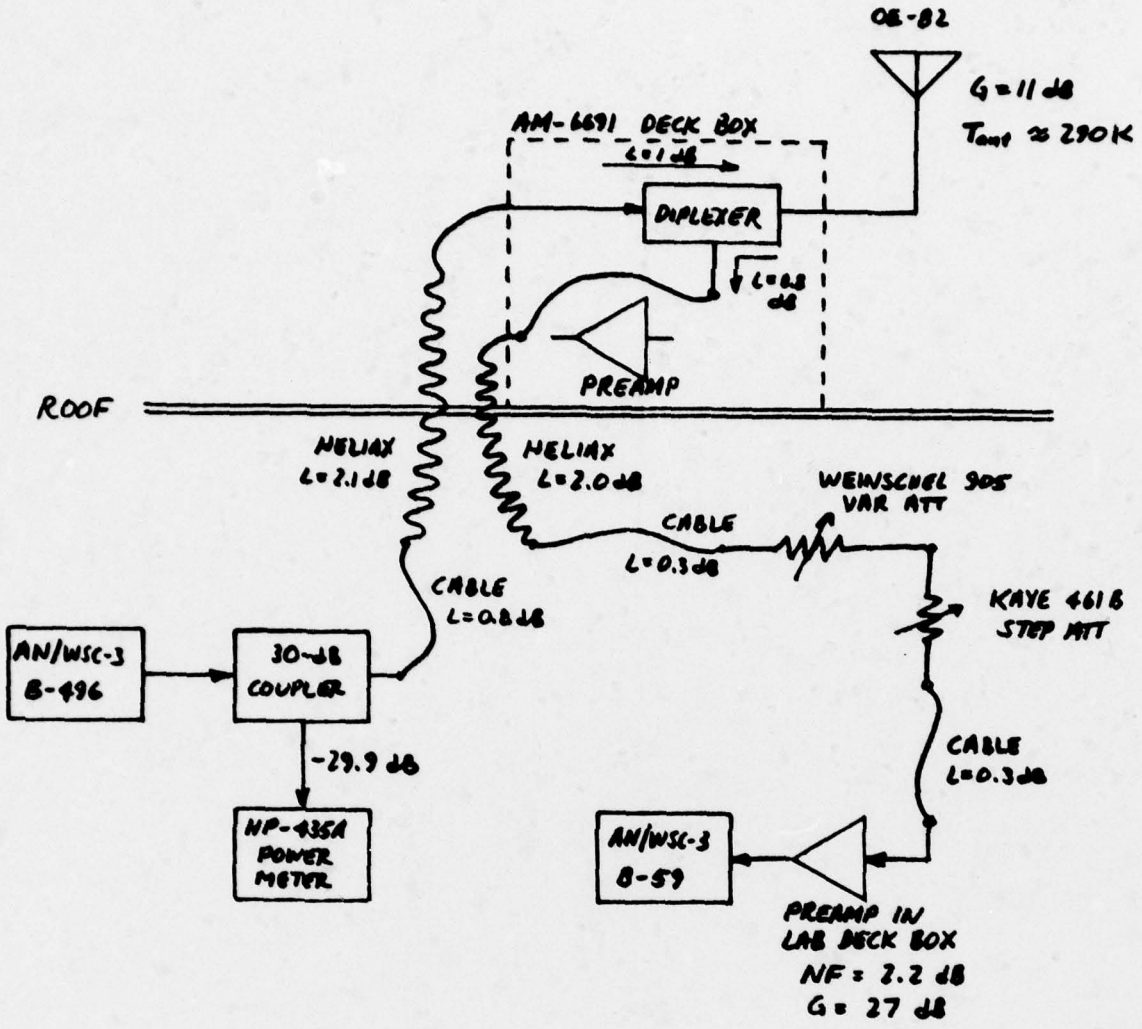

Figure C-1. Equipment Configuration for Satellite Link Tests